PB 257 095

EPA-450/3-76-027

March 1976

ANALYSIS OF POPULATION EXPOSURE TO AIR POLLUTION IN NEW YORK-NEW JERSEY-CONNECTICUT TRI-STATE REGION

U.S. ENVIRONMENTAL PROTECTION AGENCY
Office of Air and Waste Management
Office of Air Quality Planning and Standards
Research Triangle Park, North Carolina 27711

TECHNICAL REPORT DATA
(Please read Instructions on the reverse before completing)

1. REPORT NO. EPA-450/3-76-027	2.	3. RECIPIENT'S ACCESSION NO.
4. TITLE AND SUBTITLE Analysis of Population Exposure to Air Pollution in the New York-New Jersey-Connecticut Tri-State Region		5. REPORT DATE March 1976
		6. PERFORMING ORGANIZATION CODE
7. AUTHOR(S) Yuji Horie and Arthur C. Stern		8. PERFORMING ORGANIZATION REPORT NO.
9. PERFORMING ORGANIZATION NAME AND ADDRESS University of North Carolina Chapel Hill, N.C. 27514		10. PROGRAM ELEMENT NO.
		11. CONTRACT/GRANT NO. R803461-01-0
12. SPONSORING AGENCY NAME AND ADDRESS Monitoring and Data Analysis Division (MD-14) Office of Air Quality Planning and Standards U.S. Environmental Protection Agency Research Triangle Park, N.C. 27711		13. TYPE OF REPORT AND PERIOD COVERED Final
		14. SPONSORING AGENCY CODE EPA-OAQPS
15. SUPPLEMENTARY NOTES		

16. ABSTRACT

A population exposure methodology has been developed and applied to total suspended particulate (TSP) in the NY-NJ-Conn Tri-State Region. Ambient TSP data produced by 72 monitoring stations, 1971 to 1973, were used for the analysis of population exposure to TSP. Census data are aggregated into 215 points to form a demographic network. The monitored air quality data are spatially interpolated to each demographic network point to calculate a local population exposure.

Annual and quarterly geometric mean concentrations are used to estimate long-term population exposure to TSP. Long-term exposure is characterized by a population dosage spectrum that indicates a population distribution of exposures at various mean concentrations. Population average air quality is computed to indicate representative air quality levels. A health risk index indicates a percentage of the population exposed to air pollution above the annual standard.

Percentile concentrations are used to estimate short-term population exposure. Short-term exposure is characterized by a population-at-risk spectrum that indicates a population distribution for various exposures to air pollution above the 24-hour standard. A population-at-risk index indicates a percentage of time that an average person in the region is exposed to air pollution above the 24-hour standard.

Methods of forming the optimal subnetwork out of an existing monitoring network are also explored with respect to the objective of minimizing the error in estimating exposure of the population to air pollution.

17. KEY WORDS AND DOCUMENT ANALYSIS

a. DESCRIPTORS	b. IDENTIFIERS/OPEN ENDED TERMS	c. COSATI Field/Group
Air Pollution Air Quality Monitoring Interpolation Exposure Optimization		

18. DISTRIBUTION STATEMENT Unlimited	19. SECURITY CLASS (This Report) Unclassified	21. NO. OF PAGES
	20. SECURITY CLASS (This page) Unclassified	22. PI

EPA Form 2220-1 (9-73)

PRICES SUBJECT TO CHANGE

EPA-450/3-76-027

ANALYSIS OF POPULATION EXPOSURE TO AIR POLLUTION IN NEW YORK-NEW JERSEY-CONNECTICUT TRI-STATE REGION

by

Yuji Horie* and Arthur C. Stern

Department of Environmental Sciences and Engineering
University of North Carolina at Chapel Hill
Chapel Hill, North Carolina 27514

Grant No. R803461-01

EPA Project Officer: Neil H. Frank

Prepared for

ENVIRONMENTAL PROTECTION AGENCY
Office of Air and Waste Management
Office of Air Quality Planning and Standards
Research Triangle Park, North Carolina 27711

March 1976

* [illegible], Research Scientist, Technology Service Corporation, Santa Monica, California.

This report is issued by the Environmental Protection Agency to report technical data of interest to a limited number of readers. Copies are available free of charge to Federal employees, current contractors and grantees, and nonprofit organizations - in limited quantities - from the Library Services Office (MD35), Research Triangle Park, North Carolina 27711; or, for a fee, from the National Technical Information Service, 5285 Port Royal Road, Springfield, Virginia 22161.

This report was furnished to the Environmental Protection Agency by the Department of Environmental Sciences and Engineering, University of North Carolina at Chapel Hill, North Carolina 27514, in fulfillment of Grant No. R803461-01. The contents of this report are reproduced herein as received from the Department of Environmental Sciences and Engineering, University of North Carolina at Chapel Hill. The opinions, findings, and conclusions expressed are those of the author and not necessarily those of the Environmental Protection Agency. Mention of company or product names is not to be considered as an endorsement by the Environmental Protection Agency.

Publication No. EPA-450/3-76-027

Table of Contents

I. INTRODUCTION

A Population Exposure Approach[1], as contrasted with an Air Quality Approach, for reporting ambient air quality in a concise and comprehensive manner is proposed and developed in this work. Presently, ambient air quality is reported in terms of mean concentrations and/or percentile concentrations which are derived from air monitoring data through standard statistical manipulation. However, these quantities, of themselves, do not describe accurately the state of air quality to which a population is exposed. The population at risk could be any population, such as the tree population or the cattle population, but in this report "population" always means "human population".

The purpose of a Population Exposure Approach is to provide a better method to describe the state of air quality representative of the population at risk. For this purpose, air quality data[2] are merged with demographic data[3]. The New York-New Jersey-Connecticut Tri-State Region was chosen for the analysis of population exposure, and the pollutant to which they were exposed chosen was total suspended particulates (TSP). Of 164 air monitoring stations scattered over the Tri-State Region, 72 stations reported statistically valid air quality data during the study period, the second quarter of 1971 (designated 71/2) and the second quarter of 1973 (designated 73/2).

1970 census summaries[3] for county subdivisions and 1970 population traits prepared by the Tri-State Regional Planning Commission[4] were used to generate the population data set. These population data were tabulated for contiguous regional statistical areas. In order to interface the population data with the air quality data, the population data were aggregated into 215 standard network points. Each point is supposed to indicate the local population size, local subpopulations (school-age, elderly, and non-white populations), and the area in which the local population resides.

TSP air quality at each standard network point was estimated by interpolating to the point the air qualities observed at the nearest three monitoring stations to the network point. The data set of air quality and population at the 215 standard network points was then used to compute local and regional values of the various population exposure indices and variables discussed below. Geometric mean concentrations are used to estimate the long-term average exposure of the population to TSP air pollution, whereas percentile concentrations are used to describe a cumulative distribution of the short-term population exposure to various levels of TSP air pollution.

Long-term population exposure is summarized in: (a) a population average air quality which indicates the air quality level to which the population was exposed; (b) a health index which indicates the percentage of the population exposed to air pollution exceeding the United States federal primary air quality standard; (c) a welfare index which indicates the percentage of the population exposed to air pollution exceeding the United States federal secondary air quality standard; and (d) a population dosage spectrum which indicates the distribution of the population associated with various air pollution dose levels.

Short-term exposure is summarized in: (a) a risk probability which indicates the time percentage of local population exposure in excess of a given concentration threshold (the United States federal 24 hour or annual air quality standards are used for the threshold values), and (b) a population-at-risk spectrum which indicates the distribution of the population associated with various risk probabilitie

Air pollution effects on health vary among sub-populations such as the child population and the elderly population. Therefore, the population exposure parameters described above are determined not only for the whole population but also for three sub-populations: (a) school-age, (b) elderly, and (c) non-white. The working-age population was intentionally dropped from this analysis because of its great daily mobility. A population exposure analysis for the working-age population would require use of a measure of a dynamic population whose size and composition vary with time, instead of the static population exemplified by the resident population, on which this report is based.

The air quality trend on an annual base is investigated in Section VI. The annual geometric mean concentrations observed at 69 air monitoring stations during 1971 and 1973 were used for the analysis of trends in the air quality indices noted above. Of the 69 stations, 14 stations failed to report valid air quality data in one or two quarters during 1971 and 1973. Where there was missing quarterly data in one year, the air quality data in the corresponding quarters of the other year, i.e. either 1971 or 1973, was substituted.

An empirical method of upgrading an existing air monitoring network is discussed in Section VII. 130 of the 164 Tri-State Region air monitoring stations reported statistically valid air quality data during the second and third quarter of 1973. These 130 stations were used to explore optimal sub-networks.

II. AIR QUALITY AND POPULATION DATA

The area under study is the New York-New Jersey-Connecticut Tri-State air quality control region (AQCR) less the eastern half of Suffolk County. This area is a little smaller than the Tri-State Region[5] but a little larger than the New York-North Eastern New Jersey Standard Metropolitan

Statistical Area (Fig. 1). It is comprised of parts of Connecticut, New York, and New Jersey, i.e. the 19 counties listed in Table I. According to the 1970 census summaries[3], the study area includes approximately 12,000 square kilometers (4,600 square miles) and 17.0 million people in and surrounding New York City. There are 164 air monitoring stations in the area operated by federal, state or city governments. Of these, 72 stations report to the Nation Aerometric Data Bank statistically valid air quality data for TSP measured by Hi-Vol Sampler during the two quarters, 71/2 and 73/2.

The individual statistical areas for the county sub-divisions vary in area and population and have complex geographic boundaries. Air monitoring stations are not distributed uniformly over the area but tend to be concentrated in heavily populated areas. As a result, there is a very poor geographical agreement between the distribution of air monitoring stations and that of census statistical areas. To solve this problem, the standard network shown in Figure 2 was devised. The standard network consists of 215 standard network points located by considering the geographical distribution of the population. The boundaries between one point and the neighboring points were determined rather arbitrarily but geographical boundaries were considered in the partitioning process. Air quality at a standard network point was estimated by interpolating to that point the observed air qualities at neighboring monitoring stations.

2.1 Population Data

The 1970 census results have been summarized in many ways in print and on magnetic tape. Of these summaries, the "Population of County Subdivisions" was used as the population data base for this study. However, they do not include the statistics of the school-age, elderly, and non-white sub-populations. It is very time consuming to aggregate such subpopulation statistics of each census tract into subdivisions for each county. In this study, this impediment was circumvented by using "Population by Age Group" data previously aggregated by the Tri-State Regional Planning Commission[5].

The commission also issues a series of computer-produced maps called Regional Profiles[4]. The Regional Profile computer display of 1970 population distribution over the Tri-State Region was used to produce the standard network by assigning to each sub-region the number of network points approximately proportional to the population density of that sub-region. The 215 standard network points thus selected are shown on the regional map of Figure 2. Each standard network point is intended to represent its spatial location, its assigned area, and the average population density in that assigned area. These data are listed in Table II. The code number indicates the county in which the network point is located. The corresponding county name can be found from Table I. Table III lists for each network point the percentage of each sub-population in the total population.

2.2 Air Quality Data

There are 164 air monitoring stations[6] operated by federal, state, or city governments in the study area. These stations measure 24 hour average air quality of TSP with Hi-Vol samplers. The frequency of sampling is 61 samples per year, or once every 6 days. EPA's National Aerometric Data Bank (NADB) receives the observed air quality data from the local air pollution agency and stores them for retrieval and use by a variety of purposes, such as for a study like this one. NADB's quarterly summaries of TSP air quality data during the period 1970 to 1974 were examined for use in this study. Judging from the data retrieved, the performance of the Tri-State Regional air quality monitoring network is disappointingly poor. The number of stations consistently reporting statistically valid air quality data during the five year period is less than 30% of the total number of stations.

The present analysis of population exposure to TSP air pollution includes a comparison of trend in air quality and that in population exposure. Such analysis needs statistically valid air quality data from a station at two points in time. Among the many possible combinations of quarters during the three year period examined the number of monitoring stations satisfying this condition is greatest for the combination of the second quarters of 1971 (71/2) and of 1973 (73/2). There were 72 monitoring stations whose data were valid for both these periods. The geometric mean concentrations and spatial coordinates of all the 164 stations operating during the two quarters, 71/2 and 73/2 are listed in Table IV. The locations of the 72 monitoring stations valid for both periods are shown in Figure 3 by open circles, the invalid stations by solid circles. The data set presented in Table IV was used for the analysis of the long-term population exposure, i.e. for a season, discussed in Section IV. The percentile concentrations at these 72 valid stations during the same period are presented in Table V. These percentile data were used for the analysis of short-term population exposure discussed in Section V.

There are 45 monitoring stations that report statistically valid air quality data for the entire years of both 1971 and 1973. For these two years, 14 stations failed to report statistical valid air quality data for one quarter and 10 stations failed to do so for two quarters. For each of these 24 imperfect stations, valid data from the corresponding quarter of the other year was used to replace the data for the invalid quarters. In this way, the air quality data for 69 monitoring stations was generated and used for the analysis of trend in air quality and population exposure discussed in Section VI. These data are shown in Table VI.

The annual geometric mean concentration of each monitoring station was computed by taking a geometric mean of the geometric mean concentrations during each of the four individual quarters (Table VII). The resulting value is a little different from the reported value for the annual geometric mean concentration. However, the difference between the computed and the reported value is generally less than 0.1 $\mu g/m^3$. The cause of the difference is that the computed value is based on the assumption of an equal number of samples during each quarter while the reported value is based on the actual number of samples measured during each quarter.

The two consecutive quarters, second and third quarters of 1973 have the largest number of valid monitoring stations among many combinations of two quarter periods. There are 130 valid monitoring stations during these periods (Table VIII). The spatial locations of these stations are given in Table VIII and also shown in Figure 4. The data set of Table VIII was used for the sensitivity analysis of monitoring networks discussed in Section VII.

2.3 Interfacing Population and Air Quality Data Sets

To know the exposure of a person to air pollution, the spatial location of the person and the air quality at his location must be known as a function of time. In the present study, however, we are not interested in the actual exposures of individual persons to air pollution, but rather interested in the ensemble of potential exposures of a large population, say, a million people. For this purpose, an appropriate estimate of air quality at each standard network point should be sufficient to make an estimate of population exposure at that particular locale, if the assumption is made that the population size and sub-population composition will be approximately stationary over the study period. This assumption should be good for the analysis of exposure of elderly and school-age populations because these subpopulations tend to be locationally fixed, i.e. most school-age children and elderly people stay close to their residence locations most of the time.

However, the above assumption would not hold for the working-age population because a substantial percentage of that population spends a substantial part of their time at their working places where the air environment may be quite different from that of their residential location. Thus, the working-age population has been intentionally omitted from this population exposure analysis. A substantial percentage of the whole population and of the non-white population may also spend a substantial part of their time at locations with an air environment different from that of their residence. However, such percentages of the total population and of the non-white population would certainly be smaller than that for the working-age population.

A look at the census data(3) for the Tri-State Region indicates that although the daytime population of New York City is significantly greater than the nighttime population, regionwide the population which commutes to work from their residential location is small compared to the total population. Nassau County is a case in point. The census data show that, of the total population (1,428,077), the working population that commutes to working places outside of Nassau County is 263,592 (i.e. all workers [558,931] less those working in Nassau County [295,339]) or 18% of the total population. The percentage of such a population to the total population of the Tri-State region has been assumed to be somewhat lower than 18%, e.g. 10%. A 10% error in the estimate of population should not invalidate analysis of exposure of the total population or the non-white population, when compared with the error in the estimate of air quality, which may be estimated as around 10 ∿ 20%.

As mentioned earlier, the spatially distributed population over the study area was aggregated at 215 standard network points. Therefore, all the information on air quality necessary for the population exposure analysis was assumed to be contained in the air quality at the 215 network points. Their air quality was estimated from the air quality observed at the 72 valid air monitoring stations. The air quality at a network point was estimated by interpolating the observed air quality at the three nearest neighboring stations to that point as

$$\left.\begin{array}{ll} C_j = \sum_{i=1}^{3} C_i \, d_i^{-2} \Big/ \sum_{i=1}^{3} d_i^{-2} & \text{for } d_i \neq 0 \\ C_j = C_i & \text{for } d_i = 0 \end{array}\right\} \quad (1)$$

where C_j is the concentration estimated at j-th network point (X_j, Y_j), C_i $(i = 1, 2, 3)$ are the concentrations observed at the three nearest neighboring stations, i-th $(i = 1, 2, 3)$ air monitoring stations (X_i, Y_i) around the j-th network point, and d_i is the distance between the i-th monitoring station and the j-th network point, i.e.

$$d_i = \sqrt{(X_i - X_j)^2 + (Y_i - Y_j)^2} \quad (2)$$

The interpolation formula given by Equation (1) was arrived at after a careful and detailed analysis was made of various interpolation formulae and their performance. A discussion of this analysis of interpolation formulae is given in Appendix A.

III. FORMULATION OF POPULATION EXPOSURE

There are national air quality standards for particulate air pollution both for short-term (24 hour average concentration) and long-term (1 year average concentration). The reasons of having an air quality standard for two different averaging times is that adverse effects can occur from either a short exposure to higher concentrations, or longer exposure to lower concentrations. These relations are explained by the dose-response curve. For each averaging time, there are two air quality standards, a primary standard to protect public health and a secondary standard to protect public welfare.

The present analysis of population exposure to air pollution is based on these same basic dose and threshold concepts. An air pollution dose of a person at $\underline{r}$ during a time period T is given as

$$DOSE\ (\underline{r}) = \int_0^T C\ (\underline{r},\ t)\ dt \qquad (3)$$

When the mean concentration of air quality at $\underline{r}$ over T is estimated from air monitoring data, Equation (3) can be expressed as:

$$DOSE\ (\underline{r}) = T\ C_m(\underline{r}) \qquad (3\text{-}a)$$

Equation (3-a) indicates that when exposure time is given, the air pollution dose of a person is estimated from the mean concentration at his location. In this report the mean of pollution concentrations at the location of a population over a given time is called "dose $D_{(\underline{r})}$" i.e.

$$D\ (\underline{r}) = C_m(\underline{r}) \qquad (4)$$

Equation (4) says that because a population which resides at $\underline{r}$ stays close to their resident location for most of time, the ensemble average of air pollution doses of its individual members is given by the mean of concentrations over the exposure time.

3.1 Parameters Based on Mean Concentrations

A spatial average concentration may be computed by

$$AQ_s = \int_{\underline{r}} D(\underline{r})\ d\underline{r}/A_o \qquad (5)$$

where A_o is the total area under study. The spatial average air quality has been used to indicate the air quality representative of a given region. However, the air quality representative of the populace which resides in the region may be better expressed by the population average air quality,

$$AQ_p = \int_{\underline{r}} D(\underline{r})\ p(\underline{r})\ d\underline{r}/P_o \qquad (6)$$

where $p(\underline{r})$ is the population density at $\underline{r}$ and P_o is the total population of the region.

The air quality indices AQ_s and AQ_p described above indicate the air quality for the entire region or population under study. Another kind of air quality index may be defined by the percentage of population exposed to air pollution exeeeding a given level. A health index, HI, is defined by the percentage of the population exposed to air pollution exceeding the primary air quality standard D_h (the health standard).

$$HI = \int_{\underline{r}} H(\underline{r}, D)\ p(\underline{r})\ d\underline{r}/P_o \qquad (7)$$

where $H(\underline{r}, D)$ is a discriminant function defined as[7]

$$\left. \begin{array}{ll} H(\underline{r}, D) = 1 & \text{if } D(\underline{r}) \geq D_h \\ H(\underline{r}, D) = 0 & \text{otherwise} \end{array} \right\} \qquad (8)$$

Similarly, a welfare index, WI, may be defined by the percentage of the population exposed to air pollution exceeding the secondary air quality standard D_w (the welfare standard).

$$WI = \int_{\underline{r}} W(\underline{r}, D)\ p(\underline{r})\ d\underline{r}/P_o \qquad (9)$$

where
$$\left.\begin{aligned} W(\underline{r}, D) &= 1 \qquad &\text{if } D(\underline{r}) \geq D_W \\ W(\underline{r}, D) &= 0 \qquad &\text{otherwise} \end{aligned}\right\} \qquad (10)$$

The discretized forms of Equations (5), (6), (7) and (9) are written as

$$AQ_s = \sum_i D_i\ \Delta A_i/A_o \qquad (5\text{-a})$$

$$AQ_p = \sum_i D_i\ p_i\ \Delta A_i/P_o \qquad (6\text{-a})$$

$$HI = \sum_i H(D_i)\ p_i\ \Delta A_i/P_o \qquad (7\text{-a})$$

$$WI = \sum_i W(D_i)\ p_i\ \Delta A_i/P_o \qquad (9\text{-a})$$

where ΔA_i is the area represented by the i-th standard network point, D_i is the annual mean concentration at the i-th point, and p_i is the population density averaged over the area ΔA_i.

A dosage isopleth map, similar to an air quality isopleth map, can be obtained by using a threshold function such that

$$\left.\begin{aligned} N(\underline{r}, D) &= 1 \qquad &\text{if } D(\underline{r}) \geq D^* \\ N(\underline{r}, D) &= 0 \qquad &\text{otherwise} \end{aligned}\right\} \qquad (11)$$

where D^* is the dosage threshold. For a given threshold, one can draw a dosage isopleth by plotting all the points with $N(\underline{r}, D) = 1$. Using the same threshold function, one can also compute the dosage spectrum $S(D^*)$ and the population dosage spectrum $P(D^*)$ that are defined as

$$S(D^*) = \int_{\underline{r}} N(\underline{r}, D)\ d\underline{r}/A_o \qquad (12)$$

$$P(D^*) = \int_{\underline{r}} N(\underline{r}, D)\ p(\underline{r})\ d\underline{r}/P_o \qquad (13)$$

Equation (12) says that a fraction of the total area, S(D*), is polluted more than D*, or is receiving a pollution dosage greater than D*T where T is 8760 hours. Equation (13) says that a fraction of the total population, P(D*), is exposed to air pollution exceeding D*, or is receiving a pollution dosage greater than D*T.

3.2 Parameters Based on Percentile Concentrations

The individual values of 24 hour Hi-Vol measurements of TSP can be sorted in descending order of magnitude and normalized in percentile concentrations. These percentile concentrations can be used to evaluate the short-term (24 hour) population exposure to air pollution in relation to national air quality standards.

At a given location, the percentile concentrations may exceed a level of, say, the 24 hour primary standard. Then, the percentage of time during which local air pollution exceeds the prescribed level may be associated with the risks to the local populace incurred by the adverse effects of such excess. The risk probability is defined as the percentage of time during which local pollution concentration exceeds the level prescribed by each of the four air quality standards; the annual primary, annual secondary, 24 hour primary, and 24 hour secondary standards.

$$P_r(\underline{r}) = f_s(\underline{r}) \tag{14}$$

where $f_s(\underline{r})$ is the percentile that corresponds to $C(\underline{r}, f) = C_s$, a concentration threshold designated by one of the four air quality standards. By plotting $f_s(\underline{r})$ against $\underline{r}$, one can draw a risk probability map that shows a spatial distribution of risk probability.

Let us define another threshold function such that

$$\left.\begin{aligned} M(\underline{r}, f_s) &= 1 \qquad && \text{if } f_s(\underline{r}) \geq f^* \\ M(\underline{r}, f_s) &= 0 && \text{otherwise} \end{aligned}\right\} \tag{15}$$

where f* is a frequency threshold. Using this threshold function, one can compute the risk spectrum $R(f^*|C_s)$ and the population-at-risk spectrum $PR(f^*|C_s)$, defined as

$$R(f^*|C_s) = \int_{\underline{r}} M(\underline{r}, f_s)\, d\underline{r}/A_o \tag{16}$$

$$PR(f^*|C_s) = \int_{\underline{r}} M(\underline{r}, f_s)\, p(\underline{r})\, d\underline{r}/P_o \tag{17}$$

Equation (16) says that a fraction of the total area, $R(f^*|C_s)$ violates one of the air quality standards C_s more often than f*, or for a greater time than f*T where T is 8760 hours. Equation (17) says that a fraction of the total population, $PR(f^*|C_s)$ is exposed to air pollution exceeding C_s in 24 hour average concentrations more often than f*, or for a greater time than f*T.

IV. LONG-TERM POPULATION EXPOSURE

The analysis of long-term population exposure to air pollution is conducted by using the population data and the quarterly air quality data described in Section II. The geometric mean concentrations observed at each of the 164 air monitoring stations during the second quarter of 1971 (71/2) and 1973 (73/2) are listed in Table IV. Of the 164 stations, 72 stations reported statistically valid air quality data during the both quarters. These quarterly geometric mean concentrations were used for the analysis of seasonal exposure of the population whose compositions are presented in Tables II and III. Although there is no air quality standard for seasonal mean concentration, the same numerical values as the annual air quality standards (primary and secondary) were assumed as hypothetical air quality standards for quarterly geometric mean concentrations.

The air quality at each of the 215 standard network points was estimated from interpolations of the observed air qualities at the 72 valid air monitoring stations during 71/2 and 73/2 by using the interpolation formula, Equation (1). The resulting concentration isopleths are shown in Figures 5 and 6 for 71/2 and 73/2, respectively. A comparison of the two figures shows that the air quality for 73/2 was, in most parts of the Tri-State Region, much better than that for 71/2.

4.1 Air Quality Indices

The interpolated concentration at a standard network point is assumed to represent the average air quality over the area represented by ΔA_i whose value for each network point is presented in Table II. Under this assumption, the spatial average concentration AQ_s, population average concentration AQ_p, health index HI, and welfare index WI were computed for the total population using Equations (5-a), (6-a), (7-a) and (9-a), respectively (Fig. 7). Indices AQ_p, HI and WI can be used to differentiate air qualities to which individual sub-populations such as school-age, elderly, and non-white population of the study area are exposed. The sub-population data for the Tri-State Region are presented in Table III. The spatial average air quality AQ_s is constant among the sub-populations, but the population average air quality AQ_p reveals that the non-white and the elderly population are exposed to poorer air quality than the total population and the school-age population exposed.

Air quality improvement may be quantified better by the health index HI and the welfare index WI than by the average air qualities AQ_s and AQ_p. The health index indicates a percentage of the population exposed to air pollution exceeding the national primary air quality standard. Figure 7 shows that during the study period such percentages of the total population, the school-age population, the elderly population, and the non-white population all decreased, between 1971 and 1973, from 49% to 37%, 45% to 33%, 54% to 42%, and 69% to 54%, respectively. Knowing that the sizes of these four populations in the study area are, respectively, 17.0, 4.0, 1.8, and 2.7 million persons, the number of persons exposed to a below-standard air quality were reduced from 1971 to 1973 from 8.3 millions to 6.3 millions for the total population, from 1.8 millions to 1.3 millions for the school-age population, from 1.0 million to 0.8 million for the elderly population, and from 1.9 millions to 1.5 millions for the non-white population. A similar interpretation can be made for the welfare index.

4.2 Dosage and Population Dosage Spectrum

Using the threshold function $N(\underline{r}, D)$ defined by Equation (11), the interpolated air quality and the size of the population at each standard network point were stratified according to a level of air pollution dose D^*. Then, the dosage spectrum $S(D^*)$ and the population dosage spectrum $P(D^*)$ defined, respectively, by Equations (12) and (13) were computed by taking the sums, $\Sigma N(\underline{r}, D) \Delta A_i$ and $\Sigma N(\underline{r}, D) p_i \Delta A_i$, over the entire study area.

The dosage spectrum is plotted in Figure 8. It shows the fraction of the study area in which the TSP seasonal geometric mean concentration exceeds any stated dose level. From the figure we can see that in the second quarter of 1971 the primary air quality standard (annual mean 75 $\mu g/m^3$) level was exceeded in 15.5% of the area, while in the same quarter of 1973 it was exceeded in 10.3% of the area. Similarly, the secondary air quality standard (annual mean 60 $\mu g/m^3$) level was exceeded in 56.0% of the area in 71/2, but only in 29.4% of the area in 73/2. The air quality improvement was more pronounced in the higher dosage range. For instance, the percentage of area exposed to mean concentrations equal to or greater than 100 $\mu g/m^3$ was reduced from 5.7% in 71/2 to 0.5% in 73/2.

The population dosage spectrum for the total population is plotted in Figure 9. It shows the fraction of the total population exposed to air pollution exceeding any stated dose level. From the figure we can see that the number of persons exposed to air pollution exceeding any stated level was reduced substantially from 71/2 to 73/2. The air quality improvements over the higher concentration range are again emphasized in this figure. The percentage of population exposed to a mean concentration equal to or greater than 100 $\mu g/m^3$ dropped from 22.5% in 71/2 to 1.3% in 73/2. Knowing the total population of the study area, 17.0 millions, the population exposed to above 100 $\mu g/m^3$ mean concentrations dropped from 3.8 millions in 71/2 to 0.2 millions in 73/2. Similar interpretations can be made for other dose levels.

Distributions of the population dosage spectrum for sub-populations are plotted in Figures 10 and 11, which reveal that, in the Tri-State Region, the non-white population and elderly population were exposed to a dirtier air than the total population. The school-age population benefitted most by cleaner air. Population dosage spectra of 71/2 and 73/2 are plotted in Figures 10 and 11, respectively. A comparison of these figures shows that all four populations benefitted by air quality improvement from 71/2 to 73/2. In particular, the improvement for the non-white population was the greatest among the four populations. It should be noted that the non-white population which was highest of the four population groups exposed to air pollution exceeding 100 $\mu g/m^3$ in 71/2 dropped to the lowest among the four populations in 73/2.

V. SHORT-TERM POPULATION EXPOSURE

The adverse effects of particulate air pollution is caused not only by long-term exposure of persons or material to air pollution but also by short-term exposure to more severe pollution. The dose threshold above which there should be a noticable adverse effect from short-term exposure to particulate air pollution should be defined by the 24 hour air quality standards (primary and secondary standard). The percentile concentrations of 24 hour Hi-Vol measurements of total suspended particulate matter can be used to describe the short-term exposure of the population at each locale. In the present study, short-term exposure of the population to TSP air pollution is summarized by the risk probability which indicates the percentage of time exposure to air pollution exceeding any given level of concentration, and the population-at-risk spectrum which indicates the distribution of the population exposed to air pollution exceeding any given level for various percentages of time.

5.1 Risk Probability Mapping

The TSP concentrations observed at each air monitoring station were rank-ordered and tabulated in a percentile form as shown in Table V. At each percentile the concentrations observed at the 72 valid monitoring stations were interpolated to each of the 215 standard network points using the interpolation formula of Equation (1). In this way, percentile concentrations were computed for each of the 215 standard network points. Then, the risk probability defined by Equation (14) was determined at each network point from these interpolated percentile data.

Risk probabilities of total suspended particulate concentrations exceeding the level of the primary 24 hour air quality standard (260 $\mu g/m^3$) are plotted in Figure 12 for the air quality data of 71/2. It can be seen that people residing in some areas of Bergen, Hudson, New York, and Kings counties were exposed for about 5 to 10% of time to air pollution exceeding the level of the primary 24 hour air quality standard. People residing in the rest of the areas were not so exposed.

Similar risk probabilities in excess of the primary 24 hour air quality standard in 73/2 are plotted in Figure 13. A comparison of Figures

12 and 13 indicates that areas having a risk probability of greater than 5% were reduced substantially from 71/2 to 73/2. In 73/2, such areas were limited to only parts of Richmond and Hudson counties.

The risk probabilities of TSP daily concentrations exceeding the level of the secondary 24 hour air quality standard (150 $\mu g/m^3$) are plotted in Figures 14 and 15 for 71/2 and 73/2, respectively. The areas having a risk probability exceeding the secondary air quality standard for more than 5% of time were much more widespread than the corresponding areas for the primary air quality standard. The areas at such risk in 71/2 extended over most of New York City and a part each of Hudson, Passaic, Bergen, Rockland, Westchester, Nassau and Fairfield counties. In 73/2, the risk areas shrunk substantially from those of 71/2.

The risk probabilities of daily concentrations exceeding the level of 75 $\mu g/m^3$ are plotted in Figures 16 and 17 for 71/2 and 73/2, respectively. These risk probability maps are to be compared with the isopleth maps of annual geometric mean concentrations in 71/2 and 73/2 shown, respectively, in Figures 5 and 6. As seen from Figure 5, the areas exceeding 75 $\mu g/m^3$ in 24 hour average concentrations in 71/2 were limited to around New York City. However, Figure 16 shows that almost all the people in the Tri-State Region were exposed, for at least 25% of time, to TSP daily concentrations exceeding 75 $\mu g/m^3$. The greatly reduced risk probabilities in 73/2 as seen from Figure 17 reflect the air quality improvement from 71/2 to 73/2.

The risk probabilities of TSP daily concentrations exceeding the level of 60 $\mu g/m^3$ are mapped in Figures 18 and 19 for 71/2 and 73/2, respectively. The majority of the Tri-State Region experienced TSP concentrations in excess of 60 $\mu g/m^3$ at least 50% of time in 71/2, whereas in 73/2 the areas experienced such higl population exposure shrunk to about one third of the total area. However, in 73/2 the entire Tri-State Region still experienced concentrations in excess of 60 $\mu g/m^3$ at least 5% of time.

5.2 Population-At-Risk Spectrum

The risk probability $f_s(\underline{r})$ is numerically integrated with respect to an incremental area $d\underline{r}$ or ΔA, after which the integrals are stratified according to the frequency threshold f*. The results are summarized in the risk spectrum $R(f^*|C_s)$ defined by Equation (16) and in the population-at-risk spectrum $PR(f^*|C_s)$.

Figure 20 shows the risk spectrum distributions for 71/2 air quality data while Figure 21 is for 73/2 air quality data. The abcissa $R(f^*|C_s)$ indicates the fraction of the study area which experiences 24 hour average concentrations exceeding the concentration threshold C_s given by either the 24 hour primary standard, the 24 hour secondary standard, the annual primary standard, or the annual secondary standard. The ordinate f* indicates the percent of time during which exposure to 24 hour average concentrations exceeds the concentration threshold C_s given by one of these four standards. The graphic area below each curve quantifies the status of the ambient air quality under study as to the extent the ambient air quality as measured by the 24 hour average concentrations meets the air quality goal C_s designated by the 24 hour primary, the 24 hour secondary, the annual primary, or the annual secondary air quality standard.

It can be seen from Figures 20 and 21 that the higher the concentration threshold C_s, the lower the corresponding curve of the risk spectrum $R(f^*|C_s)$. This means that the higher the concentration threshold, the smaller the area and time in excess of the threshold. In these figures, the air quality improvement from 71/2 to 73/2 can be visualized by the smaller area below the curve of 73/2 as compared to that below the corresponding curve of 71/2.

The air quality improvement during this period is more pronounced in the risk spectrum curves for the annual standards (C_s = 75 and 60 $\mu g/m^3$) than in the curves for the 24 hour standards (C_s = 250 and 150 $\mu g/m^3$).

Let us define a regional risk index RI such that

$$RI(C_s) = \int_0^1 R(f^*|C_s)\ df^* \qquad (18)$$

As more fully described in Appendix B, the regional risk index indicates an average percentage of time at which a typical locale within the region is exposed to air pollution exceeding the air quality standard C_s. There are two extreme situations: "total compliance" corresponding to RI = 0, and "total violation" corresponding to RI = 1. RI = 0, which is given by the horizontal axis of Figures 20 and 21, indicates that the air quality of a given air-shed meets the air quality standard C_s everywhere all the time. On the other hand, RI = 1, which is given by a horizontal line through $R(f^*|C_s) = 1$ in the above figures, indicates that the air quality of the air-shed exceeds the standard everywhere all the time.

The regional risk index RI enables us to quantify the degree of excess of the standard over an entire air-shed or Air Quality Control Region (AQCR) based on percentile concentration statistics. The area below each curve of Figures 20 and 21, shows the improvement in short-term air quality from 71/2 to 73/2 to be RI = 0.025 to 0.025 (no change) for the 24 hour primary standard, RI = 0.042 to 0.044 (slight deteriolation) for the 24 hour secondary standard, RI = 0.328 to 0.192 for the annual primary standard, and RI = 0.492 to 0.379 for the annual secondary standard (Fig. 24).

The population-at-risk spectrum distribution is shown in Figures 22 and 23 for 71/2 and 73/2 air quality, respectively. The abscissa $PR(f^*|C_s)$ indicates the fraction of the population exposed to air pollution exceeding the concentration threshold C_s in daily average concentrations for a given percentage of time f*. The improvement in terms of population exposure during the period is more pronounced in the population-at-risk spectrum curves for the annual standards (C_s = 75 and 60 $\mu g/m^3$) than in the curves for the 24 hour standards (C_s = 250 and 150 $\mu g/m^3$).

Similar to the regional risk index RI, a population-at-risk index PRI is defined as

$$PRI = \int_0^1 PR(f^*|C_s)\ df^* \qquad (19)$$

As more fully described in Appendix B, the population-at-risk index indicates the average percentage of time during which an average (or typical) person in an air-shed or AQCR is exposed to air pollution exceeding the air quality standard C_s. Again PRI = 0 corresponds to "total compliance" and PRI = 1 to "total violation". The improvement in population exposure over an entire air-shed or AQCR can be quantified by PRI from the available percentile concentration statistics of air monitoring stations in the area.

The improvement in population exposure over the study area from 71/2 to 73/2 is quantified as PRI = 0.025 to 0.025 (no change) for the 24 hour primary standard, PRI = 0.073 to 0.053 for the 24 hour secondary standard, PRI = 0.466 to 0.292 for the annual primary standard, and PRI = 0.643 to 0.478 for the annual secondary standard (Fig. 24).

VI. ANNUAL POPULATION EXPOSURE

There was no good data base of annual geometric mean concentrations for conducting analysis of long-term exposure of the population to TSP air pollution in the Tri-State Region. Since the long-term air quality standards are given for annual geometric mean concentrations, the analysis of long-term population exposure made in Section IV based on the quarterly geometric mean concentrations may be misleading. Therefore, annual air quality data sets were created from

45 stations with complete data and 24 stations with missing data in one or two quarters during the entire year of 1971 and 1973. The quarterly geometric mean concentrations of these 69 stations are presented in Table VI. Each missing quarterly concentration in one year was replaced by that of the corresponding quarter of the other year.

The annual geometric mean concentration for each air monitoring station is computed as

$$\overline{C} = \exp \left[(\log C_1 + \log C_2 + \log C_3 + \log C_4) / 4 \right] \qquad (20)$$

where $\overline{C}$ is an annual geometric mean concentration and C_1, C_2, C_3, and C_4 are geometric mean concentrations of the 1st, 2nd, 3rd and 4th quarters, respectively. The resulting annual geometric mean concentrations of the 69 valid stations are presented in Table VII. The annual geometric mean concentration computed by Equation (20) is slightly different from the reported value, but the difference is in a order of 0.1 $\mu g/m^3$, when the mean concentration is in the range of 30 to 150 $\mu g/m^3$. The cause of such small differences is the assumption of equal sample size among the 4 quarters, when, in fact, the sample size varies from one quarter to another.

6.1 Trend in Air Quality Indices

The spatial location of each of the 69 valid monitoring stations is defined by their x-y coordinates in Table VII and is shown in Figure 25. The annual geometric mean concentrations at these stations were interpolated to each of the 215 standard network points shown in Figure 2 by using Equation (1). From the interpolated concentrations at the 215 network points, the annual concentration isopleth maps have been drawn as shown in Figures 26 and 27. It can be seen from these isopleth maps that in most places of the Tri-State Region air quality in 1973 was much better than that in 1971.

Using Equations (5-a), (6-a), (7-a) and (9-a), the four long-term air quality indices described earlier were computed for the annual air quality data. The spatial average concentration, AQ_s, population average concentration AQ_p, health index HI, and welfare index WI are all plotted in Figure 28 for the four different populations; total population, school-age population, elderly population, and non-white population.

All the indices show a substantial improvement of air quality from 1971 to 1973. The spatial average air quality AQ_s remains the same among the four populations, while the population average air quality AQ_p reveals that the non-white and elderly populations were exposed to dirtier air than that to which the total population and the school-age population were exposed.

Air quality improvement is conveniently measured by the health index HI and the welfare index WI. The health index tells the percentage of the population exposed to air pollution exceeding the annual primary standard, whereas the welfare index tells the percentage exposed to air pollution exceeding the annual secondary standard. Figure 28 shows that during the period from 1971 to 1973 the percentage of the population exposed to below primary standard air quality decreased from 49% to 32% for the total population, 44% to 27% for the school-age population, 54% to 38% for the elderly population, and 64% to 50% for the non-white population. Similarly, the percentage of the population exposed to below secondary standard air quality in 1971 and 1973 were, respectively, 82% and 56% for the total population, 80% and 51% for the school-age population, 83% and 61% for the elderly population, and 88% and 71% for the non-white population.

The sizes of the four populations within the study area (which is a little smaller than the Tri-State Region) are 17.0 millions for the total population, 4.0 millions for the school-age population, 1.8 millions for the elderly population, and 2.7 millions for the non-white population. Therefore, the number of people exposed to a below primary standard air quality decreased from 1971 to 1973 from 8.3 millions to 5.4 millions for the total population, 1.8 millions to 1.1 million for the school-age population, 1.0 million to 0.7 millions for the elderly population, and 1.7 millions to 1.4 million for the non-white population. Similarly, the number of people exposed to below secondary standard air quality decreased from 1971 to 1973 from 13.9 millions to 9.5 millions for the total population, 3.2 millions to 2.0 millions for the school-age population, 1.5 millions to 1.1 million for the elderly population, and 2.4 millions to 1.9 millions for the non-white population.

6.2 Changes in Dosage Spectra

The dosage spectrum is plotted in Figure 29. It shows the fraction of the area under study in which the TSP annual geometric mean concentration exceeds any stated dose level. It can be seen from the figure that in 1971 the primary standard (75 $\mu g/m^3$) was exceeded by 14.7% of the area, while in 1973 by 6.7% of the area. The secondary standard (60 $\mu g/m^3$) was exceeded by 67% of the area in 1971 and in 1973 only by 27% of the area. The air quality improvement during the same period is more pronounced in the higher dosage range. For instance, the percentage of the area polluted by at least an annual geometric mean of 90 $\mu g/m^3$ dropped from 5.5% in 1971 to a mere 0.2% in 1973.

The population dosage spectrum for the total population is plotted in Figure 30. It shows the fraction of the population exposed to air pollution exceeding any stated dosage level. It can be seen from the figure that the number of people exposed to air pollution exceeding any stated dose level dropped substantially from 1971 to 1973. The percentage of the total population exposed to below primary standard air quality decreased from 49% in 1971 to 35% in 1973. The percentage of the population exposed to below secondary standard air quality decreased from 82% to 56% during the same period. The improvements are again most pronounced in the higher exposure range. For instance, the percentage of the population exposed to an annual geometric mean concentration of at least 90 $\mu g/m^3$ dropped from 29% in 1971 to a mere 0.6% in 1973. This means that the number of people exposed to an annual geometric mean of at least 90 $\mu g/m^3$ dropped from 4.9 millions in 1971 to 102,000 in 1973.

Figures 31 and 32 show the distributions of population dosage spectra for various sub-populations. It can be seen from these figures that the school-age population benefitted more by being exposed to a cleaner air in 1973 than in 1971 than the other populations exposed. In both figures the population dosage spectrum of the non-white population behaved differently from those of the other populations. Although the non-white population is generally exposed to dirtier air than the other populations, the percentage of the non-white population exposed to the dirtiest air was less than for any other population. The air quality improvement, from 1971 to 1973 benefitted all the four populations by reduced exposure to air pollution.

VII. EMPIRICAL AIR MONITORING OPTIMIZATION

There have been many studies on selection of proper air monitoring sites and on the number of monitoring stations required for accurately monitoring air quality in a given area. In this section we explore an empirical method of updating an existing air monitoring network. In particular we seek a sub-network whose number of monitoring stations are smaller than the existing number, but whose monitoring performance is as good as that of the existing total network.

The 130 air monitoring stations that reported valid air quality data during the second and third quarters of 1973 were chosen as the test network.

The air quality data and spatial coordinates of these 130 stations are presented in Table VIII. The spatial locations of the individual stations are shown in Figure 3. The data set given by Table VIII was used for exploring empirical methods to improve the monitoring performance of an existing network. The concentration isopleth maps for the second and the third quarter of 1973 are shown in Figures 33 and 34, respectively.

7.1 Rank-Order of Monitoring Stations

If each monitoring station is rank-ordered according to the impact of its monitored concentration on the performance of the entire monitoring network, this should tell us of which stations can be removed from the existing network without significantly impairing network performance, or where additional stations should be located to improve the performance of the enlarged network to the maximum extent. The importance of each station is evaluated first, by the difference between its measured concentration and the concentration interpolated from the three nearest neighboring stations to that station site, second, by the sum of differences between the receptor concentrations interpolated by using all N stations and those by using (N-1) stations, and third, by the Jack Knife method (Appendix C).

The first scheme of rank-ordering monitoring stations is based on the error induced at the site of a station when that station is removed from the network. The error in concentration is measured by the difference between the concentration observed by the station and that interpolated from the three nearest neighboring stations to that station site. The maximum error among the ten stations at every ten rank interval is plotted in Figure 35. The error grows nearly linearly up to the 90-th rank and thereafter more rapidly. The 10 highest rank stations and the 10 lowest among the 130 monitoring stations are shown in Figure 36. The highest rank station may be said to be least important to the monitoring network because the concentration at that station can be estimated correctly from the readings at the neighboring stations. On the other hand, the lowest rank station may be said to be most important to the network because its concentration readings bring to the network information unavailable from any of the other monitoring stations.

The second scheme of rank-ordering monitoring stations is based on the sum of errors induced at the 215 standard network points when a station is removed from the monitoring network. The error at each network point is measured by the difference between the receptor concentration interpolated from all N monitoring stations and that from (N-1) stations. The maximum error among the ten stations at every ten rank interval is plotted in Figure 37. The sum of errors in receptor concentrations initially grows nearly linearly and thereafter grows exponentially. The 10 highest rank stations and the 10 lowest among the 130 monitoring stations are shown in Figure 38. The highest rank station may again be said to be least important to the monitoring network. However, the reasoning in Scheme II is different from that in Scheme I. Receptor concentrations around the highest rank station can be estimated correctly from the readings of neighboring monitoring stations. Thus, loss of that station would have the least impact on the performance of the monitoring network. On the other hand, loss of the lowest rank station would bring a significant deterioration in network performance because receptor concentrations around that station are estimated erroneously from the readings at the neighboring stations.

The third scheme of rank-ordering the monitoring stations is also based on the sum of errors induced at the 215 standard network points when a station is removed from the monitoring network. The third scheme is different from the second in that for the K-th rank station the error at each network point is measured by the difference between the receptor concentration interpolated from the (N-K+1) stations (N stations less the first (K-1) stations) and that from the (N-K) stations (N stations less the first K stations). The 10 highest rank stations among the 130 monitoring stations are shown in Figure 39.

Because the rank-ordering of monitoring stations according to Scheme III is quite computational, only the first 68 stations were rank-ordered. The sum of errors in receptor concentrations using Scheme III grows a little faster than the linear growth of Scheme II (Figures 37 and 40).

7.2 Performance of Sub-Networks

The entire 164 monitoring stations, of which 130 stations reported valid air quality data during the 2nd and 3rd quarters of 1973, were first divided into two classes, one with odd numbered stations and the other with even numbered stations. This division resulted in 68 valid monitoring stations for the one class and 62 valid monitoring stations for the other class. The resulting concentration isopleth maps from the sub-network with odd numbered stations and that from the one with even numbered stations are strikingly different from each other as seen from Figures 41 and 42.

Three half size sub-networks were formed by removing the 68 least important stations from the 130 station network according to Scheme I, Scheme II, and Scheme III, respectively. The performances of these sub-networks and those of the sub-networks with odd numbered and even numbered stations were then compared with that of the total network, by determining the space average air qualities AQ_s for the entire study area, each state and each county from the total network and from each of the five half size sub-networks. The results are shown in Figures 44 through 47. The meanings of the symbols used in Figure 44 and the following three figures are found from Figure 43. For each averaging area, there are two vertical bars indicating the second quarter values by the left bar and the third quarter values by the right bar. The distance between the longer horizontal bar and each symbol on a vertical bar indicates the relative error in the estimate of AQ_s by that particular sub-network.

It can be seen from Figure 44 that the performances of sub-networks with odd numbered and even numbered stations are poorer than those of sub-networks formed by Schemes I, II, and III. Among the sub-networks by the three schemes, the sub-network formed by Scheme III out-performs those by Scheme I and Scheme II. The space average air qualities estimated from the sub-network by Scheme III is close to that from the total network in every averaging area. This is in contrast to the fact that the values estimated from the other sub-networks deviate from the true values progresively as the averaging area becomes smaller. Figure 45 shows the performances of the five sub-networks in estimating population average air quality AQ_p. The performance of each sub-network is similar to that revealed in estimating AQ_s.

The health indices HI and the welfare indices WI estimated from the total network and from each of the five sub-networks are plotted in Figures 46 and 47, respectively. A comparison between these figures and the previous two figures indicates that the health index and the welfare index are more sensitive to monitoring network size than is space average air quality and population average air quality. The values estimated from the sub-networks with odd numbered and even numbered stations deviate wildly from the true values at the county level. In contrast to such wild mis-estimates by the odd and even number station sub-networks, the values estimated from the sub-network by Scheme III stay consistently close to the true values. The sub-network by Scheme II out-performed that by Scheme I in the estimates of AQ_s and AQ_p but under-performed it in the estimates of HI and WI.

Scheme III, the Jack-Knife Method, is useful to identify stations which contribute minimally among the existing stations and to form an optimal sub-network from the existing network. Further, the optimal half-size sub-network does estimate the four indices, AQ_s, AQ_p, HI, and WI down to each county level with an acceptable accuracy.

VIII. RESULTS AND DISCUSSION

A population exposure approach as contrasted to an air quality approach has been explored in order to report the state of ambient air quality more meaningfully for the population exposed to such air quality. Although the final products of this work turned out to be quite different from those initially anticipated, they appear to be useful for reporting air monitoring data in a more comprehensive manner than that currently used by control agencies.

Ways have been demonstrated for merging air quality data with demographic data to estimate the degree of exposure of a population and its components to air pollution. A methodology for quantifying population exposure using both mean concentration and percentile concentration statistics has been developed. Three indices for reporting long-term population exposure; population average air quality, a health index, and a welfare index have been proposed. New dosage spectrum and population dosage spectrum concepts have been proposed to describe long-term population exposure comprehensively but yet concisely.

A method for utilizing percentile concentration statistics for estimating short-term population exposure has been developed. A risk probability concept is proposed to describe spatial distribution of excess exposure of a population to air pollution. Risk spectrum and population-at-risk spectrum are proposed to describe short-term population exposure. A regional risk index and a population-at-risk index are developed to report the improvement or deterioration of short-term air quality over a large area.

An empirical approach to improving an existing air monitoring network has been explored. Rank-ordering of monitoring stations according to their impact on network performance has proven to be useful to identify those stations which contribute maximally and those which contribute minimally among the existing stations. A Jack-Knife method, based on receptor concentrations, appears to be useful for forming an optimal sub-network from an existing network.

REFERENCES

1. Zupan, J. M., "The Distribution of Air Quality in the New York Region," Resources for the Future, Inc., Washington, D. C., 1973.

2. "Computer Printouts of SAROAD Air Quality Data in the Tri-State Region," Private Communication with Neil Frank, USEPA, OAQPS, January 1975.

3. "Census Tracts," Bureaus of the Census, U. S. Dept. of Commerce, PHC(1)-30, 96, 145, 146, 149, 206, May 1972.

4. "Computer Printouts of Population Data in the Tri-State Region," Private Communication with personnel of the Tri-State Regional Commission, February 1975.

5. "Regional Profile - 1970 Population Traits," the Tri-State Regional Commission, Vol. II, No. 1, January 1973.

6. "Directory of Air Quality Monitoring Sites - Active in 1973," USEPA, OAQPS, EPA-450/2-75-006, March 1975.

7. Csanady, G. T., "The Dosage-Area Problems in Turbulent Diffusion," Atmospheric Environment, Vol. 1, pp. 451-459, 1967.

APPENDIX A Analysis of Interpolation Formulae

There are a number of numerical schemes to obtain a smooth continuous map from a set of discrete sampling points. One well known scheme is a (psuedo) linear interpolation formula as represented by the SYMAP computer algorithm.[1] More sophisticated is the g-spline method that is used for meteorological mapping.[2] This research explores algebraic interpolation formulae that do not contain a derivative term. The nearest three neighboring stations are used for all the interpolation schemes discussed herein.

The psuedo-linear interpolation formula can be written as:

$$\left.\begin{aligned} C &= \sum_{i=1}^{3} (C_i/r_i) \Big/ \sum_{i=1}^{3} (1/r_i) && \text{for } r_i \neq 0 \\ C &= C_i && \text{for } r_i = 0 \end{aligned}\right\} \qquad \text{(A1)}$$

where C_i is the air quality measured at an air monitoring station (x_i, y_i), and r_i is the distance between a receptor point (x_r, y_r) and the monitoring station. The three nearest monitoring stations to the receptor point are selected from many monitoring stations by computing the distances between the receptor and individual monitoring stations and by ordering them according to their distances to the receptor. This psuedo-linear formula only differs from a (true) linear interpolation formula when Equation (A1) is used to extrapolate the measured air qualities to a receptor outside of the triangle formed by the three monitoring stations. In the one dimensional case, summations are replaced by subtractions in Equation (A1) when distance r_i is greater than the distance between two monitoring stations, i.e. (the interdistance). It is expressed as

$$C = \left(\frac{s_1}{r_1} C_1 + \frac{s_2}{r_2} C_2 \right) \Bigg/ \left(\frac{s_1}{r_1} + \frac{s_2}{r_2} \right) \qquad \text{(A2)}$$

where $s_1 = \pm 1$ respectively for $r_1 \lesseqgtr \ell$, $s_2 = \pm 1$ respectively for $r_2 \lesseqgtr \ell$, and ℓ is the interdistance $\sqrt{(x_1 - x_2)^2 + (y_1 - y_2)^2}$. Referring to Figure A1, Equation (A2) may be generalized for two dimensional case as:

$$\left.\begin{array}{ll} C = \sum_{i=1}^{3} (s_i\ C_i/r_i) \ / \sum_{i=1}^{3} (s_i/r_i) & \text{for } r_i \neq 0 \\ C = C_i & \text{for } r_i = 0 \end{array}\right\} \quad \text{(A3)}$$

where $s_i = \pm 1$ respectively for $h_i \lessgtr \ell_i$ (Fig. A1). As seen from Figure A1, there are seven combinations of the signs of s_i, $i = 1, 2, 3$. For example, the signs in region II are $s_1 = -1$, $s_2 = +1$, and $s_3 = +1$ because $h_1 > \ell_1$, $h_2 < \ell_2$ and $h_3 < \ell_3$.

The straight line that goes through the points (x_2, y_2) and (x_3, y_3) in Figure A1 is given by:

$$a_1\ y + b_1\ x + c_1 = 0 \quad \text{(A4)}$$

where $a_1 = -(x_2 - x_3)$, $b_1 = y_2 - y_3$, and $c_1 = x2\ y3 - x3\ y_2$. The line parallel to the above through the receptor point (x_r, y_r) is given by

$$a_r\ y + b_r\ x + c_r = 0 \quad \text{(A5)}$$

where $a_r = a_1$, $b_r = b1$, and $c_r = (x_2 - x_3)\ y_r + (y_3 - y_2)\ x_r$. The heights ℓ_1 and h_1 are given by

$$\ell_1 = \frac{|a_1\ y_1 + b_1\ x_1 + c_1|}{\sqrt{a_1^2 + b_1^2}} \quad \text{(A6)}$$

and

$$h_1 = \frac{|a_1\ y_1 + b_1\ x_1 + c_r|}{\sqrt{a_1^2 + b_1^2}} \quad \text{(A7)}$$

The heights ℓ_2 and h_2, and ℓ_3 and h_3 can be computed by equations similar to Equations (A4) through (A7).

The performance of the (true) linear interpolation formulae [Eqn. (A2) or (A3)] is compared with that of the pseudo-linear interpolation formula [Eqn. (A1)] in Figures A2, A3 and A4. Figure A2 is the comparison of the one-dimensional case, while Figures A3 and A4 provide a comparison of the two-dimensional case. In the one-dimensional example $C_A = 80\ \mu g/m^3$ and $C_B = 20\ \mu g/m^3$ are placed 4 length units apart on the x-axis, while, in the two-dimensional example, $C_A = 85\ \mu g/m^3$, $C_B = 15\ \mu g/m^3$, and $C_C = 60\ \mu g/m^3$ are placed in the x-y plane at (5.0, 8.0), (2.0, 2.0), and (8.0, 2.0), respectively. It can be seen from Figures A2 and A3 that the (true) linear interpolation formula would either overestimate or underestimate receptor concentrations when applied to extrapolation. On the other hand, Figure A4 shows that the pseudo-linear interpolation formula does not retain the monitored concentrations C_A, C_B, and C_C in the interpolated concentration field except at those exact points A, B, and C. Thus, neither formula appears to be proper for interpolating air monitoring data to get a smooth concentration map.

Next, parabolic interpolation was examined. The pseudo-parabolic formula used is:

$$\left.\begin{array}{ll} C = \sum_{i=1}^{3} (C_i/r_i^2) \Big/ \sum_{i=1}^{3} (1/r_i^2) & \text{for } r_i \neq 0 \\ C = C_i & \text{for } r_i = 0 \end{array}\right\} \qquad \text{(A8)}$$

where C, C_i and r_i are the same as those for Equation (A1). The (true) parabolic formula used is:

$$C = \sum_{i=1}^{3} (s_i\, C_i/r_i^2) \Big/ \sum_{i=1}^{3} (s_i/r_i^2) \qquad \text{(A9)}$$

where the sign of s_i is determined in the same manner as for Equation (A3).

The performances of the (true) parabolic and pseudo-parabolic interpolation formulae are shown in Figure A5 for the one dimensional case. It can be seen from the figure that the concentrations interpolated by both formulae vary much more naturally around the monitored concentrations C_A and C_B than do those generated by the (true) linear and the pseudo-linear interpolation formulae (Fig. A2). The concentrations interpolated in two dimensional space are shown in Figures A6 and A7 for the (true) parabolic and the pseudo-parabolic interpolation formulae, respectively. Both interpolation formulae yield reasonable concentration isopleth maps. However, Figure A7 shows a better isopleth map than Figure A6 in the sense that the same numerical values as the monitored concentration values are distributed over the confined area around each monitoring station whereas this is not so in Figure A6. The concentrations interpolated by the pseudo-parabolic interpolation formula exhibit both a representative area around each monitoring station with numerical values the same as the monitored concentrations with smooth continuous concentration variation elsewhere. Thus, this is the formula used in this report as the "geographic interpolation formula".

From previous experience with air monitoring networks, it has been recognized that monitoring stations are more densely distributed in a high air pollution area than in a low pollution area and, thus, a monitoring station in a low pollution area covers air quality over a wider area than that in a high pollution area. As seen from Figures A2 and A5, both the linear and the parabolic interpolation formulae do not reflect this feature in their interpolated concentrations. Representation of area can be incorporated into the interpolated concentrations by introducing a weighting function into the interpolation formula. For example, a weighted psuedo-parabolic interpolation formula may be expressed as:

$$C = \sum_{i=1}^{3} (C_i/w_i\ r_i^2) \Big/ \sum_{i=1}^{3} (1/w_i\ r_i^2) \qquad \text{(A10)}$$

where w_i is a weight that is a function of the monitored concentration C_i.

The performances of various weighted psuedo-parabolic interpolation formulae are shown in Figure A8. The weighting functions $w_i = \ln C_i$, $w_i = C_i$, and $w_i = C_i^2$, $i = 1, 2, 3$, are used in the computations. It should be noted that the intersections between the line A-B and the curves of interpolated concentrations are progressively closer to point A as the weight w_i becomes a stronger function of monitored concentration, i.e. $w_i = \ln C_i$ to $w_i = C_i$ to $w_i = C_i^2$. These results should be compared with those of the unweighted interpolation formulae shown in Figure A5 in which the line A-B and the curves of interpolated concentrations intersected at the mid-point between points A and B. The representative areas inversely proportional to the relative magnitudes of monitored concentrations are reproduced in the two dimensional examples of the weighted interpolation formulae (Figures A9, A10 and A11). Although the representativeness of each monitored concentration is reconstructed reasonably well in these figures, a serious flaw is found in the results in that the higher polluted area A and C are now divided by a narrow strip of lower concentrations. This is obviously an artifact caused by the weighted interpolation formulae, and is contradicted by our common interpretation of monitored concentrations. Because this drawback outweighs its merit of area representation of each monitoring station, weighted interpolation formulae were not employed in this study.

APPENDIX B Regional Risk and Population-at-Risk Indices

$\{1 - R(f^*|C_s)\}$ and $\{1 - PR(f^*|C_s)\}$ are cumulative distribution functions of the random variable f_s, i.e., $P(f_s \le f^*)$ where f^* is a particular frequency threshold. Let us use the common notation for random variables.[3]

X	random variable, corresponding to f_s
x	particular value of X, corresponding to f^*
f(x)	probability density function, i.e., $f(x) = P(X = x)$
F(x)	cumulative distribution function, i.e., $F(x) = P(X \le x)$, corresponding to $\{1 - R(f^*|C_s)\}$ or $\{1 - PR(f^*|C_s)\}$.

As x varies in the range 0 to 1, the well-known statistical relations can be written as

$$F(x) = \int_0^x f(x)\, dx \quad \text{or} \quad f(x) = \frac{d}{dx} F(x) \tag{B1}$$

$$E(X) = \int_0^1 xf(x)\, dx = \int_0^1 x dF(x) \tag{B2}$$

where E(X) is the mean of a random variable X.

Using the above notations, the regional risk index RI or the population-at-risk index PRI can be written as

$$\begin{aligned} \text{RI or PRI} &= \int_0^1 \{1 - F(x)\}\, dx \\ &= 1 - \int_0^1 F(x)\, dx \end{aligned} \tag{B3}$$

Using the "integration by part" method, we can transform

$$\begin{aligned} \int_0^1 F(x)\, dx &= F(x)\, x\Big|_0^1 - \int_0^1 \frac{dF(x)}{dx} x dx \\ &= F(1)\cdot 1 - \int_0^1 x dF(x) \\ &= 1 - E(X) \end{aligned} \tag{B4}$$

Substitution of Equation (B4) into (B3) yields

$$RI \text{ or } PRI = E(X) \qquad (B5)$$

Therefore, we can interpret RI or PRI as the mean percentage of time at which a typical locale within the region or an average person in the population is exposed to air pollution exceeding the air quality standard C_s.

APPENDIX C Mathematical Formulation of Schemes I, II and III

Rank-ordering of monitoring stations according to the impact of their monitored concentrations on the performance of the air monitoring network was conducted by introducing the following performance index[4] appropriate for each of the three schemes.

Scheme I

The first scheme of rank-ordering monitoring stations is based on the magnitude of errors induced at the station location when that station is removed from the monitoring network. The performance index, P, for the first scheme may be written as

$$P_i = [|C_{1i} - D_{1i}^{(i)}| + |C_{2i} - D_{2i}^{(i)}|]/2 \qquad (C1)$$

where P_i is the value of P for the i-th station, C_{1i} and C_{2i} are the concentrations observed at the i-th station in the second and the third quarter of 1973, respectively, and $D_{1i}^{(i)}$ and $D_{2i}^{(i)}$ are the concentrations interpolated to the station location from the three nearest neighboring stations to that station in the two quarters, respectively.

The first rank station is the one having the smallest P_i among {P}, the collection of P_i. The second rank station is the one having the second smallest P_i, and so forth. In general, the K-th rank station is given by

$$S_K = \text{K-th} \min_i \{P\} \qquad K = 1, 2, \ldots, N \qquad (C2)$$

where N is the total number of monitoring stations in the network. The rank-order of each station, the second quarter error, the third quarter error, and the value of its performance index are all listed in Table C1.

Scheme II

The second scheme of rank-ordering the stations is based on the sum of errors induced at all the receptor points when a station is removed from the monitoring network. The performance index for the second scheme may be written as

$$P_i = \sum_j [|D_{1j} - D_{1j}^{(i)}| + |D_{2j} - D_{2j}^{(i)}|]/2 \qquad (C3)$$

where D_{1j} and D_{2j} are the second and third quarter concentrations interpolated to the point from the three nearest neighboring stations to the j-th receptor point, and $D_{1j}^{(i)}$ and $D_{2j}^{(i)}$ are also the second and third quarter concentrations interpolated to that point. The three nearest stations to compute D_{1j} and D_{2j} are selected among the entire N stations, whereas the three stations to compute $D_{1j}^{(i)}$ and $D_{2j}^{(i)}$ are selected among the (N-1) stations, i.e., N stations less the i-th station.

The K-th rank station is given by

$$S_K = \text{K-}\underset{i}{\text{th}} \min \{P\} \qquad K = 1, 2, \ldots, N \qquad (C4)$$

where {P} is the collection of P_i whose value is computed by Equation (C3). Table C2 lists the rank-ordered stations, and the mean error in concentration induced at the effected receptor points, which are defined by a receptor having an induced error greater than or equal to 0.01 $\mu g/m^3$.

Scheme III

As the second scheme, the third scheme is also based on the sum of errors induced at all the receptor points when a station is removed from the network. While in the second scheme the same performance index is used to rank-order the stations, the third scheme uses a different performance index for each rank station. The performance index to find the first rank station is written as

$$P_i^I = \sum_j [|D_{1j} - D_{1j}^{(i)}| + |D_{2j} - D_{2j}^{(i)}|]/2 \qquad (C5)$$

and the first rank station is given by

$$S_I = \min_i \{P^I\} \tag{C6}$$

Equations (C5) and (C6) are essentially the same as Equations (C3) and (C4) used for the second scheme. However, the difference between the second and the third scheme appears in the following rank-ordering process.

The performance index to find the second rank station is written as

$$P_i^{II} = \sum_j [|D_{1j}^{(I)} - D_{1j}^{(I,i)}| + |D_{2j}^{(I)} - D_{2j}^{(I,i)}|]/2 \tag{C7}$$

and the second rank station is given by

$$S_{II} = \min_i \{P^{II}\} \tag{C8}$$

where $D_{1j}^{(I)}$ and $D_{2j}^{(I)}$ are the concentrations interpolated from the three nearest stations among the (N-1) stations, i.e., N stations less the first rank station, and $D_{1j}^{(I,i)}$ and $D_{2j}^{(I,i)}$ are the concentrations interpolated from the three nearest stations among the (N-2) stations, i.e., N stations less the first rank station and the i-th station.

In general, the K-th rank station is given by

$$P_i^K = \sum_j [|D_{1j}^{(I,II,...,K-1)} - D_{1j}^{(I,II,...,K-1,i)}| + |D_{2j}^{(I,II,...,K-1)} - D_{2j}^{(I,II,...,K-1,i)}|]/2 \tag{C9}$$

$$S_K = \min_i \{P^K\} \qquad K = 1, 2, . . . , N-3 \tag{C10}$$

where $D_{1j}^{(I,II,...,K-1)}$ and $D_{2j}^{(I,II,...,K-1)}$ are the concentrations interpolated from the three nearest stations among the (N-[K-1]) stations, i.e., N stations less the first (K-1) stations, and $D_{1j}^{(I,II,...,K-1,i)}$ and $D_{2j}^{(I,II,...,K-1,i)}$ are the concentrations interpolated from the three nearest stations among the (N-K) stations, i.e., N stations less the first (K-1) stations and the i-th station.

The rank-order of monitoring stations by Scheme III can proceed only to K = N-3 while those by Schemes I and II can complete the entire N stations. Table C3 lists the first 68 stations and the effected receptors, mean error and performance index associated with each of the 68 stations.

Network subsets were formed by removing the first 25, 43, and 68 stations among the rank-ordered stations by Schemes I, II, and III from the 130 station network. The performance of these network subsets was measured by the mean error in concentration induced at the effected receptor points, and the number of the effected receptors. The results are plotted in Figure C1. The network subsets formed by Scheme I causes a greater number of effected receptors and a greater mean error than those by Schemes II and III. The network subsets formed by Scheme II causes a lesser number of effected receptors than those by Scheme III but causes a greater mean error than those by Scheme III. As a result, the sum of errors induced at all the receptor points is greater for the network subsets formed by Scheme II than those by Scheme III. Therefore, Scheme III can be said to be the best to form a network subset among the three schemes.

REFERENCES TO APPENDICES

1. Harvard Laboratory for Computer Graphics, "User's Reference Manual for Synagraphic Computer Mapping 'SYMAP' Version V". Harvard University, Cambridge, Massachusetts, 1968.

2. M. J. Munteanu and L. L. Schumaker, "On a Method of Carasso and Laurent for Constructing Interpolating Splines", Mathematics of Computation, Vol. 27, No. 122, April 1973.

3. E. Parzen, "Stochastic Processes", Chapter 1, Holden Day, San Francisco, California, 1967.

4. W. P. Darby, P. J. Ossenbruggen and C. J. Gregory, "Optimization of Urban Air Monitoring Networks", Journal of the Environmental Engineering Division, ASCE, Vol. 100, No. EE3, PP577-591, June 1974.

TABLE I Code representing county and state

Code	County	State
11	Fairfield	Connecticut
21	Westchester	New York
22	Rockland	New York
23	Bronx	New York
24	New York	New York
25	Queens	New York
26	Kings	New York
27	Richmond	New York
28	Nassau	New York
29	Suffolk	New York
31	Bergen	New Jersey
32	Hudson	New Jersey
33	Essex	New Jersey
34	Union	New Jersey
35	Passaic	New Jersey
36	Morris	New Jersey
37	Somerset	New Jersey
38	Middlesex	New Jersey
39	Monmouth	New Jersey

TABLE II Population data of the Tri-State Region (population density in persons/Km^2)

No.	Code	Tract	X-Coord.	Y-Coord.	Area Wt.	Population Density
1	11	New Fairfield	105.0	145.0	152.7	107.1
2	11	Danbury	105.0	135.0	113.5	4,454.5
3	11	Newtown	115.0	135.0	103.2	116.7
4	11	Newtown	125.0	135.0	68.1	116.7
5	11	Ridgefield	105.0	125.0	101.1	200.5
6	11	Redding	115.0	125.0	103.2	70.8
7	11	Shelton	125.0	125.0	125.9	367.1
8	11	Stratford	137.5	117.5	37.2	989.6
9	11	Bridgeport	122.5	117.5	25.8	4,152.3
10	11	Fairfield	117.5	117.5	25.8	750.2
11	11	Fairfield	112.5	117.5	25.8	750.2
12	11	Weston	107.5	117.5	25.8	145.7
13	11	Wilton	102.5	117.5	18.6	198.1
14	11	New Canaan	97.5	112.5	39.2	315.6
15	11	Wilton	102.5	112.5	25.8	198.1
16	11	Westport	107.5	112.5	25.8	573.5
17	11	Fairfield	112.5	112.5	25.8	750.2
18	11	Fairfield	117.5	112.5	21.7	750.2
19	11	Bridgeport	122.5	112.5	17.5	4,152.3
20	11	Greenwich	87.5	107.5	18.6	476.5
21	11	Greenwich	92.5	107.5	25.8	476.5
22	11	Stamford	97.5	107.5	25.8	1,079.3

TABLE II (continued) Population data of the Tri-State Region (population density in persons/Km^2)

No.	Code	Tract	X-Coord.	Y-Coord.	Area Wt.	Population Density
23	11	Darien	102.5	107.5	25.8	602.1
24	11	Norwalk	107.5	107.5	24.8	1,428.0
25	11	Greenwich	92.5	102.5	40.2	476.5
26	11	Stamford	97.5	102.5	25.8	1,079.3
27	11	Darien	102.5	102.5	15.5	602.1
28	21	Cortland	75.0	125.0	123.3	328.0
29	21	Yorktown	85.0	125.0	114.6	294.8
30	21	Somers	95.0	125.0	127.6	124.3
31	21	Ossining	75.0	115.0	75.7	1,065.8
32	21	New Castle	85.0	115.0	97.1	310.4
33	21	Bedford	95.0	115.0	61.2	191.2
34	21	Tarrytown	76.5	107.5	34.0	1,345.8
35	21	Mt. Pleasant	82.5	107.5	31.1	553.3
36	21	Irvington	76.5	102.5	34.0	778.0
37	21	White Plains	82.5	102.5	24.3	2,039.0
38	21	Harrison	86.5	102.5	14.6	742.5
39	21	Hastings	73.5	97.5	12.6	1,746.4
40	21	Greenburgh	77.5	97.5	24.3	1,147.1
41	21	Scarsdale	82.5	97.5	24.3	954.0
42	21	Rye	87.5	97.5	24.3	1,064.4
43	21	Yonkers	73.0	92.5	19.4	4,468.0
44	21	Eastchester	77.5	92.5	24.3	3,006.0

TABLE II (continued) Population data of the Tri-State Region (population density in persons/Km^2)

No.	Code	Tract	X-Coord.	Y-Coord.	Area Wt.	Population Density
45	21	Mamaroneck	82.5	92.5	28.2	1,545.2
46	21	New Rochelle	79.0	88.5	14.6	2,781.2
47	23	Bronx	75.0	87.0	35.7	13,857.8
48	23	Bronx	72.5	82.5	29.4	13,857.8
49	23	Bronx	77.5	82.5	18.9	13,857.8
50	24	Manhattan	67.5	77.5	15.1	25,826.1
51	24	Manhattan	65.0	73.5	9.8	25,826.1
52	24	Manhattan	63.5	70.0	10.6	25,826.1
53	24	Manhattan	69.0	83.0	12.1	25,826.1
54	25	Queens	71.5	76.0	12.4	7,102.2
55	25	Queens	72.5	72.5	33.8	7,102.2
56	25	Queens	77.5	72.5	28.1	7,102.2
57	25	Queens	68.5	76.5	21.4	7,102.2
58	25	Queens	83.0	72.5	31.5	7,102.2
59	25	Queens	82.0	66.5	34.9	7,102.2
60	25	Queens	77.0	68.0	39.4	7,102.2
61	26	Kings	72.0	66.5	16.2	14,352.0
62	26	Kings	67.0	68.0	41.0	14,352.0
63	26	Kings	63.5	62.5	18.3	14,352.0
64	26	Kings	67.5	62.5	27.0	14,352.0
65	26	Kings	72.0	63.0	17.2	14,352.0
66	26	Kings	67.0	59.0	23.7	14,352.0

TABLE II (continued) Population data of the Tri-State Region (population density in persons/Km^2)

No.	Code	Tract	X-Coord.	Y-Coord.	Area Wt.	Population Density
67	27	Richmond	57.0	62.5	22.7	1,967.0
68	27	Richmond	52.0	62.0	24.9	1,967.0
69	27	Richmond	52.0	57.5	34.6	1,967.0
70	27	Richmond	57.0	58.0	16.2	1,967.0
71	27	Richmond	48.0	52.5	20.5	1,967.0
72	28	Port Washington	87.0	83.0	30.3	1,573.7
73	28	Old Brookville	92.5	82.5	27.1	272.3
74	28	Muttontown	97.5	82.5	27.1	131.9
75	28	Mill Neck	95.0	87.0	36.8	131.6
76	28	Oyster Bay	102.5	82.5	29.2	532.3
77	28	Plainview	102.5	77.5	28.2	2,273.9
78	28	Jericho	97.5	77.5	27.1	1,339.2
79	28	Old Westbury	92.5	77.5	27.1	129.1
80	28	Manhasset	87.0	77.5	39.0	1,341.7
81	28	Garden City	88.0	72.5	23.8	2,006.1
82	28	Hempstead	92.5	72.5	27.1	2,278.6
83	28	Levittown	97.5	72.5	27.1	3,704.5
84	28	Old Bethpage	103.0	72.5	32.5	695.5
85	28	Franklin Square	87.0	67.5	32.5	4,412.7
86	28	Roosevelt	92.5	67.5	27.1	3,324.3
87	28	North Bellmore	97.5	67.5	27.1	3,308.9
88	28	Wantagh	99.0	64.0	21.7	2,239.6

TABLE II (continued) Population data of the Tri-State Region (population density in persons/Km^2)

No.	Code	Tract	X-Coord.	Y-Coord.	Area Wt.	Population Density
89	28	Massapequa	102.5	67.5	26.0	2,675.1
90	28	Oceanside	87.0	63.0	33.6	2,756.5
91	28	Freeport	92.5	63.0	23.8	3,762.8
92	29	Lloyd Harbor	106.0	87.0	42.7	134.3
93	29	Huntington Station	107.5	82.5	24.5	2,062.6
94	29	Half Hollow Hills	107.5	77.5	21.8	522.6
95	29	Babylon	108.0	72.5	18.2	553.7
96	29	Copiague	108.0	67.0	21.8	2,386.8
97	29	East Northport	115.0	85.0	89.0	1,847.0
98	29	Isliptown	115.0	73.5	121.7	1,053.7
99	29	Smithtown	125.0	85.0	95.3	982.2
100	29	Isliptown	125.0	75.0	95.3	1,053.7
101	29	Selden	135.0	85.0	90.8	786.0
102	29	East Patchogue	135.0	75.0	77.2	826.4
103	29	Brookhaven	145.0	85.0	90.8	465.6
104	29	Brookhaven	145.0	77.0	64.5	465.6
105	22	Stony Point	64.0	122.0	66.1	190.1
106	22	Ramapotown	56.0	113.0	71.6	591.6
107	22	Clarkstown	65.0	115.0	90.6	628.0
108	22	Congers	72.0	113.0	19.9	629.1

TABLE II (continued) Population data of the Tri-State Region (population density in persons/Km^2)

No.	Code	Tract	X-Coord.	Y-Coord.	Area Wt.	Population Density
109	22	Ramapotown	62.0	108.0	35.3	591.6
110	22	West Nyack	67.5	107.5	22.6	449.3
111	22	Upper Nyack	71.5	107.5	13.6	635.3
112	22	Pearl River	67.0	103.0	23.6	1,043.3
113	22	Orangetown	71.5	102.0	18.1	898.5
114	31	Ramsey	52.0	105.0	122.1	891.8
115	31	Montvale	62.0	102.0	23.3	1,659.3
116	31	Wyckoff	55.0	97.5	50.4	976.0
117	31	Westwood	62.5	97.5	24.2	302.2
118	31	Norwood	68.5	97.5	31.0	649.8
119	31	Fair Lawn	56.5	92.5	28.1	2,904.4
120	31	New Milford	62.5	92.5	24.2	3,567.7
121	31	Tenafly	67.5	93.0	31.0	1,286.5
122	31	Lodi	67.5	87.5	22.3	4,192.4
123	31	Teaneck	72.5	87.5	24.2	3,001.0
124	31	Englewood Cliffs	77.5	87.5	24.2	1,189.5
125	31	Rutherford	58.0	82.5	20.3	3,006.7
126	31	Carlstadt	62.5	82.5	22.3	756.0
127	31	Ridgefield	66.0	82.5	13.6	1,717.6
128	31	Lyndhurst	57.0	78.0	17.4	1,999.7
129	32	North Bergen	62.5	77.5	30.9	3,503.9
130	32	Jersey City	58.0	72.5	19.9	7,118.1

TABLE II (continued) Population data of the Tri-State Region (population density in persons/Km^2)

No.	Code	Tract	X-Coord.	Y-Coord.	Area Wt.	Population Density
131	32	Jersey City	61.5	72.5	14.0	7,118.1
132	32	Bayonne	57.0	68.0	15.0	5,650.8
133	32	Kearny	55.0	75.0	16.9	1,688.2
134	35	West Milford	35.0	110.0	116.4	83.8
135	35	Ringwood	44.0	110.0	83.4	137.4
136	35	West Milford	37.0	103.0	29.1	83.8
137	35	Bloomingdale	43.0	102.0	27.2	322.5
138	35	Wayne	47.0	95.0	53.3	771.0
139	35	Hawthorne	52.0	93.5	27.2	2,427.4
140	35	West Paterson	49.0	88.0	21.3	1,367.2
141	35	Cliffton	53.5	86.0	35.9	3,081.4
142	33	Fairfield	43.0	37.0	23.7	252.3
143	33	Roseland	42.5	82.5	25.8	523.8
144	33	Montclair	47.5	83.0	35.5	2,999.6
145	33	Nutley	52.0	81.0	15.1	4,379.7
146	33	Livingston	42.0	77.5	39.8	888.1
147	33	West Orange	47.5	77.5	26.9	1,492.0
148	33	Newark	51.5	77.5	19.4	6,708.2
149	33	Millburn	42.0	78.5	23.7	893.2
150	33	Newark	47.5	78.0	25.8	6,708.2
151	33	Newark	52.0	72.0	31.2	6,708.2
152	36	Rockaway	25.0	95.0	167.7	172.2

TABLE II (continued) Population data of the Tri-State Region (population density in persons/Km^2)

No.	Code	Tract	X-Coord.	Y-Coord.	Area Wt.	Population Density
153	36	Kinnelon	35.0	95.0	121.4	155.6
154	36	Roxbury	15.0	85.0	106.0	294.6
155	36	Lincoln Park	42.0	95.0	39.1	512.6
156	36	Randolph	25.0	85.0	102.9	254.3
157	36	Hanover	35.0	85.0	105.0	420.6
158	36	Chester	15.0	77.0	63.8	73.8
159	36	Mendham	27.0	75.0	95.7	130.2
160	36	Chatham	33.5	75.0	73.1	589.2
161	37	Bedminster	15.5	65.0	91.2	40.7
162	37	Warren	23.0	64.0	99.4	185.8
163	37	Hillsborough	15.0	54.0	117.9	87.2
164	37	Franklin	23.0	55.0	71.7	268.2
165	37	Montgomery	17.0	46.0	166.0	79.8
166	34	Summit	39.0	71.0	27.1	1,629.1
167	34	Berkley Heights	36.0	68.0	40.7	851.3
168	34	Cranford	42.5	67.5	26.1	2,411.6
169	34	Elizabeth	47.5	67.5	32.3	4,048.7
170	34	Plainfield	33.0	62.0	13.6	3,234.0
171	34	Scotch Plains	37.5	63.0	21.9	999.6
172	34	Clark	42.5	62.5	26.1	1,680.1
173	34	Linden	47.5	62.5	24.0	1,536.3
174	38	Piscataway	28.0	56.0	30.2	765.9

TABLE II (continued) Population data of the Tri-State Region (population density in persons/Km^2)

No.	Code	Tract	X-Coord.	Y-Coord.	Area Wt.	Population Density
175	38	South Plainfield	32.5	57.5	25.1	1,015.7
176	38	Metuchen	37.5	57.5	29.2	2,551.9
177	38	Woodbridge	42.5	57.5	25.1	1,707.3
178	38	Carteret	47.0	57.5	18.1	2,110.2
179	38	New Brunswick	32.5	52.5	25.1	2,920.9
180	38	Edison	37.5	52.5	25.1	915.7
181	38	Perth Amboy	43.0	52.5	28.2	3,230.2
182	38	North Brunswick	31.0	46.0	41.2	575.3
183	38	South River	37.5	47.5	25.1	2,291.0
184	38	Madison	42.0	47.5	23.1	518.2
185	38	South Brunswick	25.0	40.0	106.6	141.6
186	38	East Brunswick	32.5	40.0	50.3	644.0
187	38	Old Bridge	37.5	40.0	50.3	1,631.0
188	38	Madison	42.0	42.0	36.2	518.2
189	38	Plainsboro	27.0	33.0	58.3	57.0
190	38	Monroe	33.0	32.0	43.3	91.0
191	39	Matawan	47.5	42.5	23.9	914.6
192	39	Hazlet	52.5	42.5	28.9	1,523.2
193	39	Middletown	57.5	42.0	19.9	596.6
194	39	Marlboro	44.0	34.0	106.7	171.7
195	39	Colts Neck	55.0	35.0	99.7	74.0
196	39	Rumson	63.0	38.0	39.9	564.7

TABLE II (continued) Population data of the Tri-State Region (population density in persons/Km^2)

No.	Code	Tract	X-Coord.	Y-Coord.	Area Wt.	Population Density
197	39	Oceanport	63.0	32.5	29.9	888.4
198	39	Ocean	62.5	27.5	22.9	831.8
199	39	Spring Lake	61.5	21.0	33.9	1,071.7
200	39	New Shrewsbury	55.0	25.0	99.7	148.4
201	39	Howell	45.0	25.0	99.7	139.6
202	39	Freehold	35.0	24.0	111.7	102.4
203	39	Millstone	25.0	18.0	118.6	27.7
204	39	Howell	47.0	18.0	53.8	139.6
205	39	Wall	55.0	17.0	79.8	217.4
206	37	Bernardsville	18.5	71.5	84.0	207.4
207	36	Chester	7.5	82.0	85.4	73.8
208	39	Sea Bright	64.0	46.0	8.0	153.9
209	25	Queens	75.0	56.5	20.3	7,102.2
210	28	Long Beach	88.0	57.5	5.4	5,723.6
211	28	Oyster Bay	105.0	59.5	14.1	1,395.9
212	29	Islip	120.0	61.5	10.9	1,053.7
213	29	Brookhaven	132.0	64.5	16.3	465.6
214	29	Brookhaven	135.0	92.0	36.3	465.6
215	29	Brookhaven	145.0	92.0	36.3	465.6

TABLE III Sub-population data of the Tri-State Region (population density in persons/Km^2, sub-population in % of population density)

No.	Code	Tract	Population Density	School-Age	Elderly	Non-White
1	11	New Fairfield	107.1	27.0	9.0	1.5
2	11	Danbury	4,454.5	25.0	9.5	8.0
3	11	Newtown	116.7	29.0	11.0	1.0
4	11	Newtown	116.7	27.0	8.0	1.5
5	11	Ridgefield	200.5	31.0	6.5	1.5
6	11	Redding	70.8	29.0	9.0	1.5
7	11	Shelton	367.1	31.0	8.0	1.5
8	11	Stratford	989.6	27.0	9.5	0.8
9	11	Bridgeport	4,152.3	29.0	10.5	1.0
10	11	Fairfield	750.2	29.0	8.0	1.0
11	11	Fairfield	750.2	31.0	7.5	1.0
12	11	Weston	145.7	31.0	6.5	1.0
13	11	Wilton	198.1	31.0	8.0	1.0
14	11	New Canaan	315.6	25.0	9.0	7.0
15	11	Wilton	198.1	31.0	8.0	3.5
16	11	Westport	573.5	29.0	8.0	5.0
17	11	Fairfield	750.2	27.0	8.0	1.0
18	11	Fairfield	750.2	22.0	11.0	10.5
19	11	Bridgeport	4,152.3	25.0	9.5	7.0
20	11	Greenwich	476.5	25.0	11.5	3.5
21	11	Greenwich	476.5	25.0	10.0	9.0
22	11	Stamford	1,079.3	25.0	8.0	10.0

TABLE III (continued) Sub-population data of the Tri-State Region (population density in persons/Km^2, sub-population in % of population density)

No.	Code	Tract	Population Density	School-Age	Elderly	Non-White
23	11	Darien	602.1	27.0	8.0	11.0
24	11	Norwalk	1,428.0	25.0	8.0	2.0
25	11	Greenwich	476.5	25.0	11.0	4.0
26	11	Stamford	1,079.3	25.0	10.0	11.0
27	11	Darien	602.1	27.0	7.0	5.0
28	21	Cortland	328.0	26.0	11.0	9.0
29	21	Yorktown	294.8	31.0	7.0	1.5
30	21	Somers	124.3	30.0	10.5	2.0
31	21	Ossining	1,065.8	26.0	11.0	4.0
32	21	New Castle	310.4	30.0	9.0	7.0
33	21	Bedford	191.2	31.0	7.0	1.7
34	21	Tarrytown	1,345.8	27.0	9.5	7.0
35	21	Mt. Pleasant	553.3	28.0	8.5	3.5
36	21	Irvington	778.0	25.0	8.0	12.0
37	21	White Plains	2,039.0	25.0	12.0	10.0
38	21	Harrison	742.5	25.0	8.0	5.0
39	21	Hastings on Hudson	1,746.4	25.0	8.0	10.0
40	21	Greenburgh	1,147.1	27.0	9.0	4.5
41	21	Scarsdale	954.0	25.0	12.0	2.0
42	21	Rye	1,064.4	27.0	9.5	4.5
43	21	Yonkers	4,468.0	22.0	11.0	7.0
44	21	Eastchester	3,006.0	24.0	11.5	9.0

TABLE III (continued) Sub-population data of the Tri-State Region (population density in persons/Km^2, sub-population in % of population density)

No.	Code	Tract	Population Density	School-Age	Elderly	Non-White
45	21	Mamaroneck	1,545.2	27.0	11.0	6.0
46	21	New Rochelle	2,781.2	24.0	12.5	11.0
47	23	Bronx	13,857.8	22.5	11.6	26.6
48	23	Bronx	13,857.8	22.5	11.6	26.6
49	23	Bronx	13,857.8	22.5	11.6	26.6
50	24	Manhattan	25,826.1	15.6	14.0	29.2
51	24	Manhattan	25,826.1	15.6	14.0	29.2
52	24	Manhattan	25,826.1	15.6	14.0	29.2
53	24	Manhattan	25,826.1	15.6	14.0	29.2
54	25	Queens	7,102.2	19.2	12.4	14.7
55	25	Queens	7,102.2	19.2	12.4	14.7
56	25	Queens	7,102.2	19.2	12.4	14.7
57	25	Queens	7,102.2	19.2	12.4	14.7
58	25	Queens	7,102.2	19.2	12.4	14.7
59	25	Queens	7,102.2	19.2	12.4	14.7
60	25	Queens	7,102.2	19.2	12.4	14.7
61	26	Kings	14,352.0	22.7	11.1	26.8
62	26	Kings	14,352.0	22.7	11.1	26.8
63	26	Kings	14,352.0	22.7	11.1	26.8
64	26	Kings	14,352.0	22.7	11.1	26.8
65	26	Kings	14,352.0	22.7	11.1	26.8
66	26	Kings	14,352.0	22.7	11.1	26.8

TABLE III (continued) Sub-population data of the Tri-State Region (population density in persons/Km^2, sub-population in % of population density)

No.	Code	Tract	Population Density	School-Age	Elderly	Non-White
67	27	Richmond	1,967.0	25.4	8.7	6.0
68	27	Richmond	1,967.0	25.4	8.7	6.0
69	27	Richmond	1,967.0	25.4	8.7	6.0
70	27	Richmond	1,967.0	25.4	8.7	6.0
71	27	Richmond	1,967.0	25.4	8.7	6.0
72	28	Port Washington	1,573.7	25.0	8.0	7.0
73	28	Old Brookville	272.3	25.0	7.0	3.0
74	28	Muttontown	131.9	31.0	6.0	1.8
75	28	Mill Neck	131.6	30.0	9.0	1.5
76	28	Oyster Bay	532.3	31.0	6.0	1.5
77	28	Plainview	2,273.9	31.0	6.0	1.5
78	28	Jericho	1,339.2	31.0	6.5	1.5
79	28	Old Westbury	129.1	28.0	7.5	3.0
80	28	Manhasset	1,341.7	25.0	8.5	8.0
81	28	Garden City	2,006.1	26.0	8.0	8.0
82	28	Hempstead	2,278.6	26.0	8.0	7.0
83	28	Levittown	3,704.5	28.0	7.5	6.0
84	28	Old Bethpage	695.5	30.0	6.5	1.8
85	28	Franklin Square	4,412.7	27.0	8.0	8.0
86	28	Roosevelt	3,324.3	27.0	8.0	8.0
87	28	North Bellmore	3,308.9	27.0	8.0	7.0
88	28	Wantagh	2,239.6	28.0	7.5	7.0

TABLE III (continued) Sub-population data of the Tri-State Region (population density in persons/Km^2, sub-population in % of population density)

No.	Code	Tract	Population Density	School-Age	Elderly	Non-White
89	28	Massapequa	2,675.1	30.0	6.0	1.9
90	28	Oceanside	2,756.5	27.0	12.0	7.5
91	28	Freeport	3,762.8	27.0	8.0	7.5
92	29	Lloyd Harbor	134.3	31.0	6.0	3.5
93	29	Huntington Station	2,062.6	31.0	6.0	3.5
94	29	Half Hollow Hills	522.6	31.0	6.0	4.0
95	20	Babylon	553.7	31.0	6.0	10.0
96	29	Copiague	2,386.8	31.0	6.0	11.0
97	29	East Northport	1,847.0	31.0	6.0	2.0
98	29	Isliptown	1,053.7	30.0	7.0	5.0
99	29	Smithtown	982.2	30.0	7.0	1.5
100	29	Isliptown	1,053.7	29.0	8.0	4.0
101	29	Selden	786.0	29.0	8.0	4.0
102	29	East Patchgue	826.4	29.0	8.0	4.0
103	29	Brookhaven	465.6	29.0	8.5	4.0
104	29	Brookhaven	465.6	29.0	8.0	4.0
105	22	Stony Point	190.1	27.0	8.0	1.5
106	22	Ramapotown	591.6	31.0	6.0	7.5
107	22	Clarkstown	628.0	29.0	7.0	7.0
108	22	Congers	629.1	31.0	6.0	7.5
109	22	Ramapotown	591.6	31.0	6.0	7.5
110	22	West Nyack	449.3	31.0	6.0	7.5

TABLE III (continued) Sub-population data of the Tri-State Region (population density in persons/Km^2, sub-population in % of population density)

No.	Code	Tract	Population Density	School-Age	Elderly	Non-White
111	22	Upper Nyack	635.1	39.0	7.0	7.0
112	22	Pearl River	1,043.3	29.0	9.5	6.0
113	22	Orangetown	898.5	29.0	9.5	6.0
114	31	Ramsey	891.8	28.0	6.0	2.5
115	31	Montvale	1,659.3	30.0	5.0	0.5
116	31	Wyckoff	976.0	30.0	7.5	0.5
117	31	Westwood	302.2	30.0	6.0	0.8
118	31	Norwood	649.8	31.0	7.0	1.0
119	31	Fair Lawn	2,904.4	26.0	9.5	1.5
120	31	New Milford	3,567.7	30.0	8.0	2.0
121	31	Tenafly	1,286.5	28.0	8.0	2.0
122	31	Lodi	4,192.4	25.0	10.0	0.5
123	31	Teaneck	3,001.0	20.0	10.5	11.0
124	31	Englewood Cliffs	1,189.5	22.0	11.5	10.0
125	31	Rutherford	3,006.7	23.0	11.5	3.5
126	31	Carlstadt	756.0	22.0	11.5	0.9
127	31	Ridgefield	1,717.6	19.0	11.5	0.5
128	31	Lyndhurst	1,999.7	22.0	10.5	3.5
129	32	North Bergen	3,503.9	19.0	12.5	1.5
130	32	Jersey City	7,118.1	22.0	11.5	20.0
131	32	Jersey City	7,118.1	22.0	11.0	20.0
132	32	Bayonne	5,650.8	22.0	11.0	5.0

TABLE III (continued) Sub-population data of the Tri-State Region (population density in persons/Km^2, sub-population in % of population density)

No.	Code	Tract	Population Density	School-Age	Elderly	Non-White
133	32	Kearny	1,688.2	20.0	11.0	1.5
134	35	West Milford	83.8	30.0	6.0	1.5
135	35	Ringwood	137.4	29.0	4.5	4.0
136	35	West Milford	83.8	30.0	6.0	1.5
137	35	Bloomingdale	322.5	29.0	8.0	0.5
138	35	Wayne	771.0	29.0	6.0	0.9
139	35	Hawthorne	2,427.4	25.0	11.5	13.0
140	35	West Paterson	1,367.2	28.0	7.5	2.0
141	35	Cliffton	3,081.4	21.0	11.5	12.0
142	33	Fairfield	252.3	30.0	6.0	0.9
143	33	Roseland	523.8	28.0	11.0	2.0
144	33	Montclair	2,999.6	23.0	11.5	7.5
145	33	Nutley	4,379.7	23.0	12.0	10.0
146	33	Livingston	888.1	29.0	6.0	2.0
147	33	West Orange	1,492.0	21.0	11.0	20.0
148	33	Newark	6,708.2	25.0	10.0	40.0
149	33	Millburn	893.2	24	12.0	2.0
150	33	Newark	6,708.2	20	10.5	20.0
151	33	Newark	6,708.2	26.5	8.0	50.0
152	36	Rockaway	172.2	28	5.0	0.5
153	36	Kinnelon	155.6	29	4.5	2.0
154	36	Roxbury	294.6	29	6.0	1.0

TABLE III (continued) Sub-population data of the Tri-State Region (population density in persons/Km^2, sub-population in % of population density)

No.	Code	Tract	Population Density	School-Age	Elderly	Non-White
155	36	Lincoln Park	512.6	30	8.0	1.0
156	36	Randolph	254.3	28	8.0	7.0
157	36	Hanover	420.6	23	6.5	5.0
158	36	Chester	73.8	30	7.5	0.9
159	36	Mendham	130.2	27	9.0	3.0
160	36	Chatham	589.2	26	8.5	0.5
161	37	Bedminster	40.7	28	10.5	1.5
162	37	Warren	185.8	30	7.5	1.0
163	37	Hillsborough	87.2	30	6.5	1.0
164	37	Franklin	268.2	28	6.0	2.0
165	37	Montgomery	79.8	28.5	6.0	7.0
166	34	Summit	1,629.1	24	12.5	7.5
167	34	Berkley Heights	851.3	24	10.5	2.0
168	34	Cramford	2,411.6	23	11.0	5.0
169	34	Elizabeth	4,048.7	23.0	11.0	20.0
170	34	Plainfield	3,234.0	23.0	11.0	15.0
171	34	Scotch Plains	999.6	29.0	7.0	9.0
172	34	Clark	1,680.1	26.0	7.5	10.0
173	34	Linden	1,536.3	23.0	8.0	20.0
174	38	Piscataway	765.9	27.0	4.0	20.0
175	38	South Plainfield	1,015.7	30.0	4.5	10.0
176	38	Metuchen	2,551.9	28.0	5.0	4.0

TABLE III (continued) Sub-population data of the Tri-State Region (population density in persons/Km^2, sub-population in % of population density)

No.	Code	Tract	Population Density	School-Age	Elderly	Non-White
177	38	Woodridge	1,707.3	29.0	6.0	4.0
178	38	Carteret	2,110.3	28.0	7.5	5.0
179	38	New Brunswick	2,920.9	26.0	9.0	10.0
180	38	Edison	915.7	27.0	6.0	4.0
181	38	Perth Amboy	3,230.2	25.0	10.0	5.0
182	38	North Brunswick	575.3	25.0	9.0	2.0
183	38	South River	2,291.0	29.0	6.0	0.5
184	38	Madison	518.2	29.0	5.0	1.5
185	38	South Brunswick	141.6	30.0	6.0	3.5
186	38	East Brunswick	644.0	29.0	10.0	5.0
187	38	Old Bridge	1,631.0	28.0	9.5	5.0
188	38	Madison	518.2	31.0	4.5	2.0
189	39	Plainsboro	57.0	26.0	10.0	15.0
190	38	Monroe	91.0	25.0	11.0	10.0
191	39	Matawan	914.6	30.0	4.5	10.0
192	39	Hazlet	1,523.2	30.0	6.0	1.0
193	39	Middletown	596.6	31.0	6.0	3.5
194	39	Marlboro	171.7	26.0	7.5	8.0
195	39	Colts Neck	74.0	30.0	6.5	3.5
196	39	Rumson	564.7	22.0	12.0	5.0
197	39	Oceanport	888.4	28.0	11.0	10.0
198	39	Ocean	831.4	24.0	11.5	10.0

TABLE III (continued) Sub-population data of the Tri-State Region (population density in persons/Km^2, sub-population in % of population density)

No.	Code	Tract	Population Density	School-Age	Elderly	Non-White
199	39	Spring Lake	1,071.7	22.0	12.5	10.0
200	39	New Shrewsbury	148.4	27.0	8.0	10.0
201	39	Howell	139.6	31.0	7.0	5.0
202	39	Freehold	102.4	30.0	9.0	15.0
203	39	Millstone	27.7	27.0	9.5	10.0
204	39	Howell	139.6	30.0	8.0	8.0
205	39	Wall	217.4	24.0	12.5	7.5
206	37	Bernardsville	207.4	26.0	12.0	0.4
207	36	Chester	73.8	29.0	11.0	0.7
208	39	Sea Bright	153.9	30.0	6.0	3.5
209	25	Queens	7,102.2	19.2	12.4	14.7
210	28	Long Beach	5,723.6	27.0	12.0	7.5
211	28	Oyster Bay	1,395.9	30.0	8.0	10.0
212	29	Islip	1,053.7	29.0	8.0	4.0
213	29	Brookhaven	465.6	29.0	8.0	4.0
214	29	Brookhaven	465.6	29.0	8.0	4.0
215	29	Brookhaven	465.6	29.0	8.0	10.0

TABLE IV TSP air quality data, 24 hr. Hi-Vol.
(geometric mean C_m in $\mu g/m^3$)

No.	Code	SAROAD #	X-Coord.	Y-Coord.	C_m, 71/2	C_m, 73/2
1	11	070060001	124.0	116.5	--	--
2	11	070060001	124.0	116.5	52.63	42.16
3	11	070060002	123.5	114.5	--	53.29
4	11	070175001	106.0	135.5	--	73.30
5	11	070260002	118.5	116.5	59.18	40.94
6	11	070330001	92.0	100.5	45.06	46.28
7	11	070330002	94.5	103.5	61.40	63.09
8	11	070330003	91.0	99.0	56.69	51.20
9	11	070330004	87.5	107.0	--	41.40
10	11	070330007	91.5	105.5	44.62	33.03
11	11	070330008	94.5	102.5	86.48	62.45
12	11	070820001	108.5	111.0	53.23	51.13
13	11	070820005	109.0	112.0	65.98	60.53
14	11	071080001	99.5	104.5	--	--
15	11	071080003	98.5	106.5	--	--
16	11	071080004	99.5	109.0	--	129.90
17	11	071080010	96.5	110.0	--	42.76
18	11	071110001	129.0	119.0	47.51	--
19	11	071110005	129.0	116.0	--	53.99
20	32	310180001	56.5	67.5	--	--
21	34	311300002	49.5	65.5	83.25	73.90
22	32	312320001	60.5	71.5	117.35	--

TABLE IV (continued) **TSP air quality data, 24 hr. Hi-Vol. (geometric mean C_m in $\mu g/m^3$)**

No.	Code	SAROAD #	X-Coord.	Y-Coord.	C_m, 71/2	C_m, 73/2
23	33	313480001	52.0	70.0	--	--
24	35	314140001	53.0	90.5	82.44	--
25	38	314220001	43.5	51.0	--	--
26	39	310060002	64.0	28.0	76.38	53.52
27	32	310180003	57.5	66.5	102.24	83.10
28	33	310400002	51.5	83.0	--	--
29	37	310500001	24.5	58.5	76.34	--
30	39	310560001	61.0	13.5	--	34.10
31	38	310820001	48.5	58.5	67.22	70.52
32	36	311100001	24.0	88.0	--	--
33	36	311100002	23.5	89.0	--	37.08
34	33	311160002	43.0	75.0	83.38	132.39
35	33	311380001	45.0	75.0	48.77	39.07
36	31	311440001	57.0	93.5	--	42.80
37	31	311460001	65.0	81.0	125.96	79.48
38	36	311540001	36.5	77.5	--	33.26
39	31	311560001	67.0	84.0	--	--
40	31	311560002	67.5	85.0	--	46.14
41	31	311820001	62.0	89.5	214.00	--
42	32	312180001	68.5	74.0	--	116.93
43	33	312280001	47.5	72.0	68.39	55.49
44	32	312320003	60.5	73.0	145.36	108.96

TABLE IV (continued) TSP air quality data, 24 hr. Hi-Vol. (geometric mean C_m in $\mu g/m^3$)

No.	Code	SAROAD #	X-Coord.	Y-Coord.	C_m, 71/2	C_m, 73/2
45	32	312320004	58.5	71.5	95.89	81.07
46	34	312580001	47.0	61.5	76.10	67.91
47	38	313020002	38.0	54.5	--	44.61
48	38	313060001	39.0	52.5	--	--
49	38	313060002	44.5	46.5	--	39.79
50	38	313060003	23.5	39.0	--	41.73
51	39	313180001	41.5	21.0	45.52	32.57
52	39	313180002	45.0	17.5	--	30.46
53	36	313300002	29.5	79.5	55.60	--
54	33	313480002	54.5	72.5	--	151.24
55	33	313480003	53.5	71.5	45.49	--
56	38	313500001	31.0	49.5	--	--
57	33	313980001	47.5	76.5	72.95	59.28
58	35	314100001	55.5	134.0	54.63	--
59	35	314140001	54.0	139.5	82.44	--
60	38	314220002	44.0	52.0	--	53.44
61	34	314440001	44.0	61.0	67.20	53.67
62	39	314500001	59.5	35.5	--	--
63	39	314500002	58.5	34.5	--	50.52
64	34	314760001	45.5	65.5	89.22	72.95
65	38	314920001	37.5	47.5	--	--
66	38	314920002	40.5	48.5	--	56.19

TABLE IV (continued) TSP air quality data, 24 hr. Hi-Vol. (geometric mean C_m in $\mu g/m^3$)

No.	Code	SAROAD #	X-Coord.	Y-Coord.	C_m, 71/2	C_m, 73/2
67	32	314960001	60.5	78.0	—	70.40
68	37	315060002	19.5	57.5	57.08	48.54
69	38	315080001	43.0	49.5	68.27	52.21
70	32	315420001	61.5	75.5	109.22	80.24
71	34	315440001	47.5	67.0	—	46.97
72	31	315500001	57.5	105.0	—	35.15
73	33	315860001	46.5	79.0	—	57.03
74	31	315920001	62.5	98.0	61.79	46.03
75	38	316040001	42.5	57.0	73.39	68.89
76	38	316040002	45.5	56.0	—	50.65
77	23	334680001	70.5	80.0	120.69	—
78	21	337620001	73.5	92.0	—	—
79	29	330280001	107.0	71.5	—	52.94
80	21	331560001	75.0	100.0	—	50.52
81	28	332300001	94.5	64.0	—	—
82	28	332300002	95.5	65.0	74.34	50.85
83	28	332360001	92.0	71.0	—	52.63
84	28	332460001	92.0	86.0	81.82	—
85	28	332900001	91.0	62.5	98.53	53.98
86	28	332900003	86.5	67.5	85.57	59.04
87	28	332900004	87.0	63.0	66.48	50.06
88	28	332900005	95.0	71.0	69.87	71.31

TABLE IV (continued) TSP air quality data, 24 hr. Hi-Vol. (geometric mean C_m in $\mu g/m^3$)

No.	Code	SAROAD #	X-Coord.	Y-Coord.	C_m, 71/2	C_m, 73/2
89	28	332900007	84.0	62.5	--	74.57
90	28	333480001	83.5	80.0	74.22	40.10
91	21	334100001	84.5	94.0	64.02	54.46
92	21	334100002	84.0	93.0	49.38	73.64
93	21	334480001	77.5	89.5	--	--
94	21	334480003	77.0	91.0	--	76.08
95	28	334520001	96.5	72.5	56.34	53.17
96	28	334520002	103.5	65.5	60.37	60.09
97	28	334520004	101.0	84.5	--	--
98	28	334520005	99.5	85.0	51.91	42.58
99	28	334520006	104.0	79.0	72.45	46.30
100	21	334620002	81.5	90.5	77.71	58.19
101	24	334680050	68.0	75.5	90.95	75.97
102	24	334680057	68.0	75.5	87.12	83.92
103	21	334880001	76.0	107.0	59.69	40.74
104	21	335200001	75.5	114.5	54.89	48.04
105	21	335360001	71.5	127.0	91.11	73.29
106	21	335520001	89.5	99.0	71.94	50.46
107	29	33550001	134.5	93.5	--	--
108	29	335550002	135.0	92.5	--	--
109	22	335780001	67.0	107.0	53.71	53.08
110	22	335780002	71.0	101.0	--	50.36

TABLE IV (continued) TSP air quality data, 24 hr. Hi-Vol. (geometric mean C_m in $\mu g/m^3$)

No.	Code	SAROAD #	X-Coord.	Y-Coord.	C_m, 71/2	C_m, 73/2
111	28	335800001	90.5	65.0	93.18	67.60
112	21	335910001	88.5	97.5	72.18	52.96
113	29	336340001	160.0	89.0	37.25	43.54
114	22	336560001	54.5	110.5	52.78	65.23
115	29	336580001	129.5	91.0	64.87	45.43
116	29	336580002	139.0	79.0	65.26	38.28
117	29	336580011	119.0	73.0	52.06	48.18
118	29	336580023	118.0	83.5	37.08	48.84
119	21	337320003	78.5	108.5	44.98	35.81
120	21	337320004	82.0	125.5	40.74	30.78
121	21	337320005	85.0	129.0	53.51	32.45
122	21	337320006	77.5	103.5	98.99	52.04
123	22	337400001	66.0	119.0	—	53.02
124	21	337480001	82.5	101.0	83.98	52.72
125	21	337620001	73.0	93.0	117.81	--
126	24	334680002	68.0	81.5	--	84.99
127	23	334680003	72.0	84.0	—	84.20
128	25	334680004	78.0	73.0	--	55.25
129	24	334680005	65.5	75.0	—	80.44
130	23	334680006	72.5	87.0	—	71.22
131	26	334680007	69.0	58.5	—	63.35
132	25	334680008	77.0	77.5	--	102.09

TABLE IV (continued) TSP air quality data, 24 hr. Hi-Vol.
(geometric mean C_m in $\mu g/m^3$)

No.	Code	SAROAD #	X-Coord.	Y-Coord.	C_m, 71/2	C_m, 73/2
133	23	334680009	78.5	80.5	--	53.89
134	26	334680010	64.0	65.5	--	85.52
135	26	334680011	68.0	72.5	--	87.03
136	24	334680014	69.0	79.0	--	78.53
137	25	334680015	80.5	76.5	--	57.08
138	25	334680016	85.5	73.5	--	60.13
139	24	334680017	66.0	73.0	--	85.45
140	26	334680018	67.0	68.0	--	50.94
141	26	334680019	70.5	67.0	--	69.49
142	25	334680020	73.5	69.5	--	74.62
143	26	334680021	73.5	64.5	--	--
144	23	334680022	73.0	81.0	--	84.76
145	26	334680025	68.0	64.0	--	--
146	25	334680029	76.5	64.5	--	56.81
147	25	334680030	82.0	66.0	--	53.12
148	27	334680031	51.5	62.5	--	75.46
149	27	334680032	58.0	63.5	--	75.52
150	27	334680033	50.0	57.5	--	79.58
151	27	334680034	54.5	59.5	--	60.50
152	27	334680035	57.5	58.0	--	68.10
153	27	334680036	46.5	51.5	--	53.65
154	24	334680037	64.0	72.0	--	62.63

TABLE IV (continued) TSP air quality data, 24 hr. Hi-Vol. (geometric mean C_m in μg/m^3)

No.	Code	SAROAD #	X-Coord.	Y-Coord.	C_m, 71/2	C_m, 73/2
155	23	334680038	77.0	83.0	--	61.87
156	23	334680039	77.0	87.0	--	71.61
157	25	334680040	71.5	77.0	--	86.41
158	25	334680041	74.0	75.5	--	65.43
159	25	334680042	70.5	75.5	--	83.56
160	25	334680044	83.0	69.5	--	73.72
161	26	334680045	62.5	63.0	--	67.70
162	26	334680046	72.5	62.5	--	63.90
163	25	334680047	77.0	57.0	--	103.32
164	26	334680064	66.0	62.0	--	60.00

TABLE V **TSP percentile concentrations in 71/2 and 73/2 (71/73 values in $\mu g/m^3$)**

No.	SAROAD #	Min.	10%	30%	50%	70%	90%	95%	Max.
2	070060001	19/23	37/25	46/35	50/41	66/42	95/79	106/94	106/94
5	070260002	23/30	23/34	41/38	44/39	88/45	107/49	176/59	176/59
6	070330001	16/29	17/31	43/36	49/42	55/50	80/79	96/83	96/83
7	070330002	19/36	38/39	52/48	61/52	83/88	115/122	129/122	129/12
8	070330003	14/25	41/28	50/45	60/50	65/71	95/88	101/89	101/89
10	070330007	12/20	28/20	39/29	44/30	52/38	92/58	95/79	95/79
11	070330008	60/25	60/27	67/56	69/60	100/79	172/88	172/248	172/24
12	070820001	21/26	36/34	47/41	54/43	61/76	92/98	100/110	100/11
13	070820005	31/28	50/33	55/47	64/59	78/71	92/111	125/139	125/13
18	071110001	29/22	29/22	38/48	40/52	48/58	70/75	107/75	107/75
21	311300002	59/56	59/56	64/70	67/70	91/73	183/110	183/110	183/11
22	312320001	73/46	73/46	81/62	109/73	150/120	227/161	227/161	227/16
24	314140001	49/56	49/56	75/63	81/66	87/91	147/109	147/109	147/10
26	310060002	47/28	56/36	64/46	71/52	84/72	134/78	147/88	147/88
27	310180003	25/26	45/35	89/66	104/71	127/107	179/293	239/331	239/33
29	310500003	37/28	46/29	64/48	79/57	89/80	129/90	144/94	144/94
31	310820001	47/36	47/41	48/56	68/68	77/77	107/136	107/154	107/15
34	311160002	54/81	56/89	68/107	80/120	95/174	126/196	134/240	134/24
35	311380001	20/18	30/23	46/35	52/36	64/55	75/67	78/68	78/68
37	311460001	55/43	86/55	114/62	121/74	148/109	211/138	218/155	218/15
41	311820001	110/77	110/89	151/118	214/121	232/127	339/226	339/258	339/25
43	312280001	31/30	43/31	61/47	68/51	81/77	103/68	121/87	121/87

TABLE V (continued) TSP percentile concentrations in 71/2 and 73/2 (71/73 values in μg/m^3)

No.	SAROAD #	Min.	10%	30%	50%	70%	90%	95%	Max.
44	312320003	62/60	87/60	98/80	156/101	168/160	323/177	372/177	327/177
45	312320004	35/41	64/48	85/72	91/83	126/97	132/118	196/134	196/134
46	312580001	43/32	43/33	58/63	85/69	98/92	130/111	130/114	130/114
51	313180001	18/14	20/20	36/24	43/38	52/47	98/54	107/54	107/54
53	313300002	20/23	41/26	48/37	57/43	61/60	100/74	101/75	101/75
56	313500001	32/19	32/40	35/49	45/54	56/69	71/71	72/75	72/75
57	313980001	28/39	55/41	67/49	69/56	93/76	104/82	115/98	115/98
58	314100001	28/31	28/37	53/48	59/56	65/73	88/116	88/125	88/125
59	314140001	49/56	49/56	75/63	81/66	87/91	147/109	147/109	147/109
61	314440001	30/31	46/34	57/45	68/52	79/65	104/85	127/88	127/88
64	314760001	55/34	67/37	74/60	88/77	99/83	158/112	159/124	159/124
68	315060002	23/21	31/25	50/41	59/52	79/60	91/72	104/112	104/112
69	315080001	36/28	51/29	57/39	62/51	83/71	91/89	146/107	146/107
70	315420001	56/44	83/48	92/63	112/78	128/105	158/142	200/150	200/150
74	315920001	35/23	40/23	51/40	62/44	73/66	98/84	103/95	103/95
75	316040001	29/40	43/40	63/58	70/65	92/72	123/126	139/146	139/146
77	334680001	94/59	94/59	107/89	111/98	124/107	186/144	186/144	186/144
82	332300002	33/24	51/27	58/46	67/55	101/64	113/78	233/85	233/85
85	332900001	64/38	66/39	80/44	89/48	121/63	142/87	235/92	235/92
86	332900003	39/29	59/29	68/52	74/62	119/75	147/102	171/110	171/110
87	332900004	28/25	41/29	59/41	61/63	86/64	119/74	124/77	124/77
88	332900005	25/21	40/21	53/63	66/64	100/78	123/332	149/332	149/332

TABLE V (continued) TSP percentile concentrations in 71/2 and 73/2 (71/73 values in $\mu g/m^3$)

No.	SAROAD #	Min.	10%	30%	50%	70%	90%	95%	Max.
90	333480001	24/16	51/18	60/34	67/42	99/47	132/84	166/88	166/88
91	334100001	19/26	19/30	57/44	64/55	66/78	109/97	144/101	144/101
92	334100002	17/39	36/51	45/65	45/74	55/83	70/120	131/124	131/124
95	334520001	21/23	28/30	49/45	57/51	71/60	95/89	117/107	117/107
96	334520002	33/25	37/26	54/53	59/70	75/81	92/92	98/96	98/96
98	334520005	17/20	34/26	44/33	55/45	69/55	84/69	109/74	109/74
99	334520006	26/23	50/23	61/33	72/51	86/58	114/62	143/108	143/108
100	334620002	57/24	57/38	67/39	73/60	82/90	114/108	119/124	119/124
101	334680050	37/44	71/48	85/53	86/67	97/112	148/134	168/143	168/143
102	334680057	53/52	62/60	81/67	91/71	100/119	118/130	119/156	119/156
103	334880001	18/10	37/20	47/33	68/38	76/45	105/100	118/134	118/134
104	335200001	18/23	36/26	44/41	63/47	69/67	86/82	97/86	97/86
105	335360001	31/29	61/43	80/56	94/67	116/109	149/125	178/134	178/134
106	335520001	32/25	35/35	58/41	77/46	81/59	124/89	192/93	192/93
109	335780001	19/27	35/36	40/39	56/50	72/78	78/88	111/94	111/94
111	335800001	48/31	66/31	81/59	90/73	115/79	135/96	181/112	181/112
112	335910001	31/22	53/30	63/47	76/51	86/80	99/83	104/105	104/105
113	336340001	11/15	22/23	31/36	41/49	51/65	58/71	79/76	79/76
114	336560001	23/30	33/34	46/52	54/68	68/91	91/110	92/133	92/133
115	336580001	19/16	38/26	53/40	66/42	86/49	110/74	115/75	115/75
116	336580002	20/14	36/22	58/32	69/43	102/48	107/56	109/67	109/67
117	336580011	20/18	48/30	60/36	64/37	75/67	88/84	94/118	94/118

TABLE V (continued) TSP percentile concentrations in 71/2 and 73/2 (71/73 values in µg/m^3)

No.	SAROAD #	Min.	10%	30%	50%	70%	90%	95%	Max.
118	336580023	15/22	16/22	31/41	37/51	54/58	60/78	82/84	82/84
119	337320003	13/16	24/17	40/27	53/33	56/58	85/70	87/89	87/89
120	337320004	9/15	16/17	42/26	46/28	57/39	70/61	84/68	84/68
121	337320005	13/16	21/16	47/21	59/31	64/52	112/65	112/71	112/71
122	337320006	33/26	66/31	88/39	100/48	125/69	152/92	178/98	178/98
124	337480001	31/31	60/31	60/38	84/54	115/65	133/92	171/93	171/93

TABLE VI TSP air quality data
(quarterly geometric mean in $\mu g/m^3$)

SAROAD	1971				1973			
	1	2	3	4	1	2	3	4
070060001	62.29	52.63	53.46	64.01	--	42.16	50.00	45.78
070260002	69.61	59.18	50.74	129.51	--	40.94	48.43	47.48
070330001	67.39	45.06	53.93	56.88	--	46.28	49.95	39.77
070330002	69.80	61.40	53.37	61.97	--	63.09	63.80	44.62
070330003	70.64	56.69	52.47	56.48	--	51.20	53.69	45.37
070330007	43.38	44.62	43.78	50.31	--	33.03	44.53	27.34
070330008	94.32	86.48	70.36	62.94	--	62.45	70.40	56.37
070820001	66.97	53.23	54.69	66.84	--	51.13	72.37	47.91
070820005	86.14	65.98	63.17	81.11	--	60.53	63.94	55.90
071080004	49.05	30.85	61.04	49.38	--	129.90	83.98	73.31
311300002	95.10	83.25	71.76	102.58	70.67	73.90	--	--
312320001	96.23	117.35	93.85	93.37	74.47	87.94	--	--
310060002	90.94	76.38	70.88	67.16	48.87	53.52	61.22	44.05
310180003	91.38	102.24	97.91	73.49	53.41	83.10	88.04	64.08
310500001	75.44	76.34	73.42	77.07	31.06	34.10	43.96	33.39
310820001	81.40	67.22	90.16	73.36	60.52	70.52	77.92	64.33
311160002	80.38	83.38	--	127.92	123.99	132.39	137.70	55.78
311380001	38.65	48.77	48.07	44.86	28.00	39.07	48.83	30.30
311460001	127.16	125.96	114.23	91.35	78.73	79.49	--	--
312280001	60.50	68.39	65.37	63.16	46.12	55.49	58.67	38.44
312320003	126.93	145.36	109.07	96.09	85.39	108.96	98.01	73.17
312320004	106.34	95.89	95.46	96.04	75.22	81.07	110.30	80.12

TABLE VI (continued) TSP air quality data (quarterly geometric mean in $\mu g/m^3$)

SAROAD	1971				1973			
	1	2	3	4	1	2	3	4
312580001	103.62	76.10	79.21	88.60	76.35	67.91	88.59	69.60
313180001	56.44	45.52	36.06	34.99	23.34	32.57	--	--
313300002	60.00	55.60	53.99	58.34	51.43	43.97	--	--
313500001	39.36	45.49	39.43	38.41	46.74	52.12	--	--
313980001	70.59	72.95	64.84	75.56	54.24	59.28	62.11	50.74
314220002	81.48	67.59	62.54	71.85	53.02	53.44	66.26	53.88
314440001	67.79	67.20	61.80	--	53.14	53.67	66.33	48.41
314760001	95.85	89.22	79.12	80.84	70.79	72.95	76.94	60.93
315080001	86.23	68.27	61.14	73.13	57.34	52.21	63.78	60.13
315420001	109.13	109.22	91.49	96.06	86.61	80.24	--	--
315920001	61.80	61.79	61.83	64.63	41.46	46.03	--	--
316040001	75.80	73.39	68.58	78.33	62.49	68.89	81.42	89.11
332300002	66.21	74.34	79.69	70.53	50.22	50.85	62.99	60.74
332360001	73.62	56.16	82.99	61.90	51.43	52.63	64.38	52.04
332460001	101.33	81.82	80.33	81.78	59.75	--	--	72.11
332900001	195.26	98.53	83.34	66.78	92.07	53.98	73.08	61.42
332900003	107.79	85.57	73.79	67.83	56.93	59.04	61.37	61.49
332900004	87.63	66.48	71.04	66.53	53.95	50.06	72.99	57.59
332900005	89.95	69.87	74.24	72.93	58.20	71.31	72.29	78.30
333480001	73.46	74.22	79.03	45.04	39.56	40.10	57.47	43.66
334100001	69.50	64.02	60.56	57.67	51.86	54.46	49.02	50.21
334520001	62.75	56.34	67.67	57.54	51.45	53.17	62.87	54.24

TABLE VI (continued) TSP air quality data
(quarterly geometric mean in µg/m³)

SAROAD	1971				1973			
	1	2	3	4	1	2	3	4
334520002	72.20	60.37	107.60	132.95	52.81	60.09	57.57	60.72
334520005	58.40	51.91	60.47	43.26	38.05	42.58	50.44	38.08
334520006	80.55	72.45	68.06	57.03	43.20	45.30	58.60	49.24
334620002	97.19	77.71	76.25	72.22	57.48	58.19	90.75	58.54
334680050	87.76	90.95	81.04	74.75	69.40	75.97	83.95	64.32
334680057	109.40	87.12	87.14	80.12	75.65	83.92	80.76	70.43
334880001	61.81	59.69	50.36	51.09	45.88	40.74	51.81	47.10
335200001	54.15	54.89	49.14	42.79	51.83	48.04	41.07	37.37
335360001	83.50	91.11	58.54	63.29	72.77	73.29	63.85	53.38
335520001	77.14	71.94	66.25	54.37	51.42	50.46	52.69	50.07
335780001	50.25	53.71	57.98	46.36	59.24	53.08	54.08	38.81
335800001	108.65	93.18	84.71	82.59	75.83	67.60	77.12	72.92
335910001	82.37	72.18	64.81	71.89	58.06	52.96	55.44	68.10
336340001	37.78	37.25	36.91	30.42	54.63	43.54	42.80	33.96
336560001	57.23	52.78	57.59	47.08	59.86	65.23	68.83	41.34
336580001	96.28	64.87	63.12	80.13	58.21	45.43	55.24	52.05
336580002	83.06	65.26	125.81	40.79	33.93	38.28	49.10	43.50
336580011	62.12	52.06	54.99	48.91	45.84	48.18	53.79	58.30
336580023	53.52	37.08	44.10	38.68	46.57	48.84	52.12	45.93
337320003	44.48	44.98	45.75	38.09	39.99	35.81	55.05	32.30
337320004	38.58	40.74	38.13	26.97	33.49	30.78	38.65	27.25
337320005	61.82	53.51	38.22	32.91	39.44	32.45	41.54	33.36

TABLE VI (continued) TSP air quality data (quarterly geometric mean in $\mu g/m^3$)

SAROAD	1971				1973			
	1	2	3	4	1	2	3	4
337320006	103.30	98.99	79.47	65.88	72.77	52.04	57.35	57.54
337480001	108.56	83.98	68.55	72.40	59.77	52.72	65.05	50.40
337620001	113.21	117.81	104.37	65.77	--	--	83.60	60.95

TABLE VII TSP air quality data, 24 hr. Hi-Vol. (geometric mean C_m in $\mu g/m^3$)

No.	Code	SAROAD #	X-Coord.	Y-Coord.	C_m, 71	C_m, 73
2	11	070060001	124.0	116.5	57.83	49.45
5	11	070260002	118.5	116.5	72.13	50.53
6	11	070330001	92.0	100.5	55.30	49.81
7	11	070330002	94.5	103.5	61.51	59.56
8	11	070330003	91.0	99.0	58.70	54.53
10	11	070330007	91.5	105.5	45.47	36.40
11	11	070330008	94.5	102.5	77.52	69.44
12	11	070820001	108.5	111.0	59.92	58.55
13	11	070820005	109.0	112.0	73.62	65.75
16	11	071080004	99.5	109.0	46.17	79.14
21	34	311300002	49.5	65.5	87.15	78.65
22	32	312320001	60.5	71.5	99.90	87.14
26	39	310060002	64.0	28.0	75.94	51.49
27	32	310180003	57.5	66.5	90.79	70.81
29	37	310500001	24.5	58.5	75.65	35.32
31	38	310820001	48.5	58.5	77.58	68.10
34	33	311160002	43.0	75.0	104.36	106.20
35	33	311380001	45.0	75.0	44.85	35.70
37	31	311460001	65.0	81.0	114.00	89.92
43	33	312280001	47.5	72.0	64.32	49.02
44	32	312320003	60.5	73.0	117.78	90.47
45	32	312320004	58.5	71.5	98.37	85.70

TABLE VII (continued) TSP air quality data, 24 hr. Hi-Vol. (geometric mean C_m in $\mu g/m^3$)

No.	Code	SAROAD #	X-Coord.	Y-Coord.	C_m, 71	C_m, 73
46	34	312580001	47.0	61.5	86.15	75.19
51	39	313180001	41.5	21.0	42.47	31.34
53	36	313300002	29.5	79.5	56.97	51.68
56	38	313500001	31.0	49.5	40.53	43.71
57	33	313980001	47.5	76.5	70.90	56.36
60	38	314220002	44.0	52.0	70.46	56.36
61	34	314440001	44.0	61.0	60.79	54.87
64	34	314760001	45.5	65.5	85.89	70.10
69	38	315080001	43.0	49.5	71.52	58.41
70	32	315420001	61.5	75.5	100.99	88.46
74	31	315920001	62.5	98.0	62.33	52.46
75	38	316040001	42.5	57.0	74.07	74.81
82	28	332300002	95.5	65.0	72.60	55.98
83	28	332360001	92.0	71.0	68.03	54.73
84	28	332460001	92.0	86.0	85.84	72.97
85	28	332900001	91.0	62.5	101.49	68.72
86	28	332900003	86.5	67.5	82.48	59.74
87	28	332900004	87.0	63.0	72.42	57.97
88	28	332900005	95.0	71.0	76.52	69.76
90	28	333480001	83.5	80.0	66.52	44.70
91	21	334100001	84.5	94.0	62.65	51.42
95	28	334520001	96.5	72.5	60.79	55.15

TABLE VII (continued) TSP air quality data, 24 hr. Hi-Vol. (geometric mean C_m in $\mu g/m^3$)

No.	Code	SAROAD #	X-Coord.	Y-Coord.	C_m, 71	C_m, 73
96	28	334520002	103.5	65.5	88.90	57.83
98	28	334520005	99.5	85.0	53.12	41.99
99	28	334520006	104.0	79.0	68.89	48.79
100	21	334620002	81.5	90.5	80.24	64.88
101	24	334680050	68.0	75.5	83.10	72.97
102	24	334680057	68.0	75.5	90.47	77.48
103	21	334880001	76.0	107.0	55.42	46.29
104	21	335200001	75.5	114.5	50.02	44.26
105	21	335360001	71.5	127.0	72.76	65.37
106	21	335520001	89.5	99.0	67.02	51.03
109	22	335780001	67.0	107.0	51.94	50.65
111	28	335800001	90.5	65.0	91.61	73.33
112	21	335910001	88.5	97.5	72.60	58.41
113	29	336340001	160.0	89.0	35.52	43.16
114	22	336560001	54.5	110.5	53.52	57.69
115	29	336580001	129.5	91.0	75.00	52.46
116	29	336580002	139.0	79.0	72.60	40.65
117	29	336580011	119.0	73.0	53.92	51.42
118	29	336580023	118.0	83.5	42.95	48.30
119	21	337320003	78.5	108.5	43.27	40.04
120	21	337320004	82.0	125.5	35.61	32.30
121	21	337320005	85.0	129.0	45.04	36.51

TABLE VII (continued) TSP air quality data, 24 hr. Hi-Vol. (geometric mean C_m in $\mu g/m^3$)

No.	Code	SAROAD #	X-Coord.	Y-Coord.	C_m, 71	C_m, 73
122	21	337320006	77.5	103.5	85.84	59.44
124	21	337480001	82.5	101.0	82.06	56.68
125	21	337620001	73.0	93.0	98.00	90.92

TABLE VIII TSP 24 hr. Hi-Vol. air quality data in 73/2 and 73/3 (geometric mean C_m in μg/m^3)

No.	Code	SAROAD #	X-Coord.	Y-Coord.	C_m, 73/2	C_m, 73/3
1	11	070060001	124.0	116.5	--	--
2	11	070060001	124.0	116.5	42.16	50.00
3	11	070060002	123.5	114.5	53.29	65.13
4	11	070175001	106.0	135.5	73.30	66.08
5	11	070260002	118.5	116.5	40.94	48.43
6	11	070330001	92.0	100.5	46.28	49.95
7	11	070330002	94.5	103.5	63.09	63.80
8	11	070330003	91.0	99.0	51.20	53.69
9	11	070330004	87.5	107.0	41.40	52.53
10	11	070330007	91.5	105.0	33.03	44.53
11	11	070330008	94.5	102.5	62.45	70.40
12	11	070820001	108.5	111.0	51.13	72.37
13	11	070820005	109.0	112.0	60.53	63.94
14	11	071080001	99.5	104.5	--	--
15	11	071080003	98.5	106.5	--	--
16	11	071080004	99.5	109.0	129.90	83.98
17	11	071080010	96.5	110.0	42.76	82.89
18	11	071110001	129.0	119.0	--	--
19	11	071110005	129.0	116.0	53.99	47.00
20	32	310180001	56.5	67.5	--	--
21	34	311300002	49.5	65.5	--	--
22	32	312320001	60.5	71.5	--	--

TABLE VIII (continued) TSP 24 hr. Hi-Vol. air quality data in 73/2 and 73/3 (geometric mean C_m in $\mu g/m^3$)

No.	Code	SAROAD #	X-Coord.	Y-Coord.	C_m, 73/2	C_m, 73/3
23	33	313480001	52.0	70.0	--	--
24	35	314140001	53.0	90.5	--	--
25	38	314220001	43.5	51.0	--	--
26	39	310060002	64.0	28.0	53.52	61.22
27	32	310180003	57.5	66.5	83.10	88.04
28	33	310400002	51.5	83.0	--	--
29	37	310500001	24.5	58.5	--	--
30	39	310560001	61.0	13.5	34.10	43.96
31	38	310820001	48.5	58.5	70.52	77.92
32	36	311100001	24.0	88.0	--	--
33	36	311100002	23.5	89.0	37.08	53.08
34	33	311160002	43.0	75.0	132.39	137.70
35	33	311380001	45.0	75.0	39.07	48.83
36	31	311440001	57.0	93.5	42.80	52.32
37	31	311460001	65.0	81.0	79.48	85.00
38	36	311540001	36.5	77.5	33.26	46.37
39	31	311560001	67.0	84.0	--	--
40	31	311560002	67.5	85.0	46.14	51.22
41	33	311820001	62.0	89.5	--	--
42	32	312180001	68.5	74.0	116.93	98.00
43	33	312280001	47.5	72.0	55.49	58.67
44	32	312320003	60.5	73.0	108.96	98.01

TABLE VIII (continued) TSP 24 hr. Hi-Vol. air quality data in 73/2 and 73/3 (geometric mean C_m in μg/m^3)

No.	Code	SAROAD #	X-Coord.	Y-Coord.	C_m, 73/2	C_m, 73/3
45	32	312320004	58.5	71.5	81.07	110.30
46	34	312580001	47.0	61.5	67.91	88.59
47	38	313020002	38.0	54.5	44.61	58.87
48	38	313060001	39.0	52.5	--	--
49	38	313060002	44.5	46.5	39.79	60.42
50	38	313060003	23.5	39.0	41.73	57.54
51	39	313180001	41.5	21.0	32.57	42.00
52	39	313180002	45.0	17.5	30.46	49.45
53	36	313300002	29.5	79.5	--	--
54	33	313480002	54.5	72.5	151.24	118.48
55	33	313480003	53.5	71.5	--	--
56	38	313500001	31.0	49.5	--	--
57	33	313980001	47.5	76.5	59.28	62.11
58	35	314100001	55.5	134.0	--	--
59	35	314140001	54.0	139.5	--	--
60	38	314220002	44.0	52.0	53.44	66.26
61	34	314440001	44.0	61.0	53.67	66.33
62	39	314500001	59.5	35.5	--	--
63	39	314500002	58.5	34.5	36.70	50.52
64	34	314760001	45.5	65.5	72.95	76.94
65	38	314920001	37.5	47.5	--	--
66	38	314920002	40.5	48.5	56.19	78.26

TABLE VIII (continued) TSP 24 hr. Hi-Vol. air quality data in 73/2 and 73/3 (geometric mean C_m in μg/m^3)

No.	Code	SAROAD #	X-Coord.	Y-Coord.	C_m, 73/2	C_m, 73/3
67	32	314960001	60.5	78.0	70.40	72.01
68	37	315060002	19.5	57.5	48.54	57.00
69	38	315080001	43.0	49.5	52.21	63.78
70	32	315420001	61.5	75.5	80.24	74.00
71	34	315440001	47.5	67.0	46.97	63.24
72	31	315500001	57.5	105.0	35.15	45.70
73	33	315860001	46.5	79.0	57.03	60.90
74	31	315920001	62.5	98.0	46.03	64.00
75	38	316040001	42.5	57.0	68.89	81.42
76	38	316040002	45.5	56.0	50.65	69.20
77	23	334680001	70.5	80.0	--	--
78	21	337620001	73.5	92.0	--	--
79	29	330280001	107.0	71.5	52.94	60.43
80	21	331560001	75.0	100.0	50.52	46.36
81	28	332300001	94.5	64.0	--	--
82	28	332300002	95.5	65.0	50.85	62.99
83	28	332360001	92.0	71.0	52.63	64.38
84	28	332460001	92.0	86.0	--	--
85	28	332900001	91.0	62.5	53.98	73.08
86	28	332900003	86.5	67.5	59.04	61.37
87	28	332900004	87.0	63.0	50.06	72.99
88	28	332900005	95.0	71.0	71.31	72.29

TABLE VIII (continued) TSP 24 hr. Hi-Vol. air quality data in 73/2 and 73/3 (geometric mean C_m in $\mu g/m^3$)

No.	Code	SAROAD #	X-Coord.	Y-Coord.	C_m, 73/2	C_m, 73/3
89	28	332900007	84.0	62.5	74.57	74.79
90	28	333480001	83.5	80.0	40.10	57.47
91	21	334100001	84.5	94.0	54.46	49.02
92	21	334100002	84.0	93.0	73.64	61.16
93	21	334480001	77.5	89.5	--	--
94	21	334480003	77.0	91.0	76.08	82.21
95	28	334520001	96.5	72.5	53.17	62.87
96	28	334520002	103.5	65.5	60.09	57.57
97	28	334520004	101.0	84.5	--	--
98	28	334520005	99.5	85.0	42.58	50.44
99	28	334520006	104.0	79.0	46.30	58.60
100	21	334620002	81.5	90.5	58.19	90.75
101	24	334680050	68.0	75.5	75.97	83.69
102	24	334680057	68.0	75.5	83.92	80.76
103	21	334880001	76.0	107.0	40.74	51.81
104	21	335200001	75.5	114.5	48.04	41.07
105	21	335360001	71.5	127.0	73.29	63.85
106	21	335520001	89.5	99.0	50.46	52.69
107	29	335550001	134.5	93.5	--	--
108	29	335550002	135.0	92.5	--	--
109	22	335780001	67.0	107.0	53.08	54.08
110	22	335780002	71.0	101.0	50.36	64.35

TABLE VIII (continued) TSP 24 hr. Hi-Vol. air quality data in 73/2 and 73/3 (geometric mean C_m in $\mu g/m^3$)

No.	Code	SAROAD #	X-Coord.	Y-Coord.	C_m, 73/2	C_m, 73/3
111	28	335800001	90.5	65.0	67.60	77.12
112	21	335910001	88.5	97.5	52.96	55.44
113	29	336340001	160.0	89.0	43.54	42.80
114	22	336560001	54.5	110.5	65.23	68.83
115	29	336580001	129.5	91.0	45.43	55.24
116	29	336580002	139.0	79.0	38.28	49.10
117	29	336580011	119.0	73.0	48.18	53.79
118	29	336580023	118.0	83.5	48.84	52.12
119	21	337320003	78.5	108.5	35.81	55.05
120	21	337320004	77.5	75.5	30.78	38.65
121	21	337320005	85.0	79.0	32.45	41.54
122	21	337320006	77.5	103.5	52.04	57.35
123	22	337400001	66.0	119.0	53.02	55.85
124	21	337480001	82.5	101.0	52.72	65.05
125	21	337620001	73.0	93.0	--	--
126	24	334680002	68.0	81.5	84.99	83.94
127	23	334680003	72.0	84.0	84.20	95.92
128	25	334680004	78.0	73.0	55.25	70.90
129	24	334680005	65.5	75.0	80.44	89.25
130	23	334680006	72.5	87.0	71.22	76.51
131	26	334680007	69.0	58.5	63.35	71.38
132	25	334680008	77.0	77.5	73.62	102.09

TABLE VIII (continued) TSP 24 hr. Hi-Vol. air quality data in 73/2 and 73/3 (geometric mean C_m in µg/m^3)

No.	Code	SAROAD #	X-Coord.	Y-Coord.	C_m, 73/2	C_m, 73/3
133	23	334680009	78.5	80.5	53.89	80.86
134	26	334680010	64.0	65.5	85.52	95.77
135	26	334680011	68.0	72.5	87.03	89.97
136	24	334680014	69.0	79.0	78.53	104.58
137	25	334680015	80.5	76.5	57.08	66.65
138	25	334680016	85.5	73.5	60.13	47.00
139	24	334680017	66.0	73.0	85.45	93.41
140	26	334680018	67.0	68.0	50.94	60.55
141	26	334680019	70.5	67.0	69.49	89.96
142	25	334680020	73.5	69.5	74.62	66.00
143	26	334680021	73.5	64.5	--	--
144	23	334680022	73.0	81.0	84.76	86.00
145	26	334680025	68.0	64.0	--	--
146	25	334680029	76.5	64.5	56.81	65.90
147	25	334680030	82.0	66.0	53.12	57.65
148	27	334680031	51.5	62.5	75.46	105.73
149	27	334680032	58.0	63.5	75.52	93.09
150	27	334680033	50.0	57.5	79.58	122.73
151	27	334680034	54.5	59.5	60.50	71.36
152	27	334680035	57.5	58.0	68.10	76.47
153	27	334680036	46.5	51.5	53.65	71.87
154	24	334680037	64.0	72.0	62.63	77.24

TABLE VIII (continued) TSP 24 hr. Hi-Vol. air quality data in 73/2 and 73/3 (geometric mean C_m in $\mu g/m^3$)

No.	Code	SAROAD #	X-Coord.	Y-Coord.	C_m, 73/2	C_m, 73/3
155	23	334680038	77.0	83.0	61.87	70.43
156	23	334680039	77.0	87.0	71.61	75.67
157	25	334680040	71.5	77.0	86.41	111.00
158	25	334680041	74.0	75.5	65.43	62.00
159	25	334680042	70.5	75.5	83.46	93.39
160	25	334680044	83.0	69.5	73.72	62.00
161	26	334680045	62.5	63.0	67.70	77.00
162	26	334680046	72.5	62.5	63.90	104.68
163	25	334680047	77.0	57.0	103.32	115.08
164	26	334680064	66.0	62.0	60.00	82.97

TABLE C1 Rank-order of monitoring stations according to the first scheme (errors and PI in μg/m³)

Rank	Station #	Code	2nd Q. Error	3rd Q. Error	PI
1	101	24	0.0	0.0	0.0
2	102	24	0.0	0.0	0.0
3	9	11	0.93	0.56	0.76
4	106	21	0.70	1.11	0.91
5	79	29	1.08	1.45	1.27
6	156	23	2.00	0.70	1.35
7	60	38	0.84	1.97	1.41
8	8	11	1.88	1.60	1.74
9	152	27	3.11	0.72	1.92
10	129	24	1.89	2.18	2.04
11	117	29	1.59	2.48	2.04
12	99	28	2.44	1.70	2.07
13	115	29	0.51	3.88	2.20
14	103	21	1.91	3.17	2.54
15	118	29	1.89	3.25	2.57
16	112	21	2.73	2.77	2.75
17	36	31	0.75	5.34	3.05
18	69	38	1.06	5.59	3.31
19	153	27	1.00	5.66	3.33
20	137	25	6.45	0.46	3.46
21	7	11	3.55	3.68	3.62
22	85	28	6.86	0.93	3.90

TABLE C1 (continued) Rank order of monitoring stations according to the first scheme (errors and PI in $\mu g/m^3$)

Rank	Station #	Code	2nd Q. Error	3rd Q. Error	PI
23	37	31	4.68	3.22	3.95
24	113	29	0.43	7.82	4.13
25	68	37	2.06	6.30	4.18
26	123	22	6.42	2.30	4.36
27	51	39	1.63	7.22	4.43
28	130	23	2.90	6.17	4.54
29	52	39	3.18	6.42	4.80
30	43	33	7.94	1.89	4.92
31	94	21	9.26	1.08	5.17
32	124	21	0.22	10.45	5.34
33	11	11	2.23	8.70	5.47
34	109	22	9.36	1.91	5.64
35	133	23	11.12	0.20	5.66
36	149	27	0.49	10.92	5.71
37	90	28	2.56	8.98	5.77
38	119	21	8.28	3.38	5.83
39	96	28	7.80	4.25	6.03
40	6	11	6.85	6.63	6.74
41	138	25	3.61	10.02	6.82
42	155	23	3.54	10.14	6.84
43	164	26	12.55	1.13	6.84
44	116	29	8.72	4.98	6.85

TABLE C1 (continued) Rank order of monitoring stations according to the first scheme (errors and PI in μg/m³)

Rank	Station #	Code	2nd Q. Error	3rd Q. Error	PI
45	74	31	3.46	10.40	6.93
46	86	28	5.47	8.46	6.97
47	27	32	7.56	6.38	6.97
48	80	21	0.92	13.25	7.09
49	126	24	14.09	1.05	7.57
50	110	22	0.98	14.19	7.59
51	159	25	7.97	7.33	7.65
52	139	24	8.01	7.49	7.75
53	50	38	8.31	7.33	7.82
54	57	33	9.43	6.23	7.83
55	30	39	6.81	8.97	7.89
56	122	21	9.20	6.59	7.90
57	19	11	7.66	8.68	8.17
58	13	11	8.54	8.31	8.44
59	136	24	4.72	12.21	8.47
60	144	23	1.35	16.07	8.71
61	135	26	13.88	4.45	9.17
62	5	11	8.40	10.03	9.22
63	73	33	8.70	9.75	9.23
64	12	11	10.21	8.29	9.98
65	131	26	0.70	18.43	9.57
66	87	28	17.17	1.97	9.57

TABLE C1 (continued) Rank order of monitoring stations according to the first scheme (errors and PI in μg/m^3)

Rank	Station #	Code	2nd Q. Error	3rd Q. Error	PI
67	70	32	7.75	11.78	9.77
68	111	28	13.67	6.08	9.88
69	46	34	4.10	15.86	9.98
70	83	28	13.71	6.30	10.01
71	104	21	7.27	12.96	10.12
72	98	28	9.25	11.29	10.27
73	2	11	9.89	11.01	10.45
74	66	38	6.48	14.77	10.63
75	95	28	13.96	7.61	10.79
76	161	26	7.84	14.24	11.04
77	76	38	14.88	7.41	11.15
78	160	25	16.87	5.72	11.30
79	49	38	13.85	9.15	11.50
80	142	25	11.58	11.56	11.57
81	67	32	15.13	8.29	11.71
82	82	28	12.84	11.42	12.13
83	141	26	7.10	17.47	12.29
84	128	25	10.99	14.60	12.80
85	3	11	10.06	15.62	12.84
86	147	25	17.29	8.53	12.91
87	63	39	14.72	11.87	13.30
88	158	25	3.99	22.86	13.43

TABLE C1 (continued) Rank order of monitoring stations according to the first scheme (errors and PI in μg/m³)

Rank	Station #	Code	2nd Q. Error	3rd Q. Error	PI
89	121	21	11.08	15.94	13.51
90	92	21	18.89	8.27	13.58
91	88	28	18.48	8.95	13.72
92	4	11	22.72	5.14	13.93
93	64	34	20.41	7.81	14.11
94	26	39	18.05	12.27	15.16
95	157	25	7.87	22.58	15.23
96	89	28	22.15	8.33	15.24
97	91	21	17.53	13.49	15.51
98	146	25	6.94	24.32	15.63
99	127	23	12.30	20.36	16.33
100	31	38	2.71	30.65	16.68
101	61	34	15.58	17.87	16.73
102	75	38	18.56	15.06	16.81
103	47	38	16.45	17.45	16.95
104	162	26	1.13	32.97	17.05
105	71	34	22.27	12.20	17.24
106	151	27	12.35	24.14	18.25
107	148	27	9.70	26.84	18.27
108	105	21	24.11	12.63	18.37
109	100	21	10.99	27.00	19.00
110	44	32	31.92	7.80	19.86

TABLE C1 (continued) Rank order of monitoring stations according to the first scheme (errors and PI in μg/m^3)

Rank	Station #	Code	2nd Q. Error	3rd Q. Error	PI
111	72	31	22.25	18.66	20.46
112	10	11	23.52	17.93	20.73
113	154	24	26.47	16.11	21.29
114	45	32	33.06	11.35	22.21
115	114	22	24.74	20.39	22.57
116	134	26	24.25	21.68	22.97
117	42	32	34.62	13.19	23.91
118	33	36	27.76	20.62	24.19
119	150	27	12.36	46.48	29.42
120	140	26	28.53	31.44	29.99
121	17	11	62.19	8.01	35.1
122	40	31	37.19	36.27	36.73
123	163	25	42.06	36.05	39.06
124	54	33	62.67	15.85	39.26
125	120	21	33.68	46.38	40.03
126	132	25	31.07	49.61	40.34
127	16	11	82.17	5.09	43.63
128	38	36	54.49	47.67	51.08
129	35	33	61.83	56.38	59.11
130	34	33	88.67	85.79	87.23

TABLE C2 Rank order of monitoring stations according to the second scheme (mean error and PI in μg/m3)

Rank	Station #	Code	# Receptors	Mean Error	PI
1	42	32	0	0.0	0.0
2	135	26	0	0.0	0.0
3	8	11	1	0.155	0.155
4	129	24	2	0.332	0.664
5	106	21	2	0.503	1.006
6	137	25	2	0.573	1.146
7	6	11	2	0.746	1.492
8	133	23	2	0.948	1.896
9	146	25	2	0,972	1.944
10	89	28	2	0.974	1.948
11	101	24	1	2.026	2.026
12	144	23	1	2.181	2.181
13	102	24	1	2.673	2.673
14	134	26	2	1.394	2.788
15	113	29	3	0.953	2.859
16	46	34	2	1.458	2.916
17	136	24	1	3.252	3.252
18	112	21	2	1.731	3.462
19	160	25	3	1.251	3.753
20	90	28	3	1.315	3.945
21	103	21	6	0.665	3.990
22	111	28	3	1.438	4.314

TABLE C2 (continued) Rank order of monitoring stations according to the second scheme (mean error and PI in μg/m3)

Rank	Station #	Code	# Receptors	Mean Error	PI
23	85	28	2	2.189	4.378
24	60	38	2	2.403	4.806
25	155	23	2	2.471	4.942
26	159	25	2	2.791	5.582
27	152	27	2	2.818	5.636
28	91	21	2	3.096	6.192
29	139	24	2	3.155	6.310
30	118	29	8	0.795	6.360
31	119	21	4	1.680	6.720
32	161	26	2	3.444	6.888
33	141	26	2	3.488	6.976
34	31	38	2	3.569	7.138
35	117	29	8	0.895	7.160
36	115	29	7	1.081	7.567
37	126	24	2	3.802	7.604
38	157	25	1	7.640	7.640
39	86	28	2	3.997	7.994
40	79	29	8	1.001	8.008
41	123	22	4	2.028	8.112
42	151	27	4	2.030	8.120
43	9	11	5	1.667	8.335
44	127	23	5	1.683	8.415

TABLE C2 (continued) Rank order of monitoring stations according to the second scheme (mean error and PI in $\mu g/m^3$)

Rank	Station #	Code	# Receptors	Mean Error	PI
45	164	26	3	2.857	8.571
46	69	38	9	0.976	8.784
47	131	26	4	2.461	9.844
48	19	11	3	3.282	9.846
49	30	39	5	1.980	9.900
50	92	21	2	5.020	10.04
51	100	21	3	3.567	10.70
52	76	38	3	3.592	10.78
53	132	25	1	10.965	10.97
54	153	27	5	2.231	11.16
55	43	33	2	5.698	11.40
56	149	27	3	3.935	11.81
57	147	25	1	11.844	11.84
58	122	21	7	1.708	11.96
59	82	28	6	2.020	12.12
60	148	27	1	12.888	12.89
61	99	28	11	1.175	12.93
62	87	28	2	6.534	13.07
63	138	25	3	4.389	13.17
64	158	25	3	4.568	13.70
65	52	39	6	2.342	14.05
66	70	32	4	3.584	14.34

TABLE C2 (continued) Rank order of monitoring stations according to the second scheme (mean error and PI in $\mu g/m^3$)

Rank	Station #	Code	# Receptors	Mean Error	PI
67	156	23	7	2.056	14.39
68	130	23	6	2.404	14.42
69	37	31	3	5.002	15.01
70	10	11	4	3.788	15.15
71	11	11	3	5.290	15.87
72	128	25	2	7.996	15.99
73	110	22	6	2.675	16.05
74	27	32	2	8.064	16.13
75	7	11	6	2.709	16.25
76	142	25	3	5.490	16.47
77	109	22	7	2.365	16.56
78	83	28	5	3.341	16.71
79	94	21	4	4.177	16.71
80	124	21	4	4.193	16.77
81	96	28	6	2.851	17.11
82	71	34	2	8.681	17.36
83	2	11	9	2.025	18.23
84	74	31	9	2.068	18.61
85	162	26	3	6.251	18.75
86	154	24	3	6.315	18.95
87	120	21	2	9.702	19.40
88	61	34	8	2.470	19.76

TABLE C2 (continued) Rank order of monitoring stations according to the second scheme (mean error and PI in $\mu g/m^3$) .

Rank	Station #	Code	# Receptors	Mean Error	PI
89	3	11	7	2.840	19.88
90	150	27	3	6.643	19.93
91	95	28	9	2.243	20.19
92	44	32	3	7.303	21.91
93	116	29	8	2.764	22.11
94	64	34	6	3.750	22.50
95	50	38	10	2.334	23.34
96	45	32	3	7.973	23.92
97	80	21	5	4.855	24.28
98	121	21	3	8.278	24.83
99	88	28	6	4.157	24.94
100	105	21	3	8.555	25.67
101	104	21	7	3.803	26.62
102	36	31	10	2.747	27.47
103	13	11	7	4.072	28.50
104	67	32	5	5.919	29.60
105	12	11	9	3.428	30.85
106	98	28	7	4.433	31.03
107	163	25	1	31.464	31.46
108	75	38	5	6.335	31.68
109	51	39	8	4.227	33.82
110	66	38	9	3.790	34.11

TABLE C2 (continued) Rank order of monitoring stations according to the second scheme (mean error and PI in $\mu g/m^3$)

Rank	Station #	Code	# Receptors	Mean Error	PI
111	57	33	7	5.097	35.679
112	49	38	10	3.603	36.03
113	140	26	2	18.840	37.68
114	26	39	6	6.303	37.82
115	35	33	7	5.755	40.29
116	72	31	11	3.956	43.52
117	5	11	9	5.068	45.61
118	73	33	10	4.686	46.86
119	68	37	9	5.643	50.79
120	114	22	6	8.703	52.22
121	47	38	8	6.677	53.42
122	40	31	6	8.909	53.45
123	4	11	6	9.476	56.86
124	63	39	11	5.371	59.08
125	17	11	7	9.863	69.04
126	38	36	7	13.737	96.16
127	54	33	6	19.170	115.02
128	16	11	10	14.973	149.73
129	33	36	11	14.301	157.31
130	34	33	7	27.421	191.95

TABLE C3 Rank order of monitoring stations according to the third scheme (mean error and PI in μg/m^3)

Rank	Station #	Code	# Receptors	Mean Error	PI
1	42	32	0	0.0	0.0
2	135	26	0	0.0	0.0
3	8	11	1	0.155	0.155
4	106	21	2	0.461	0.922
5	129	24	2	0.502	1.004
6	137	25	2	0.573	1.146
7	133	23	2	0.709	1.418
8	146	25	2	0.972	1.944
9	89	28	2	0.974	1.948
10	6	11	3	0.687	2.061
11	144	23	2	1.224	2.448
12	159	25	2	1.292	2.584
13	102	24	1	2.612	2.612
14	136	24	1	2.708	2.708
15	134	26	2	1.394	2.788
16	113	29	3	0.953	2.859
17	46	34	2	1.458	2.916
18	85	28	2	1.733	3.466
19	103	21	6	0.665	3.990
20	164	26	3	1.348	4.044
21	161	26	3	1.274	3.822
22	160	25	3	1.520	4.560

TABLE C3 (continued) Rank order of monitoring stations according to the third scheme (mean error and PI in $\mu g/m^3$)

Rank	Station #	Code	# Receptors	Mean Error	PI
23	60	38	2	2.403	4.806
24	90	28	3	1.852	5.556
25	101	24	3	1.994	5.982
26	158	25	3	1.964	5.892
27	118	29	8	0.795	6.360
28	91	21	3	2.162	6.486
29	152	27	2	3.289	6.578
30	31	38	2	3.354	6.708
31	9	11	5	1.402	7.010
32	115	29	8	0.952	7.616
33	123	22	5	1.626	8.130
34	79	29	10	0.877	8.770
35	86	28	5	1.969	9.835
36	30	39	5	1.980	9.900
37	139	24	2	5.219	10.44
38	149	27	4	2.720	10.88
39	147	25	4	2.852	11.41
40	43	33	2	5.726	11.45
41	126	24	3	3.857	11.57
42	153	27	5	2.359	11.80
43	11	11	3	4.229	12.69
44	112	21	5	2.187	10.94

TABLE C3 (continued) Rank order of monitoring stations according to the third scheme (mean error and PI in $\mu g/m^3$)

Rank	Station #	Code	# Receptors	Mean Error	PI
45	19	11	5	2.552	12.76
46	122	21	7	1.880	13.16
47	156	23	7	2.051	14.36
48	52	39	8	1.842	14.74
49	130	23	6	2.509	15.05
50	117	29	10	1.507	15.07
51	141	26	5	3.078	15.39
52	76	38	4	3.950	15.80
53	109	22	10	1.626	16.26
54	132	25	3	5.721	17.16
55	70	32	6	3.022	18.13
56	7	11	7	2.901	20.31
57	83	28	7	2.955	20.69
58	111	28	4	5.249	21.00
59	82	28	11	1.989	21.88
60	69	38	11	2.093	23.02
61	50	38	11	2.095	23.04
62	142	25	6	3.846	23.08
63	100	21	6	3.847	23.08
64	155	23	7	3.309	23.16
65	3	11	8	2.909	23.27
66	154	24	4	5.867	23.47
67	2	11	9	2.661	23.95
68	119	21	9	2.767	24.90

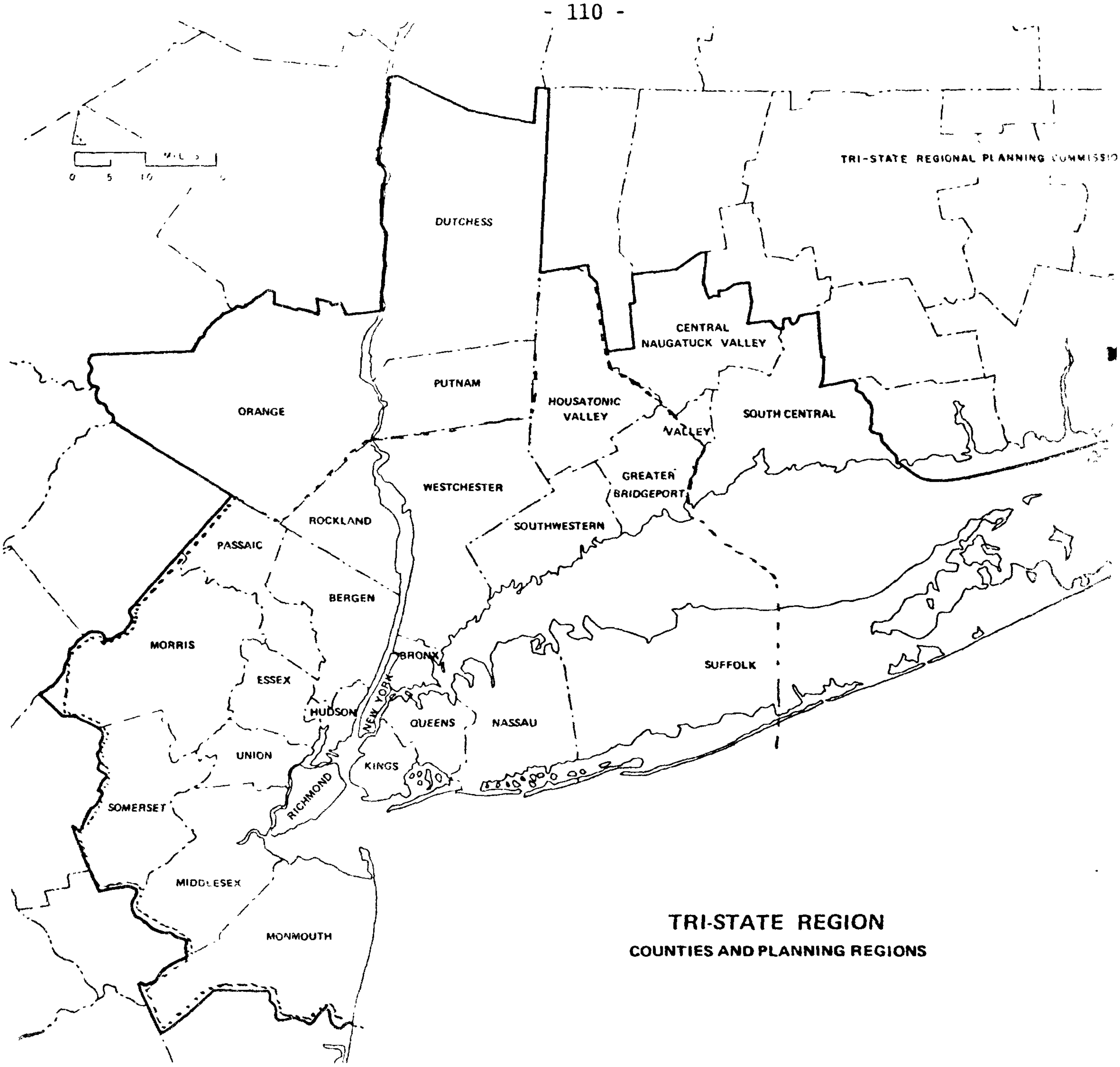

FIGURE 1. Tri-State Regional, SMSA*, and Study Areas

The boundary of the Tri-State Region is indicated by the solid line, whereas that of the study area by the dotted line. The NE New Jersey-New York SMSA is the same as the study area but excluding the Connecticut portion.

*SMSA - Standard Metropolitan Statistical Area

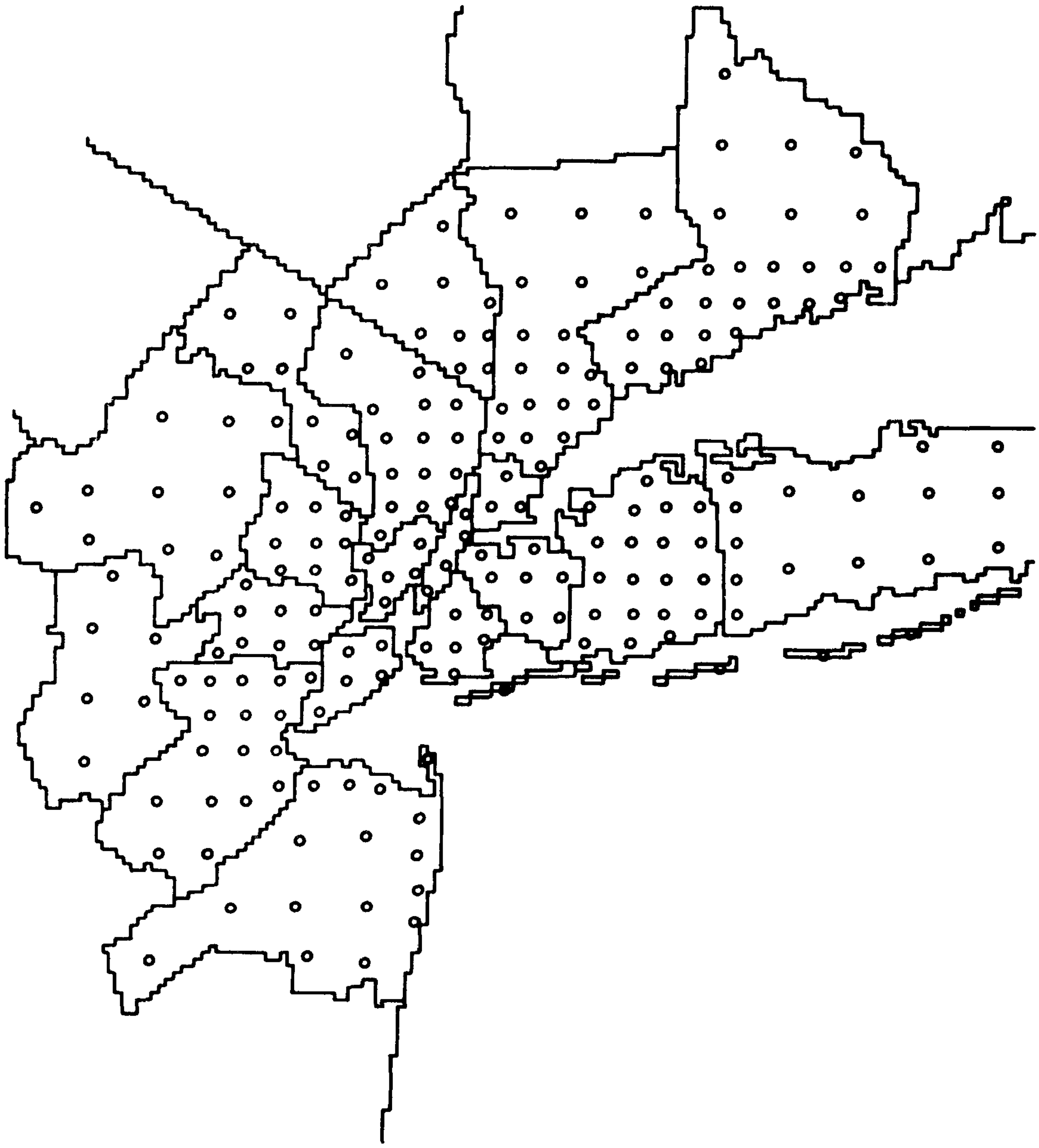

Figure 2: Standard network for environmental management.

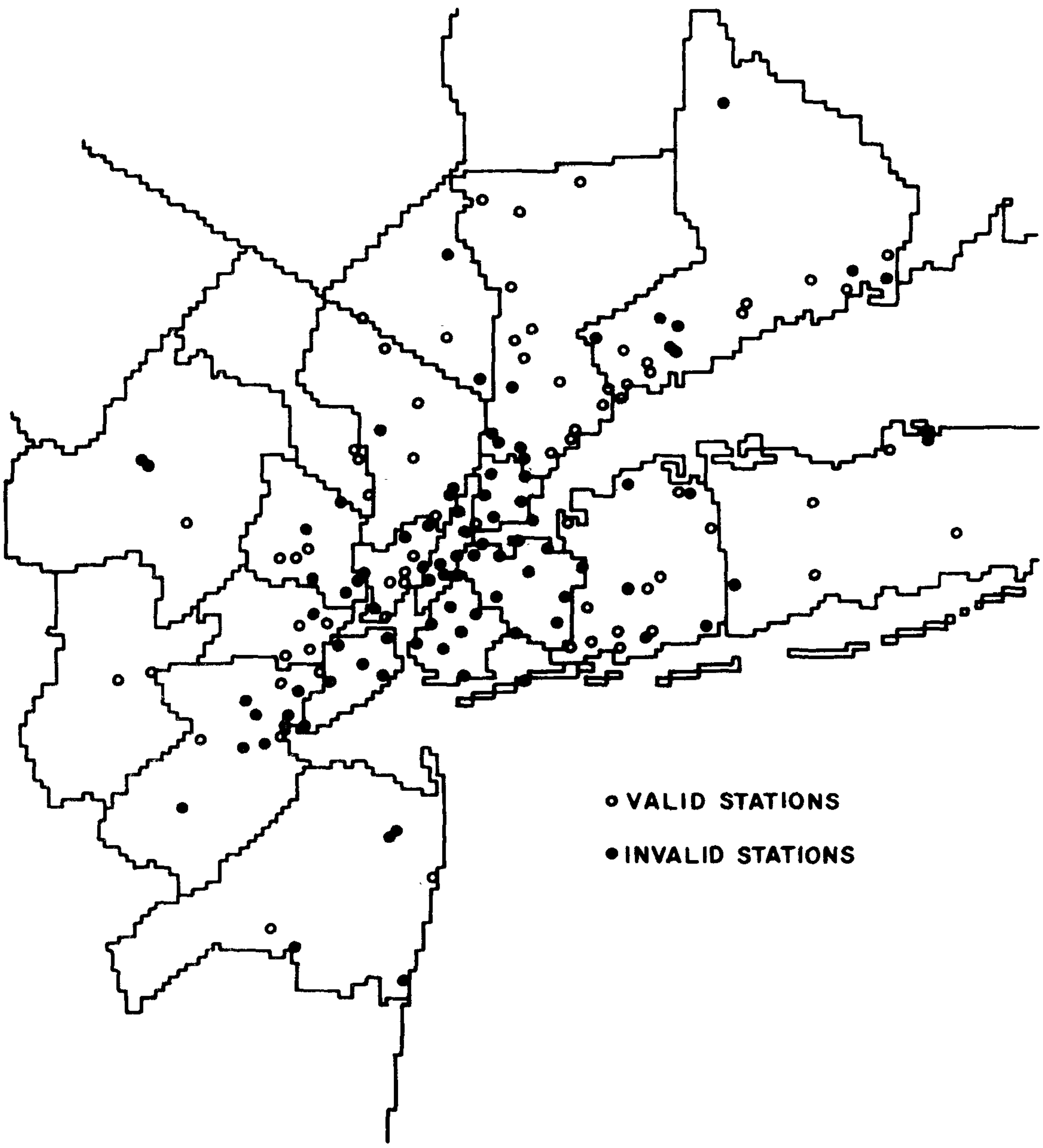

Figure 3: Monitoring stations for the periods 71/2 and 73/2.

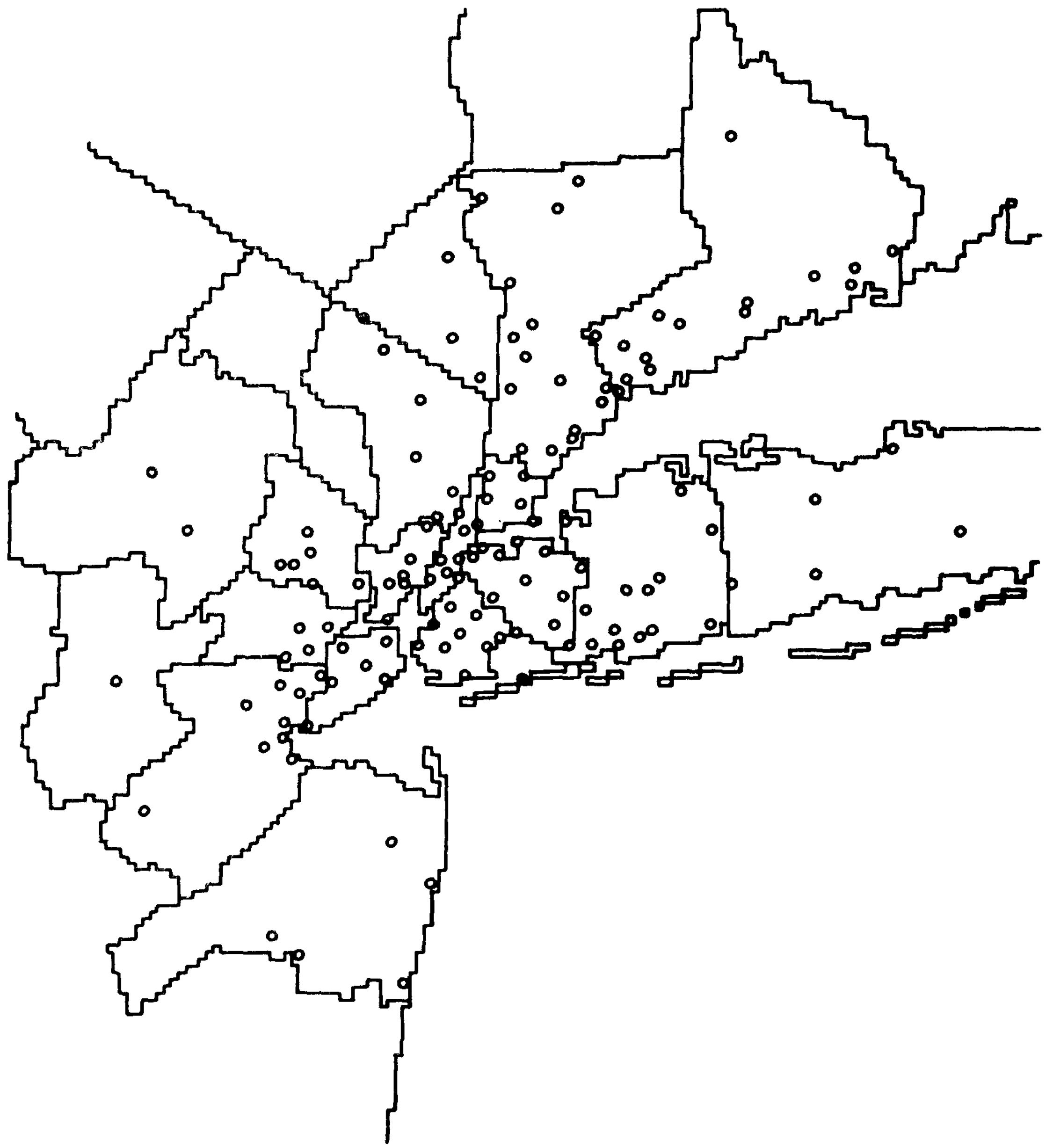

Figure 4: Air monitoring stations reported valid data during 73/2 and 73/3.

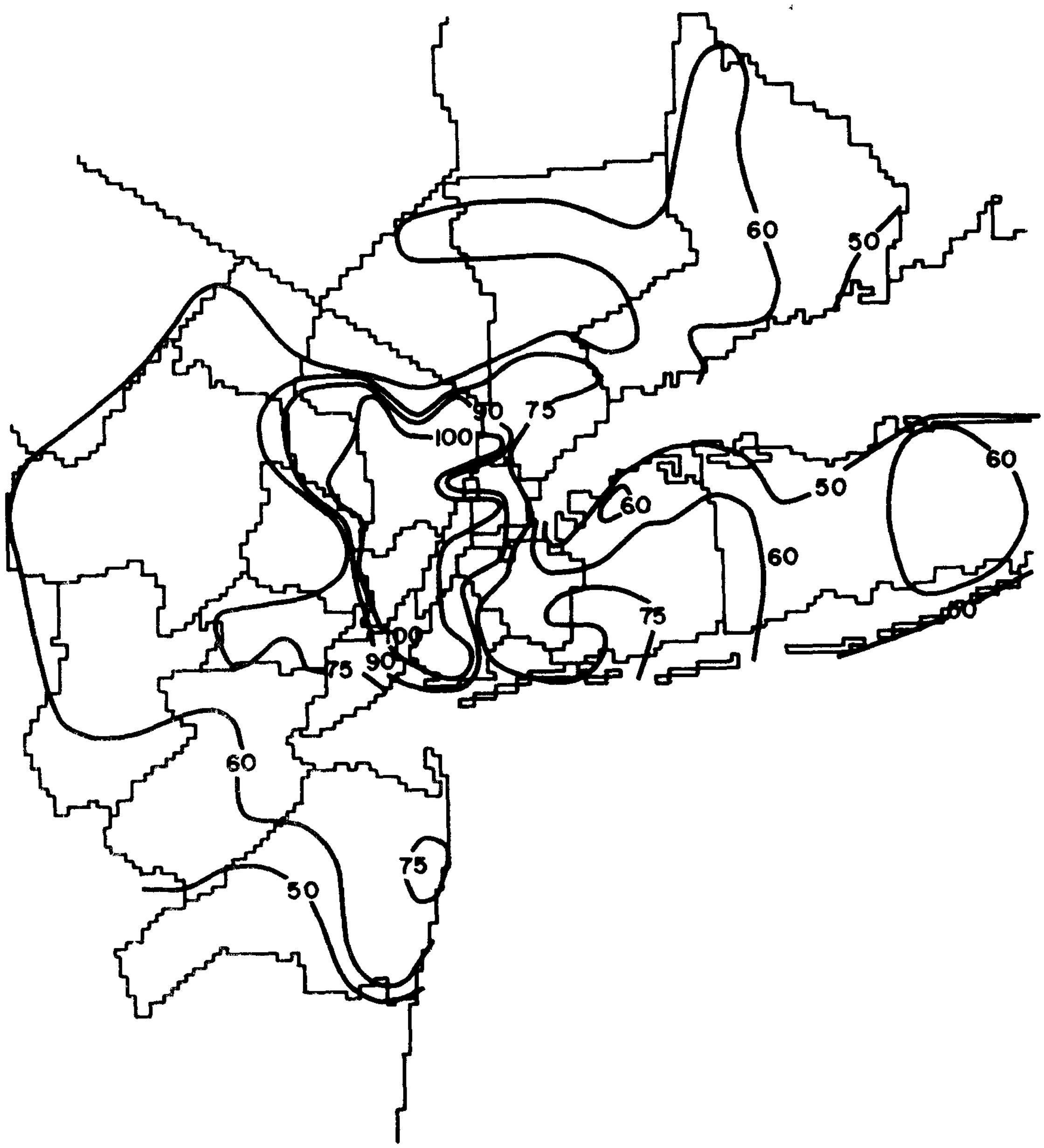

Figure 5: Concentration isopleths in 71/2 ($\mu g/m^3$).

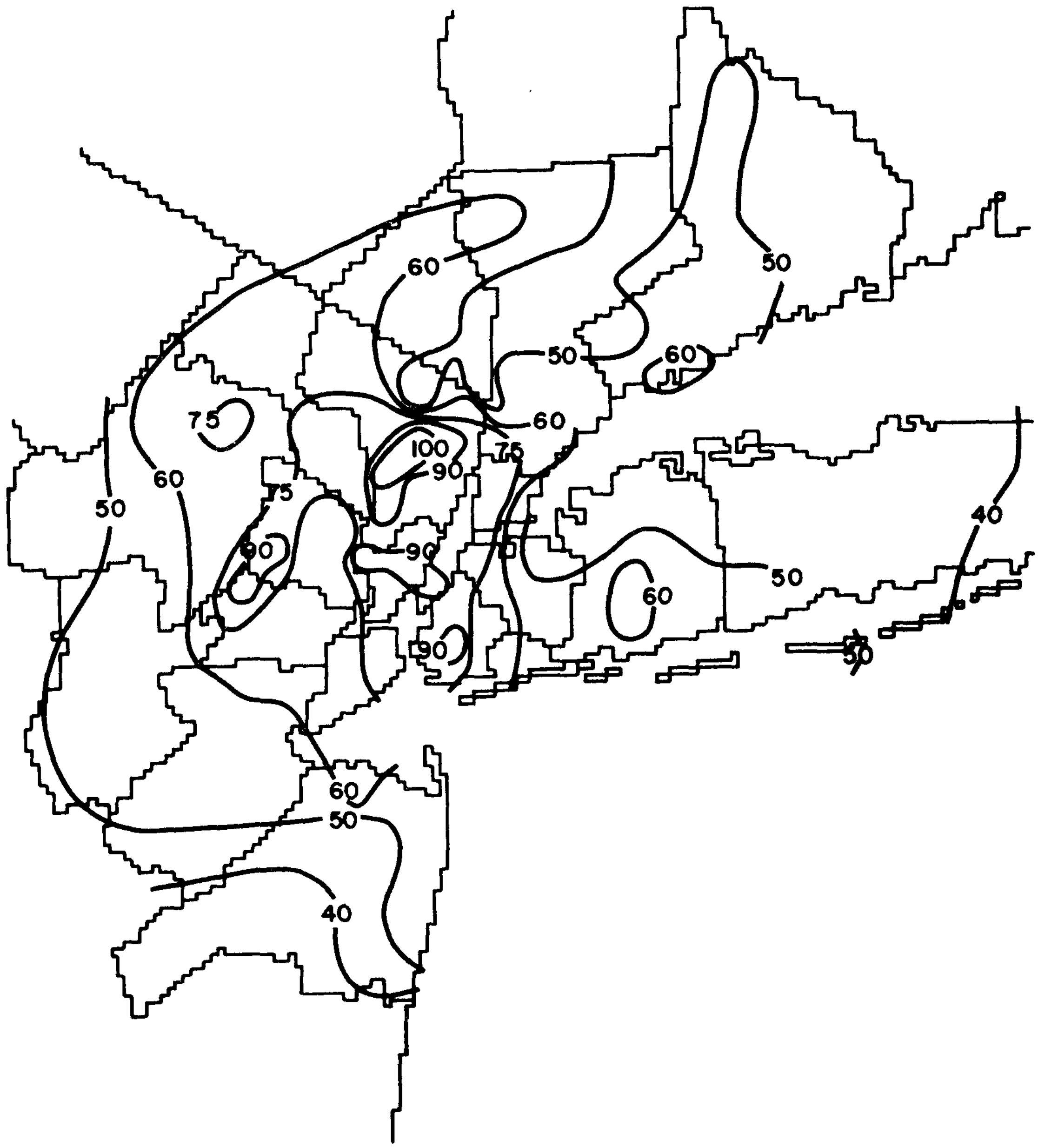

Figure 6. Concentration isopleths in 73/2 ($\mu g/m^3$).

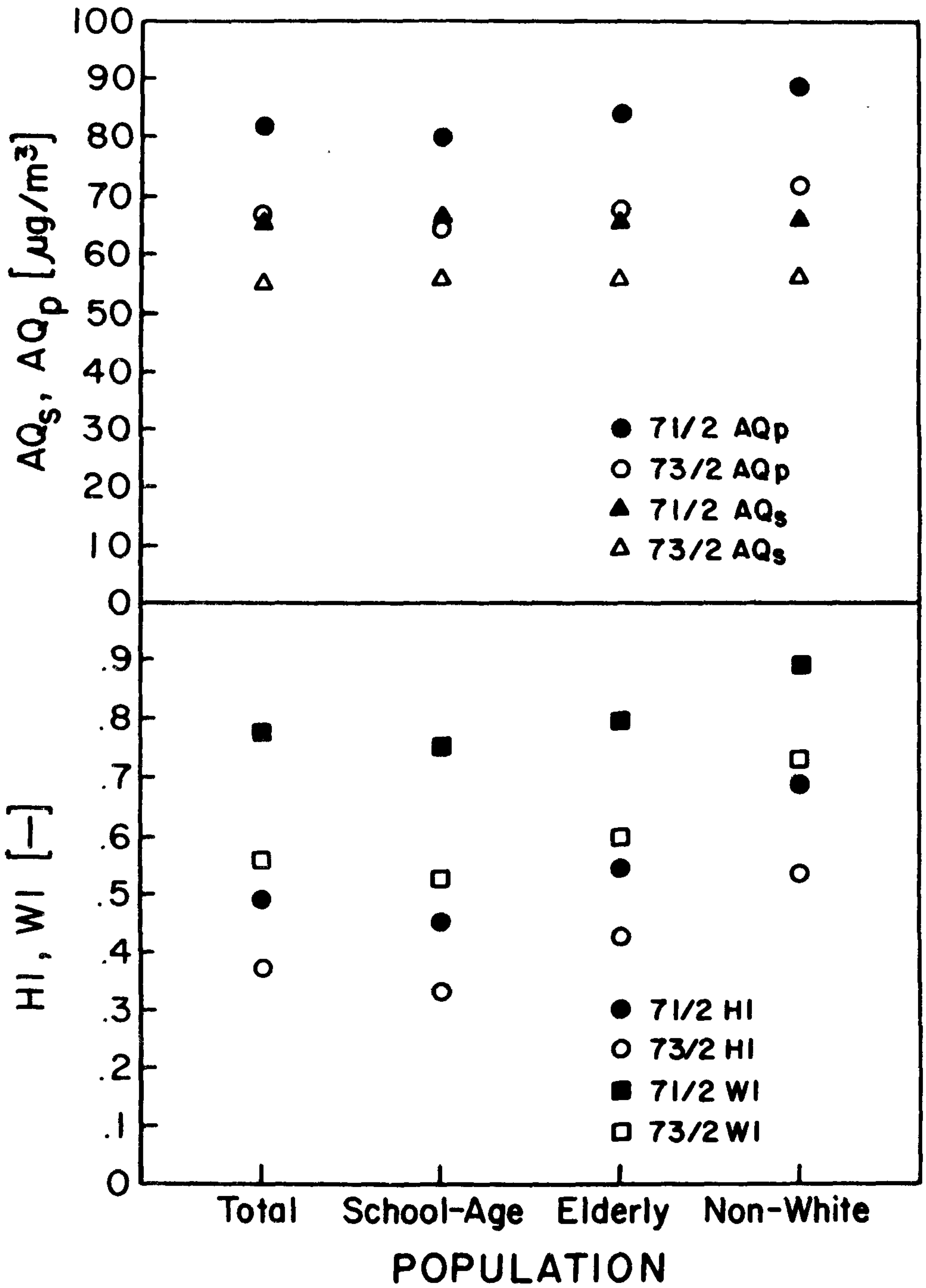

Figure 7: Changes in space average air quality, population average air quality, health index, and welfare index during 71/2 and 73/2.

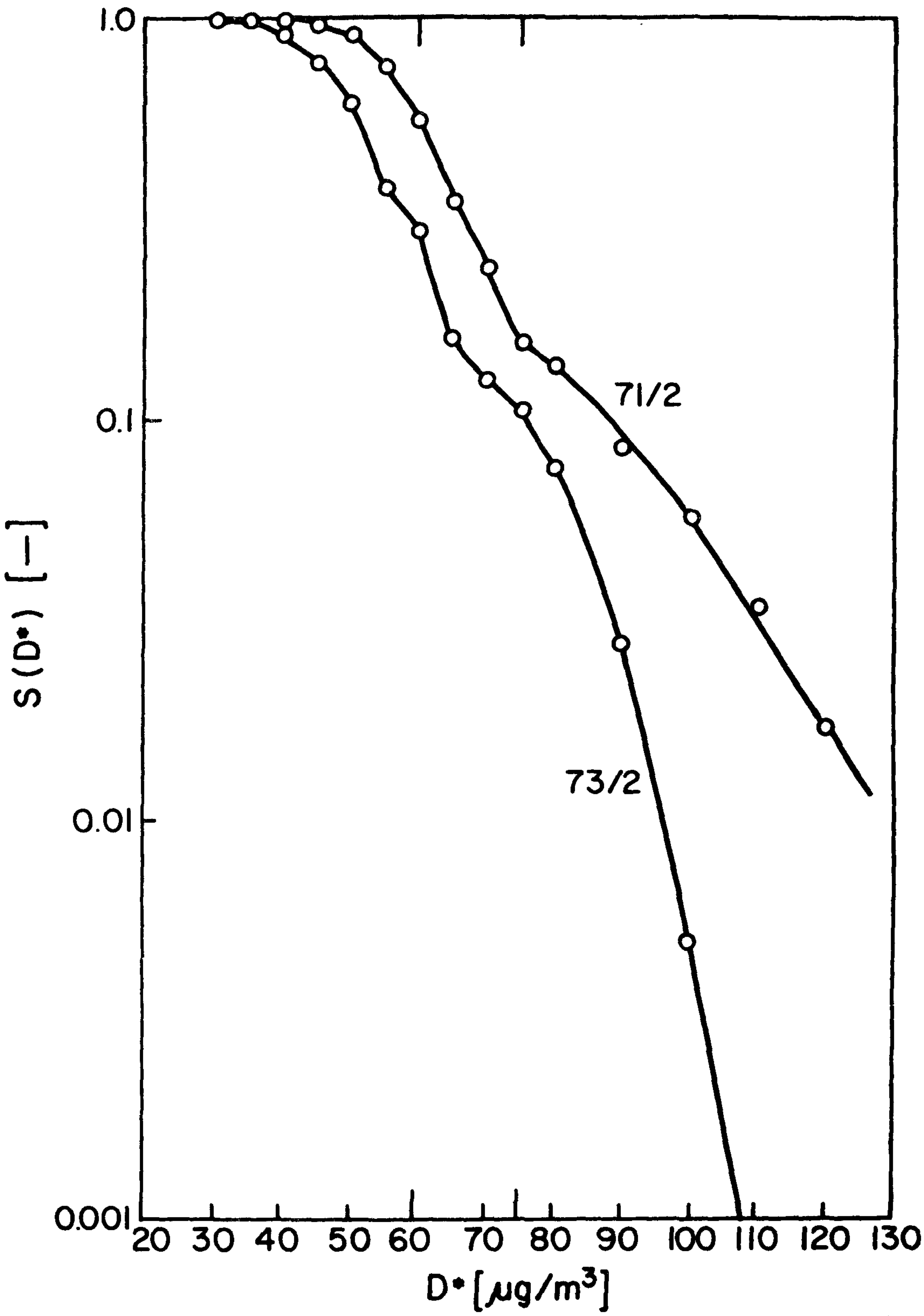

Figure 8: Dosage spectrum distribution in the Tri-State Region.

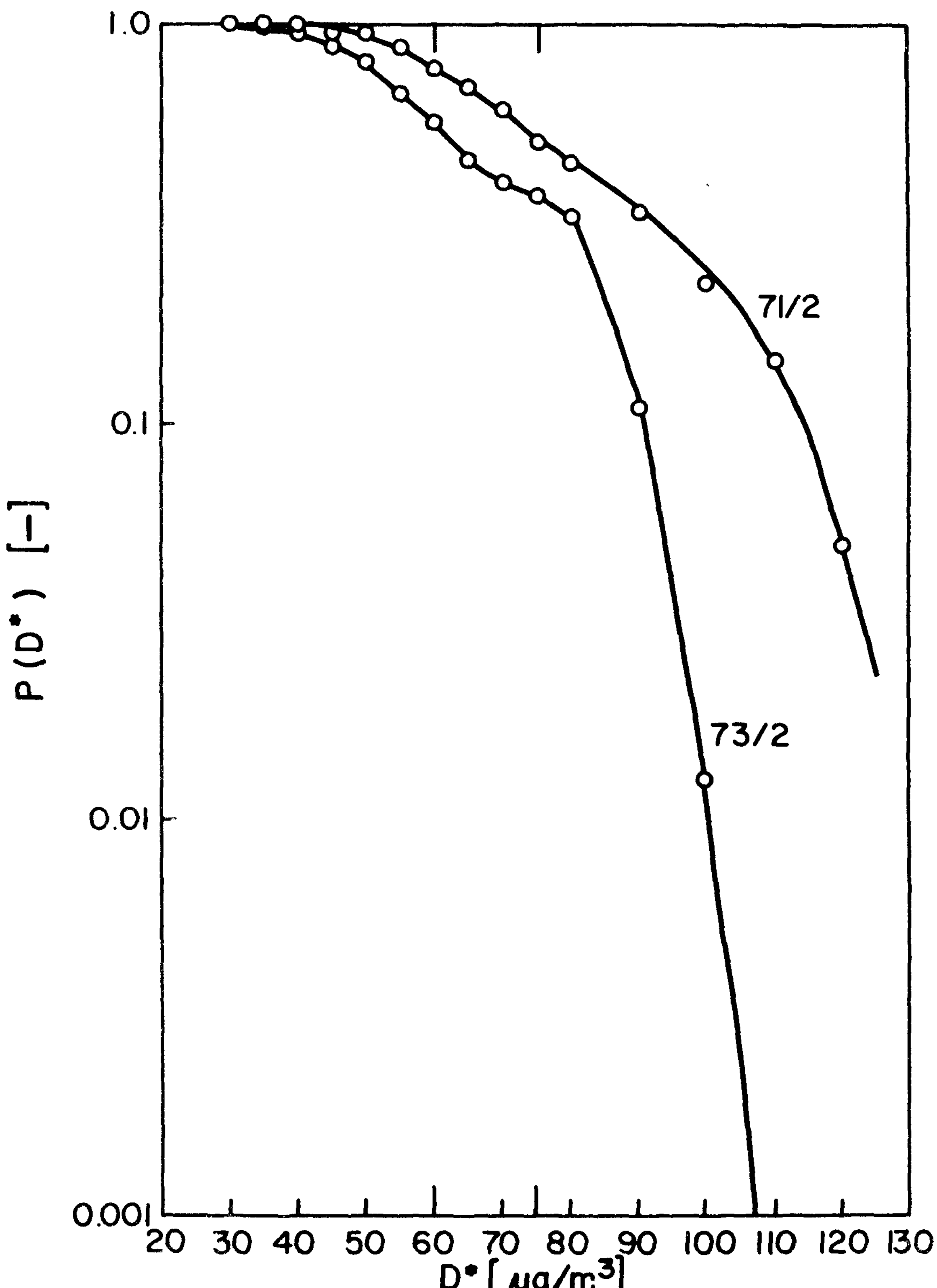

Figure 9: Population dosage spectrum distribution for total population.

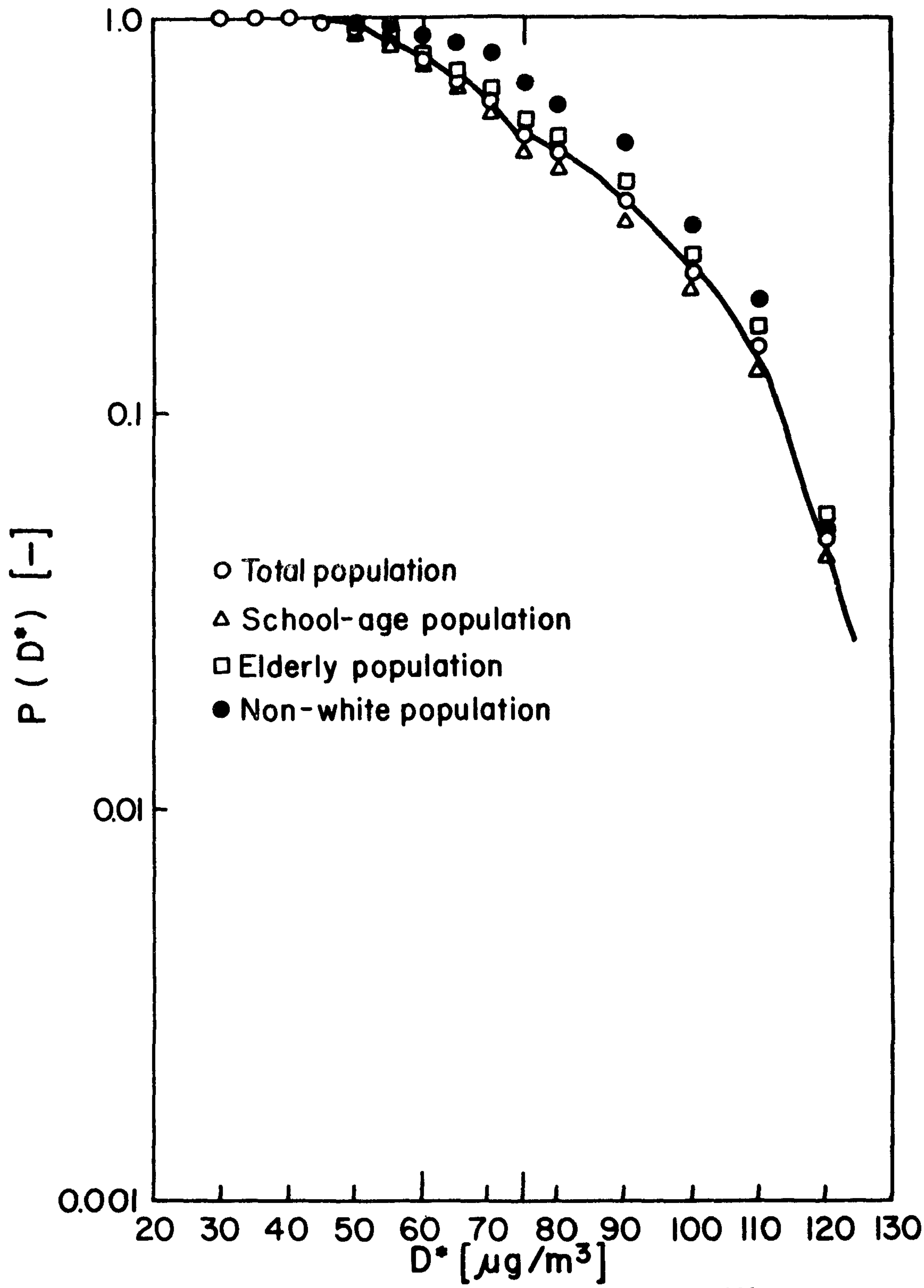

Figure 10: Population dosage spectra for four different populations in 71/2.

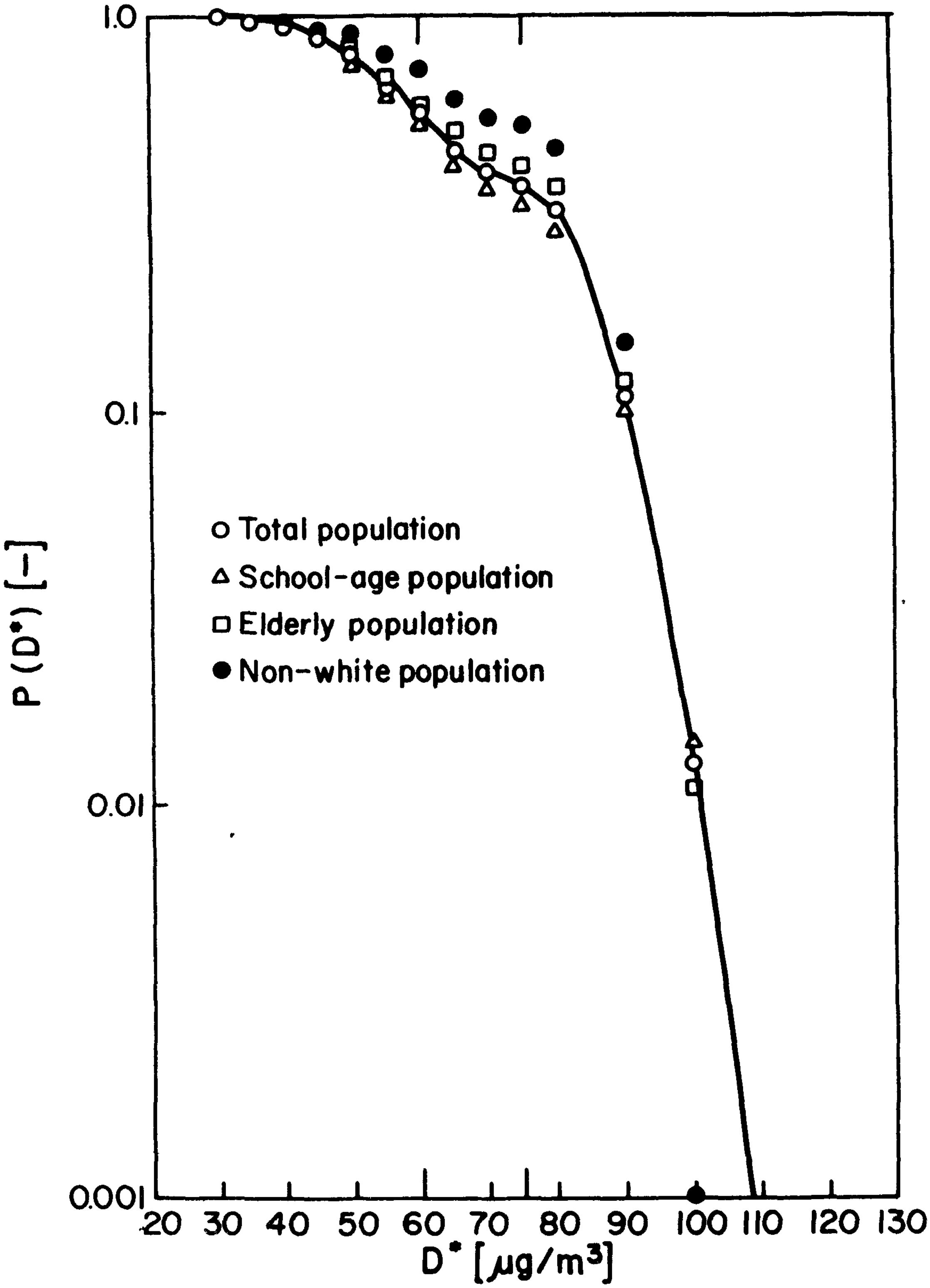

Figure 11: Population dosage spectra for four different populations in 73/2.

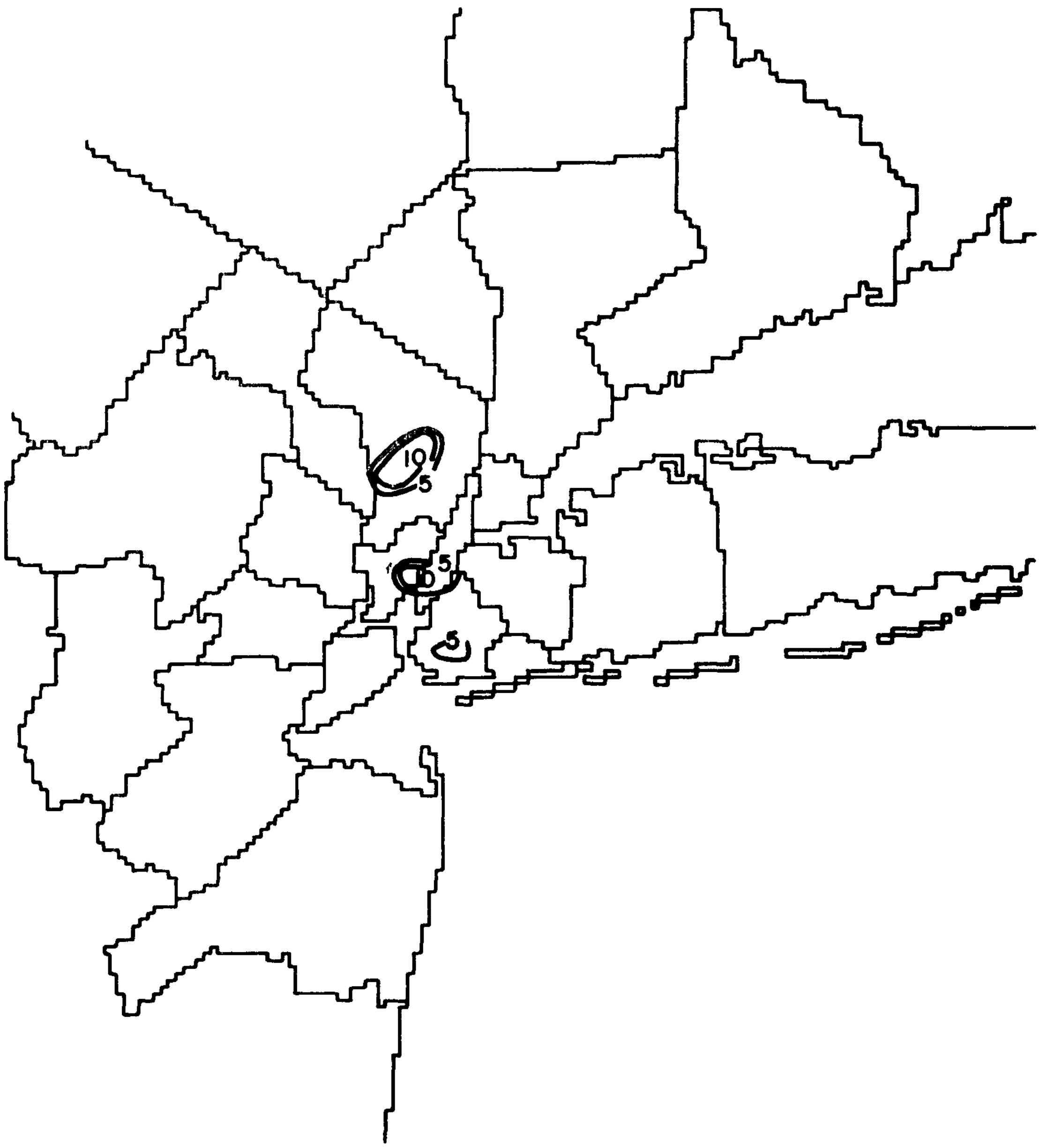

Figure 12: Risk probability of daily concentrations exceeding the primary 24 hour average air quality standard in 71/2.

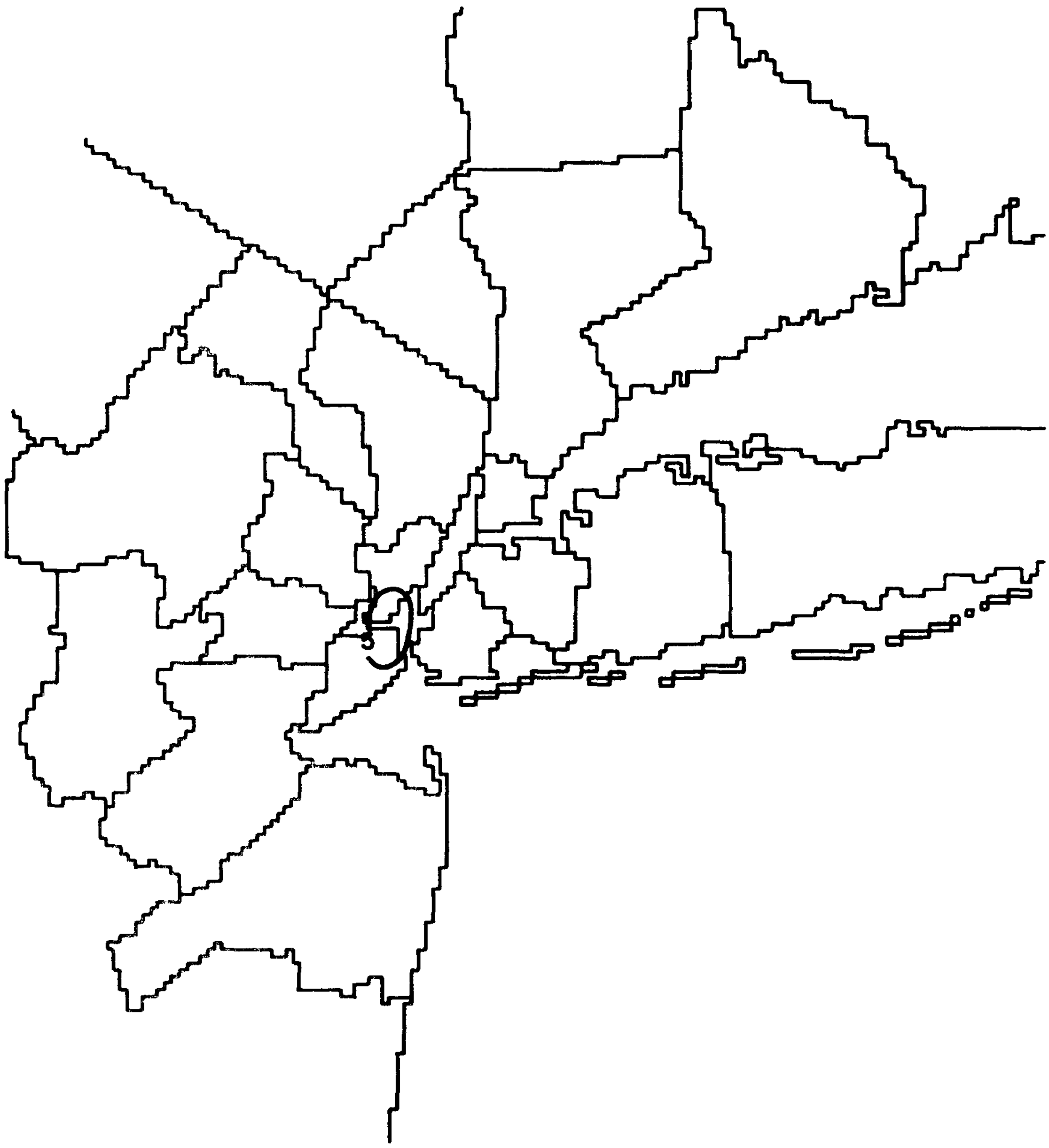

Figure 13: Risk probability of daily concentrations exceeding the level of the primary 24 hour average air quality standard in 73/2.

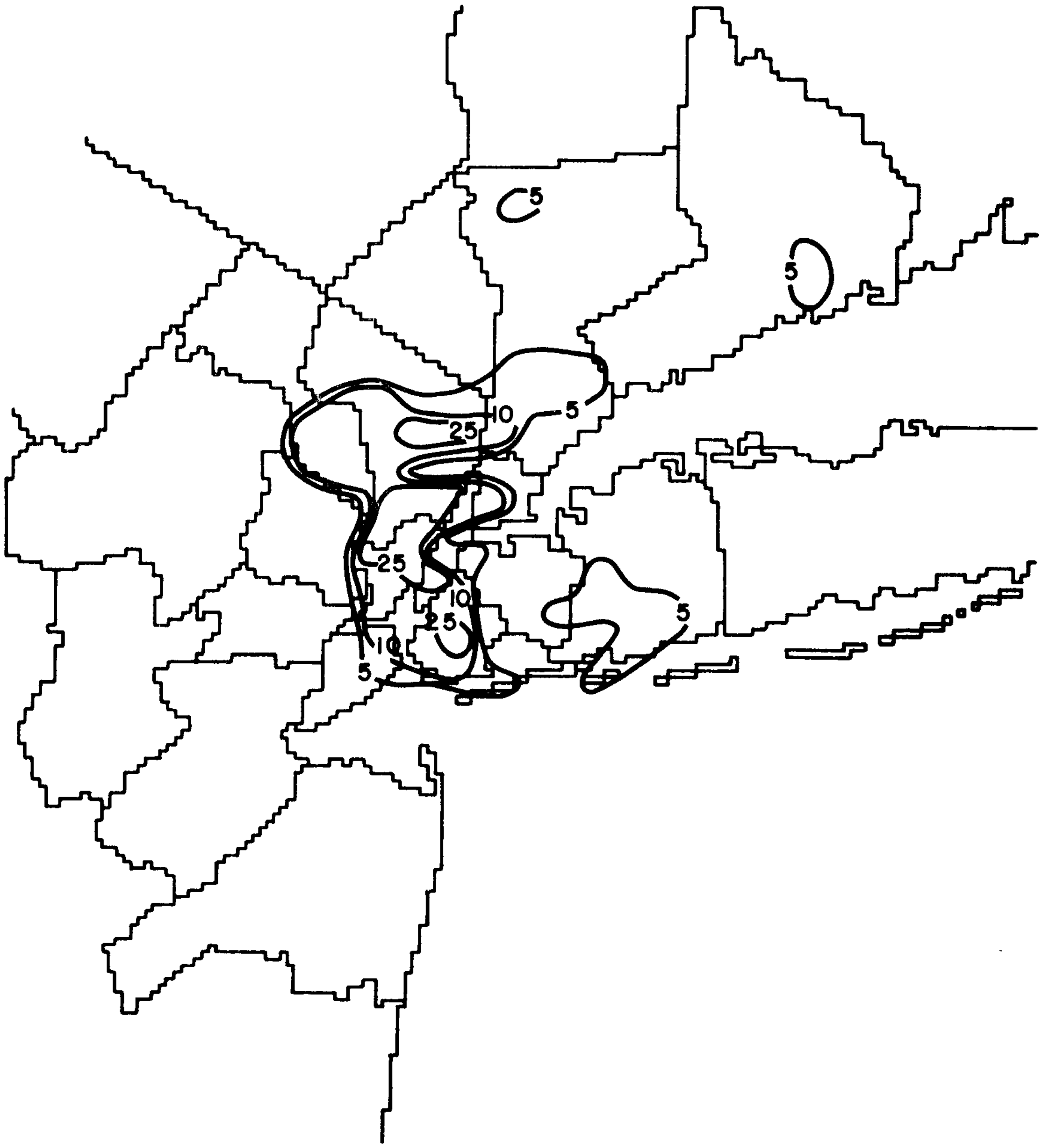

Figure 14: Risk probability of daily concentrations exceeding the secondary 24 hour average air quality standard in 71/2.

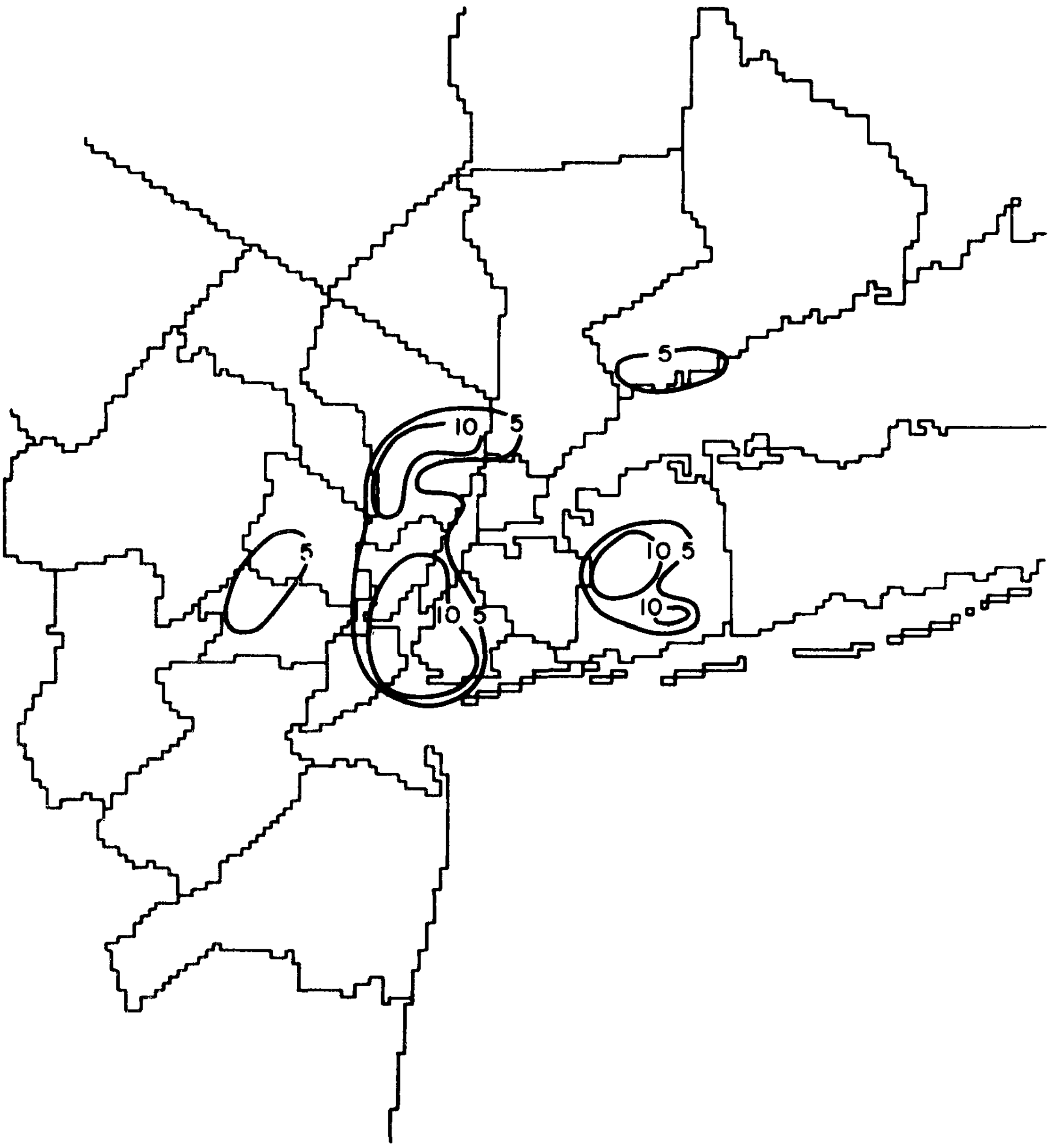

Figure 15: Risk probability of daily concentrations exceeding the secondary 24 hour average air quality standard in 73/2.

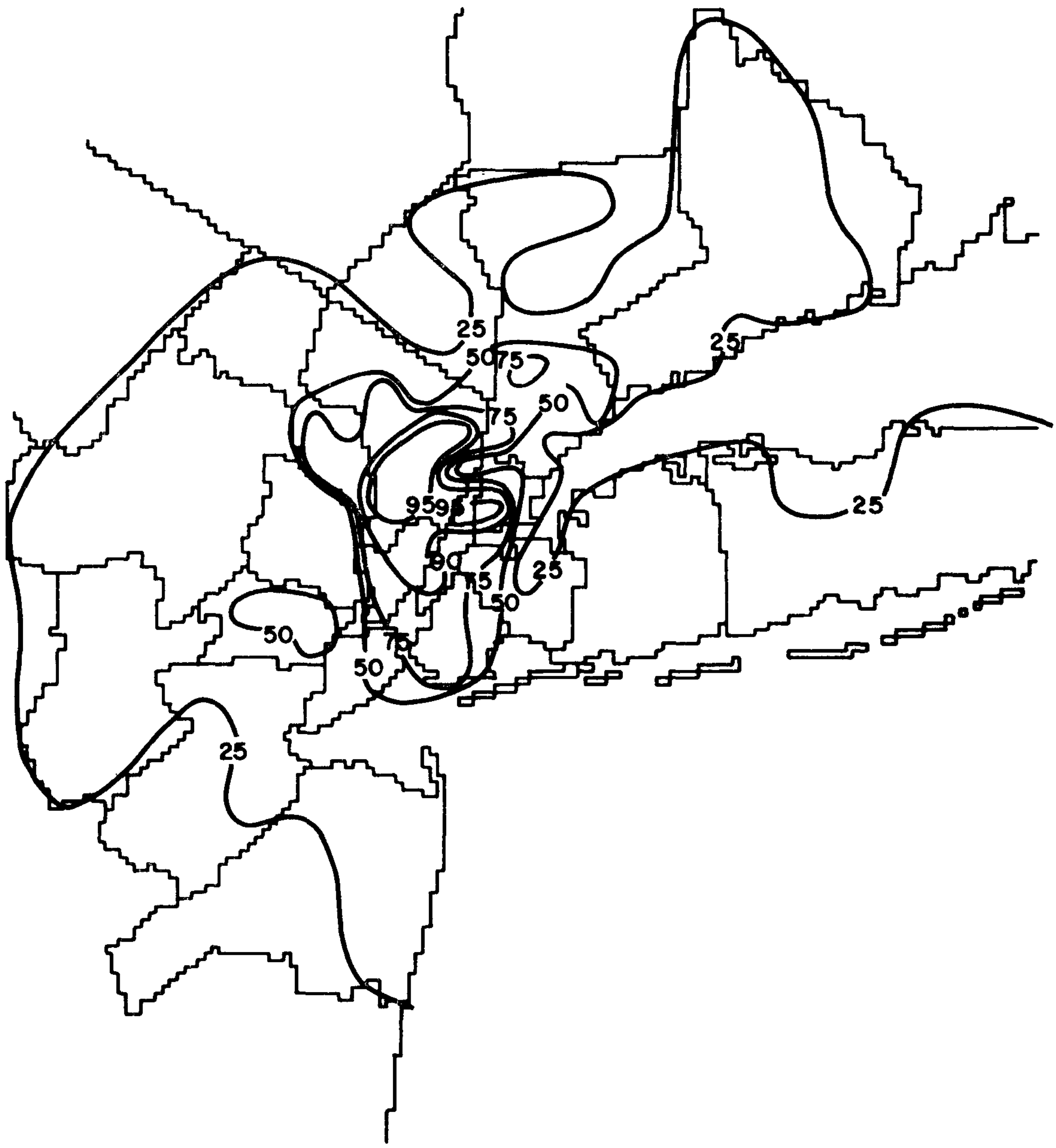

Figure 16: Risk probability of daily concentrations exceeding 75 $\mu g/m^3$ in 71/2.

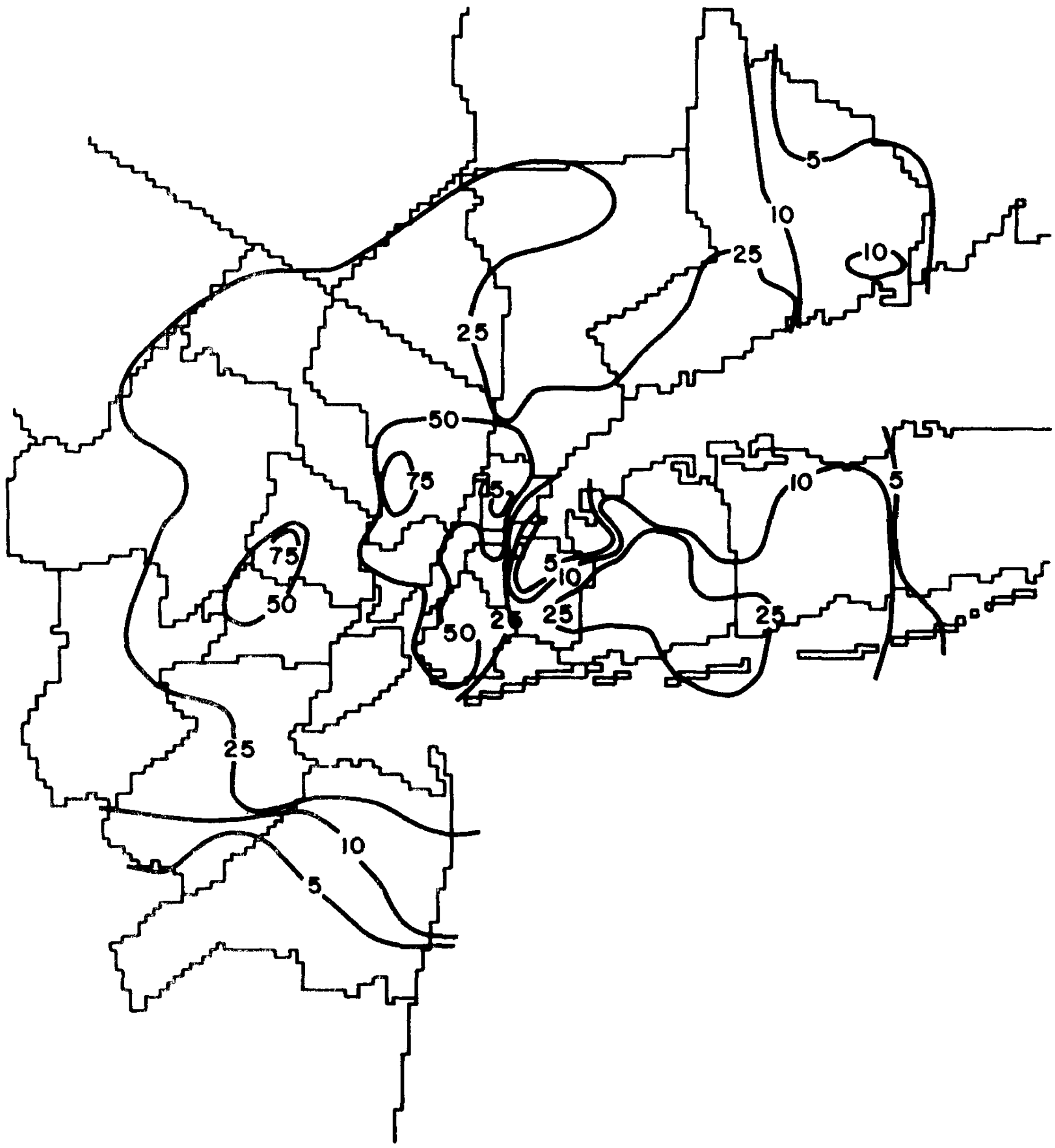

Figure 17: Risk probability of daily concentrations exceeding 75 $\mu g/m^3$ in 73/2.

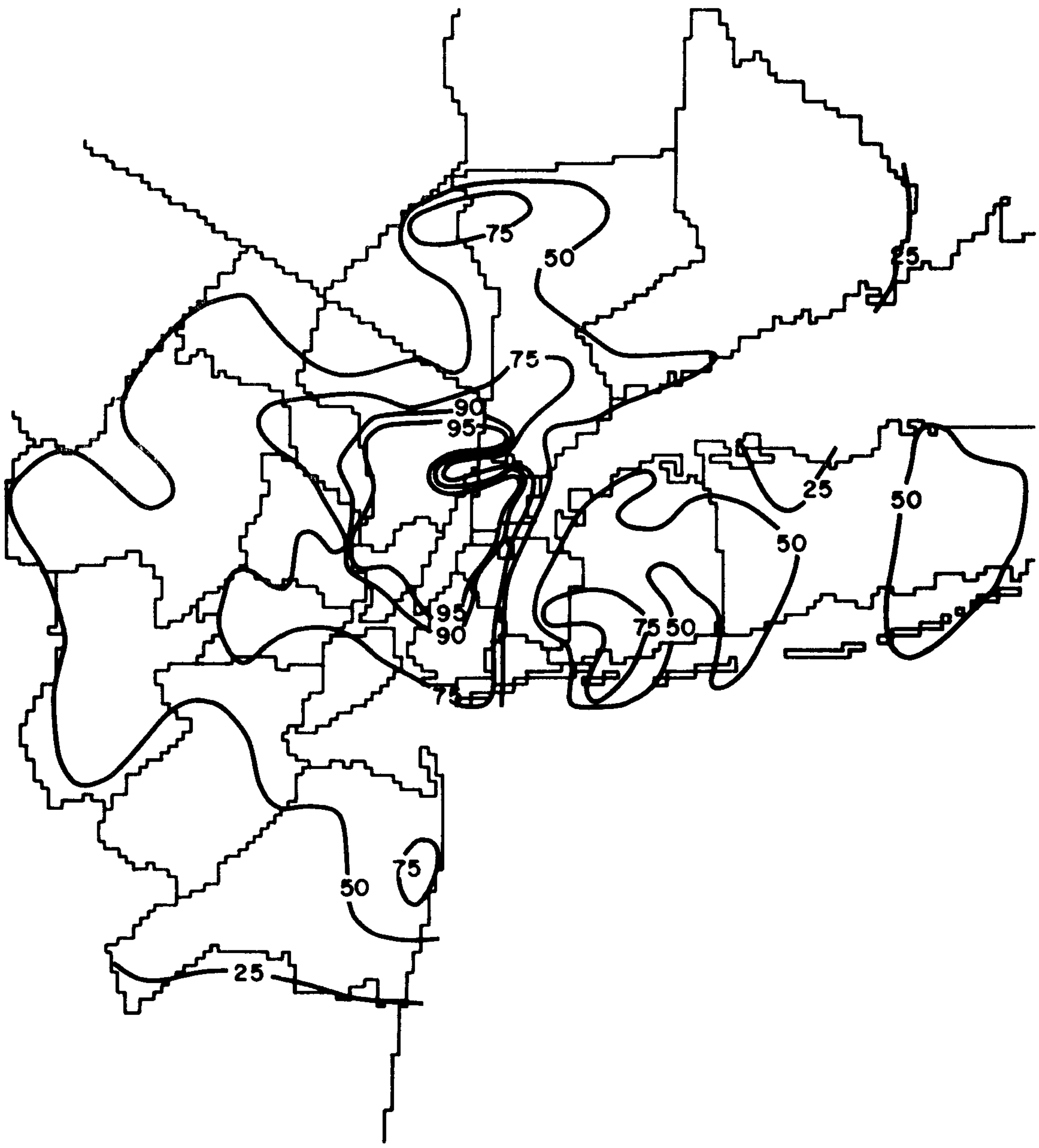

Figure 18: Risk probability of daily concentrations exceeding 60$\mu g/m^3$ in 71/2.

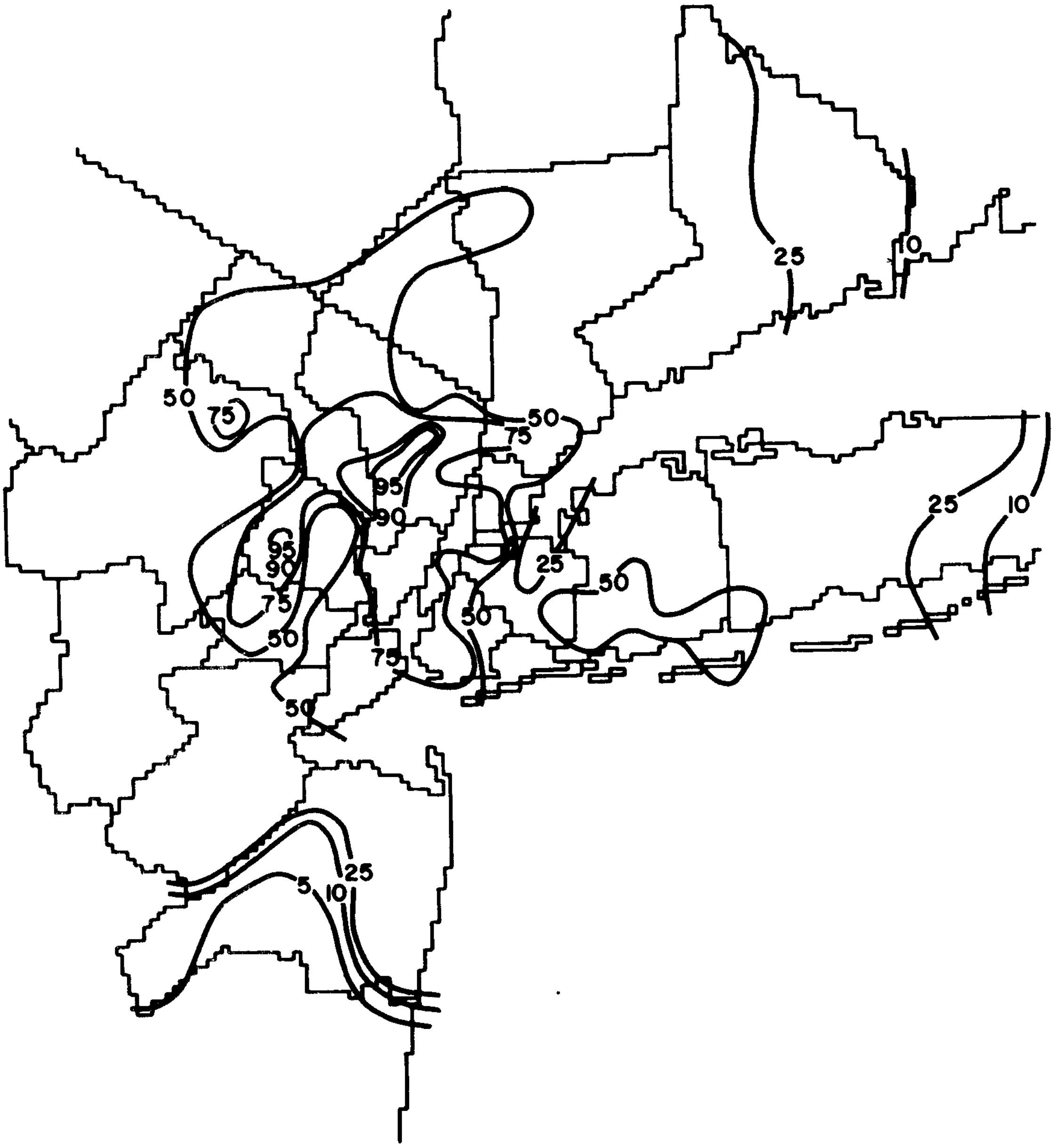

Figure 19: Risk probability of daily concentrations exceeding 60 $\mu g/m^3$ in 73/2.

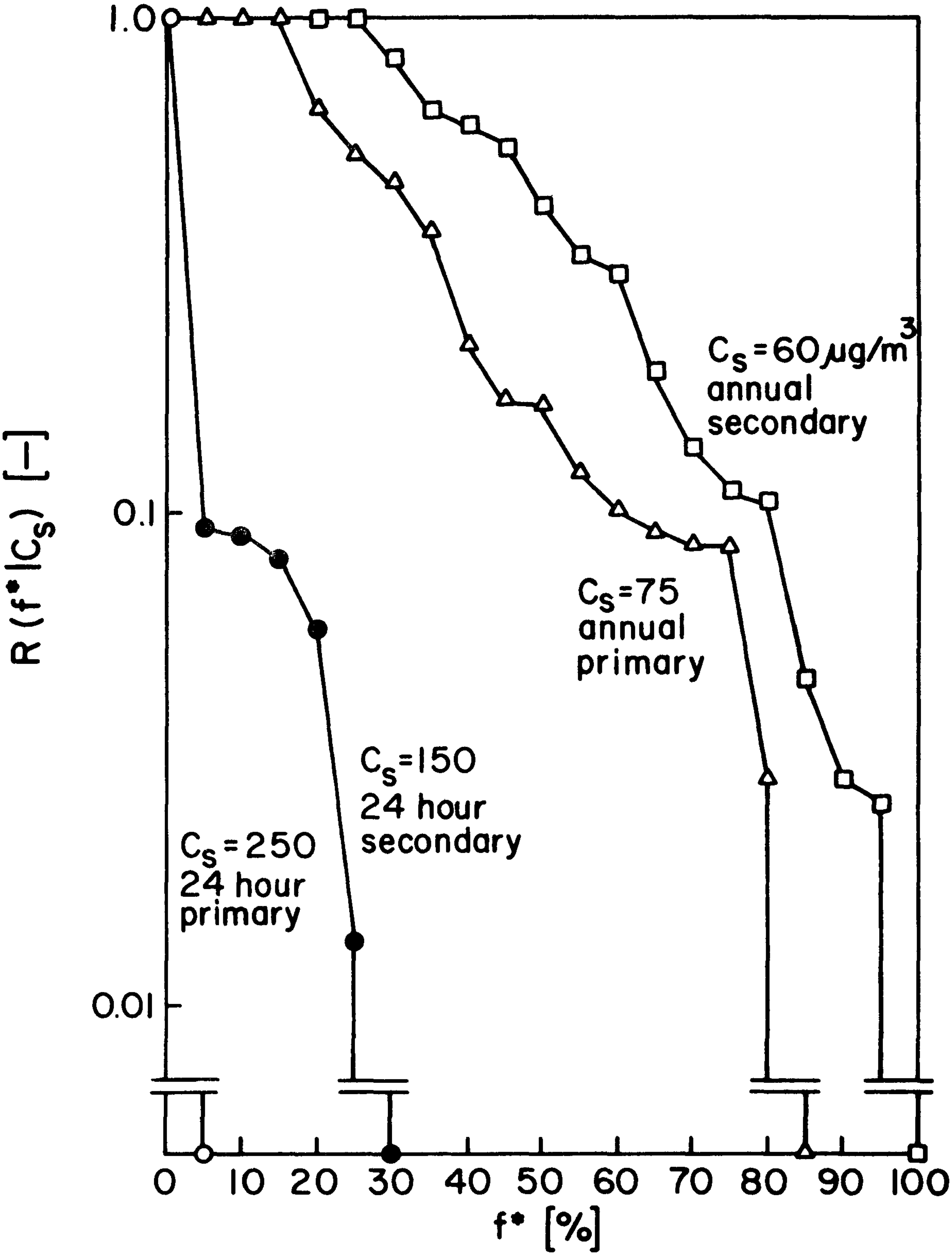

Figure 20: Risk spectrum distribution in 71/2.

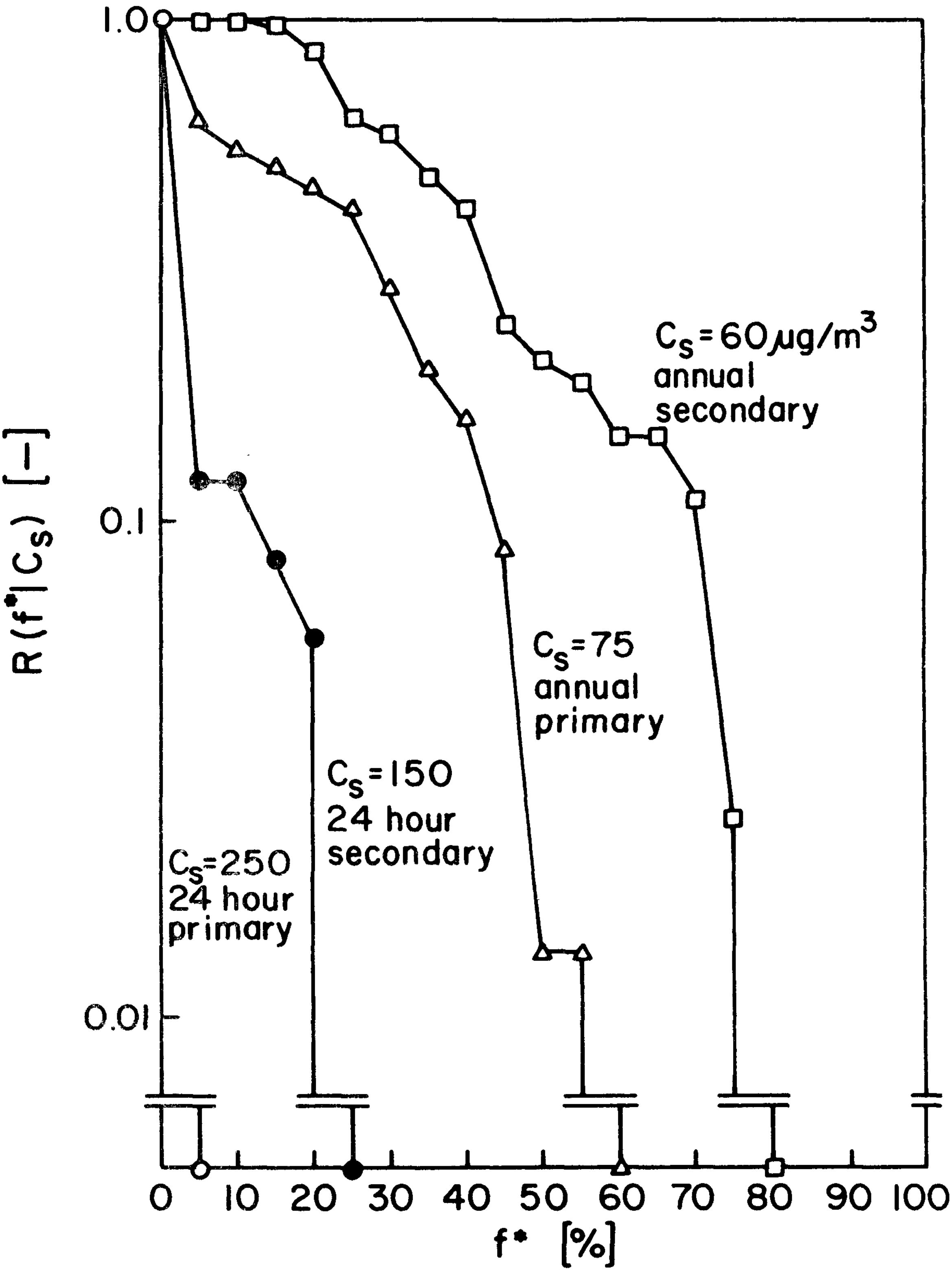

Figure 21: Risk spectrum distribution in 73/2.

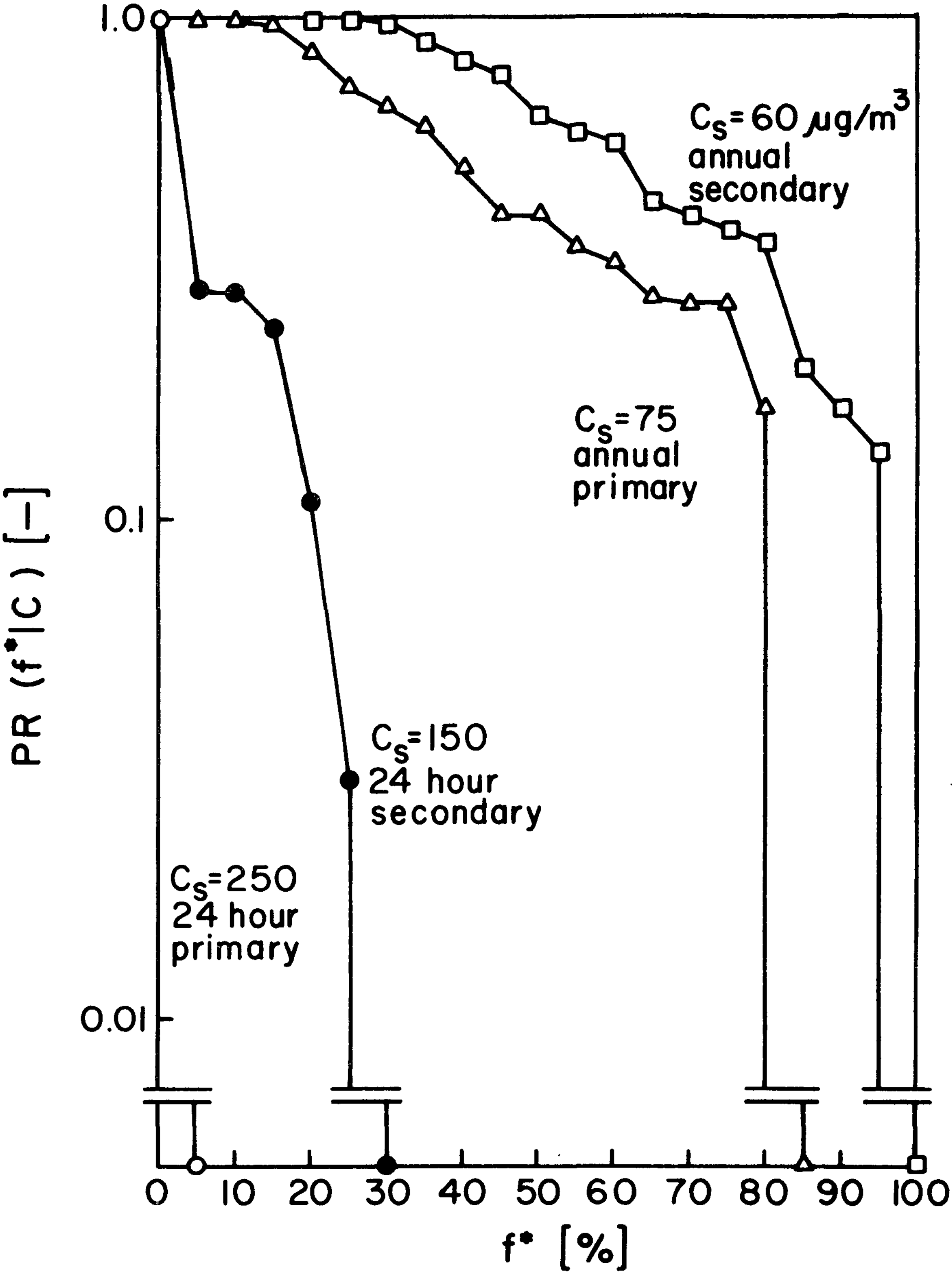

Figure 22: Population-at-risk spectrum distribution in 71/2.

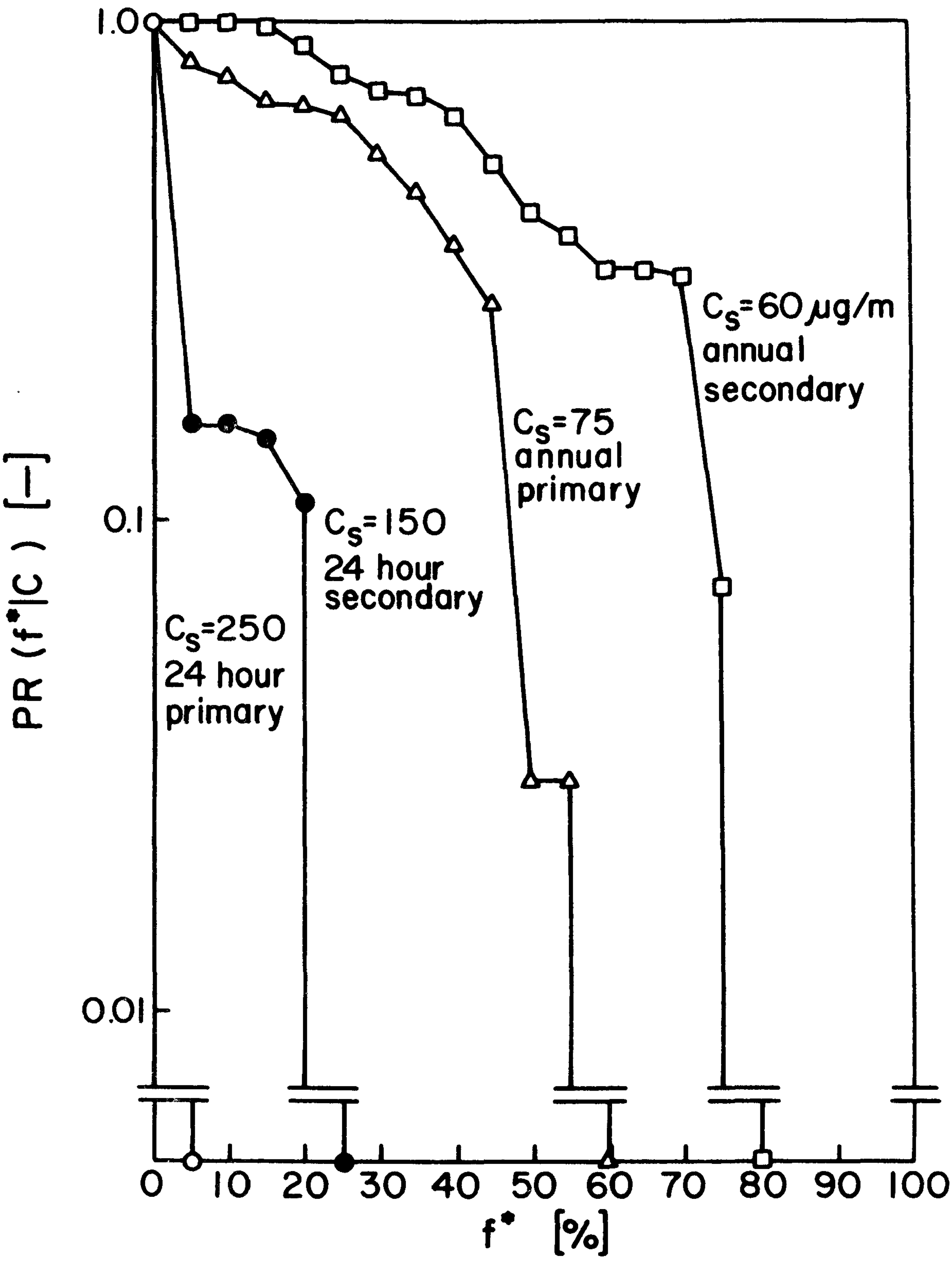

Figure 23: Population-at-risk spectrum distribution in 73/2.

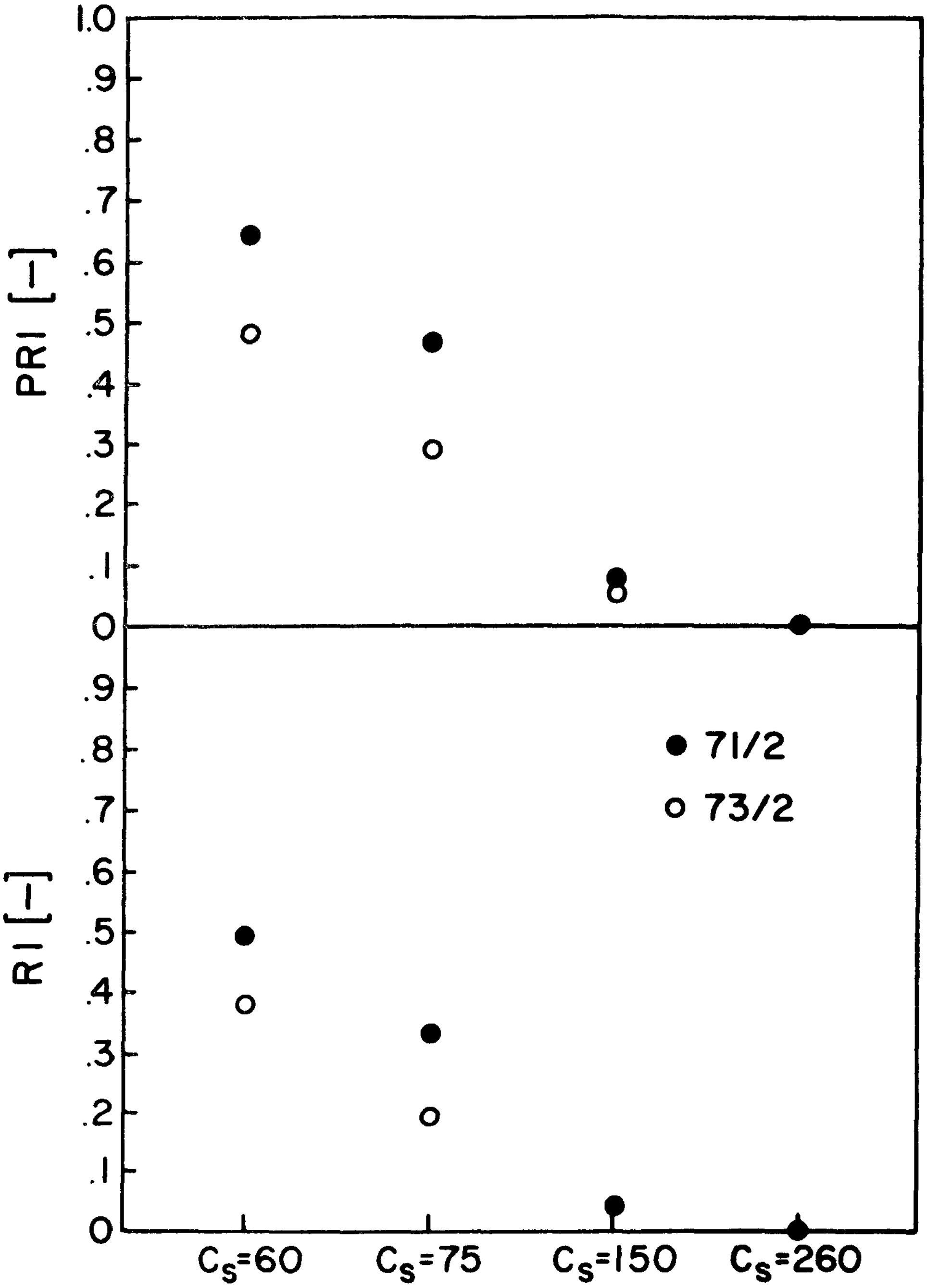

Figure 24: Regional risk index and population-at-risk index in 71/2 and 73/2.

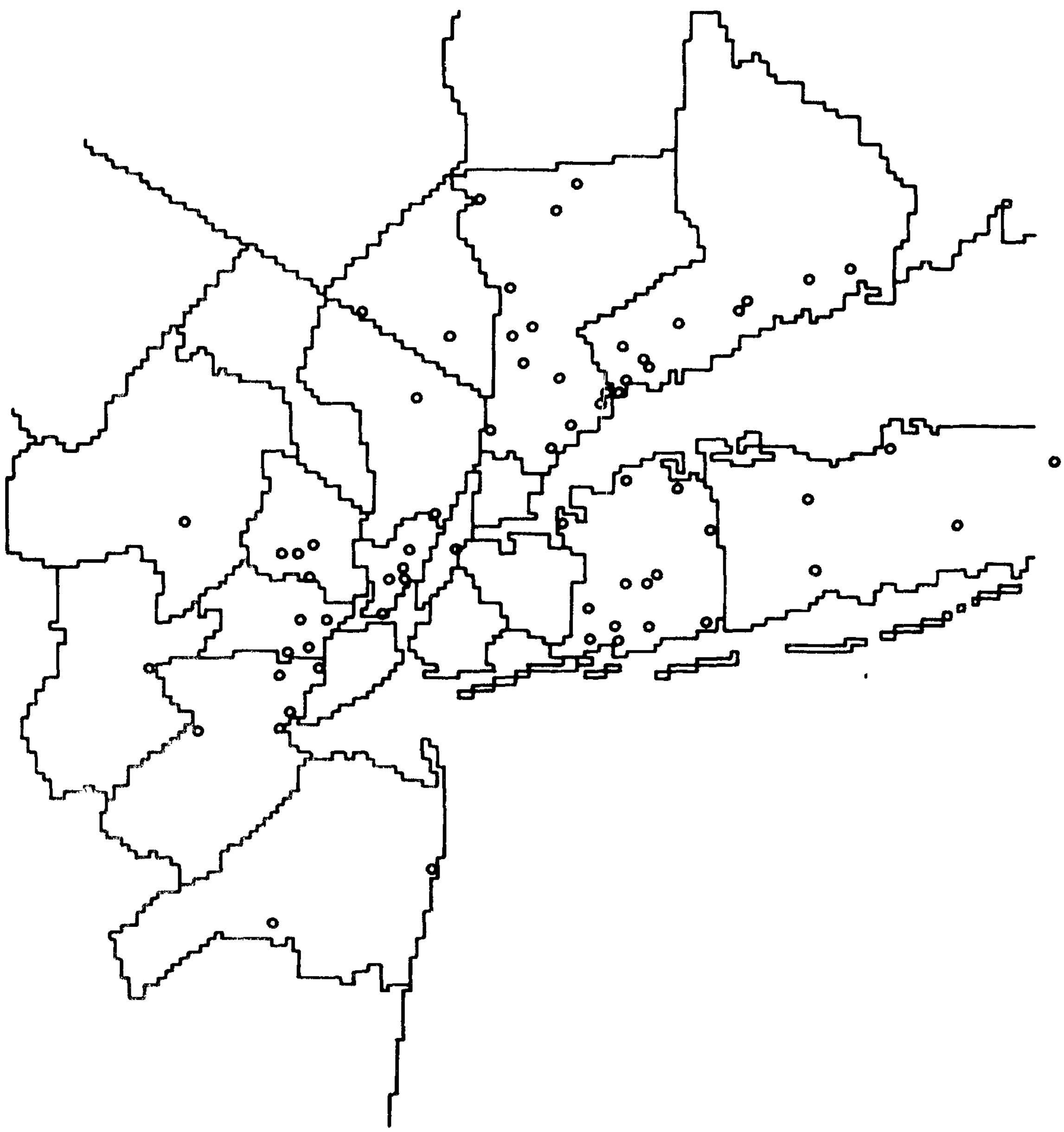

Figure 25: Valid monitoring stations for 1971 and 1973.

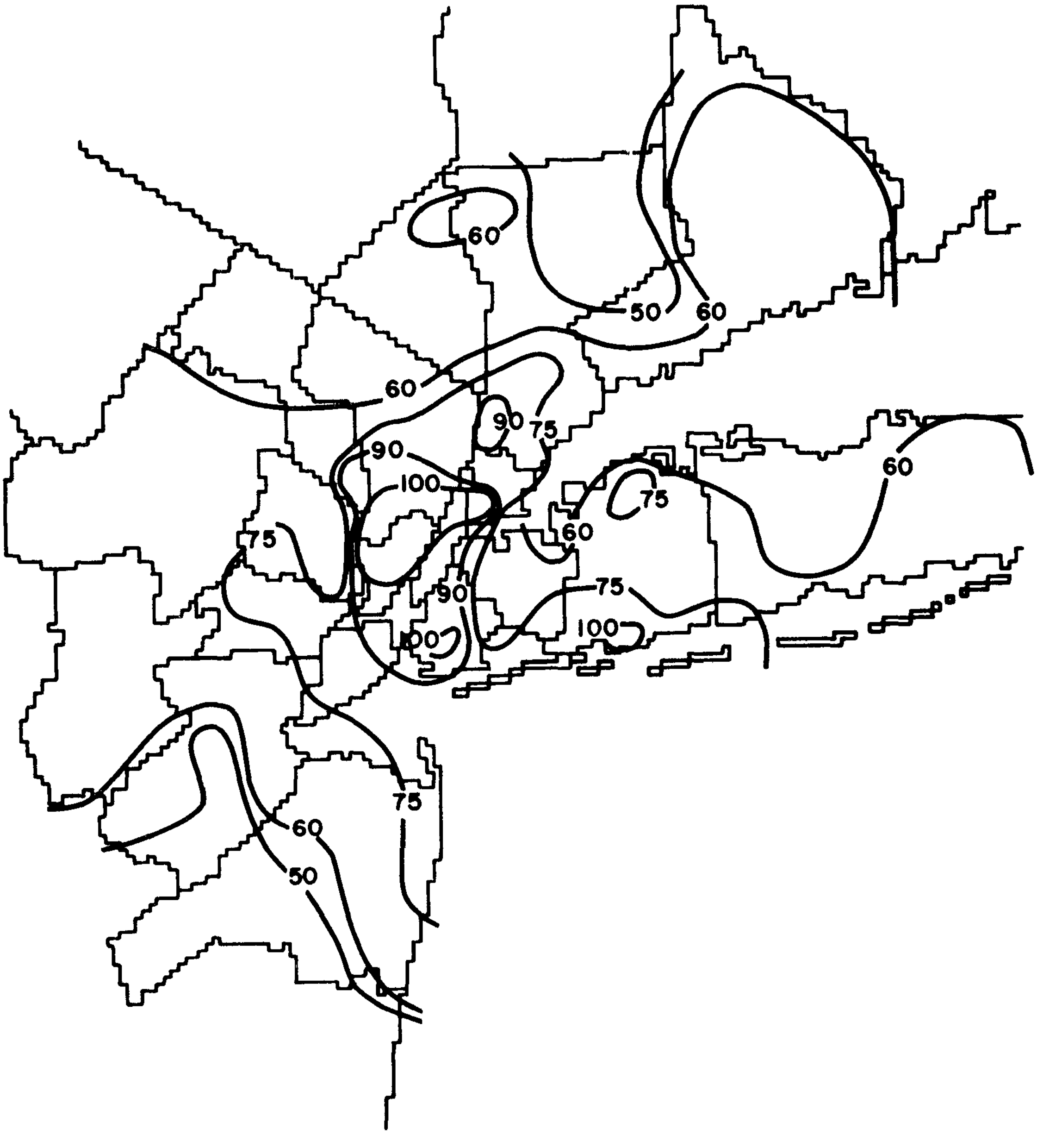

Figure 26: Concentration isopleths in 1971 ($\mu g/m^3$).

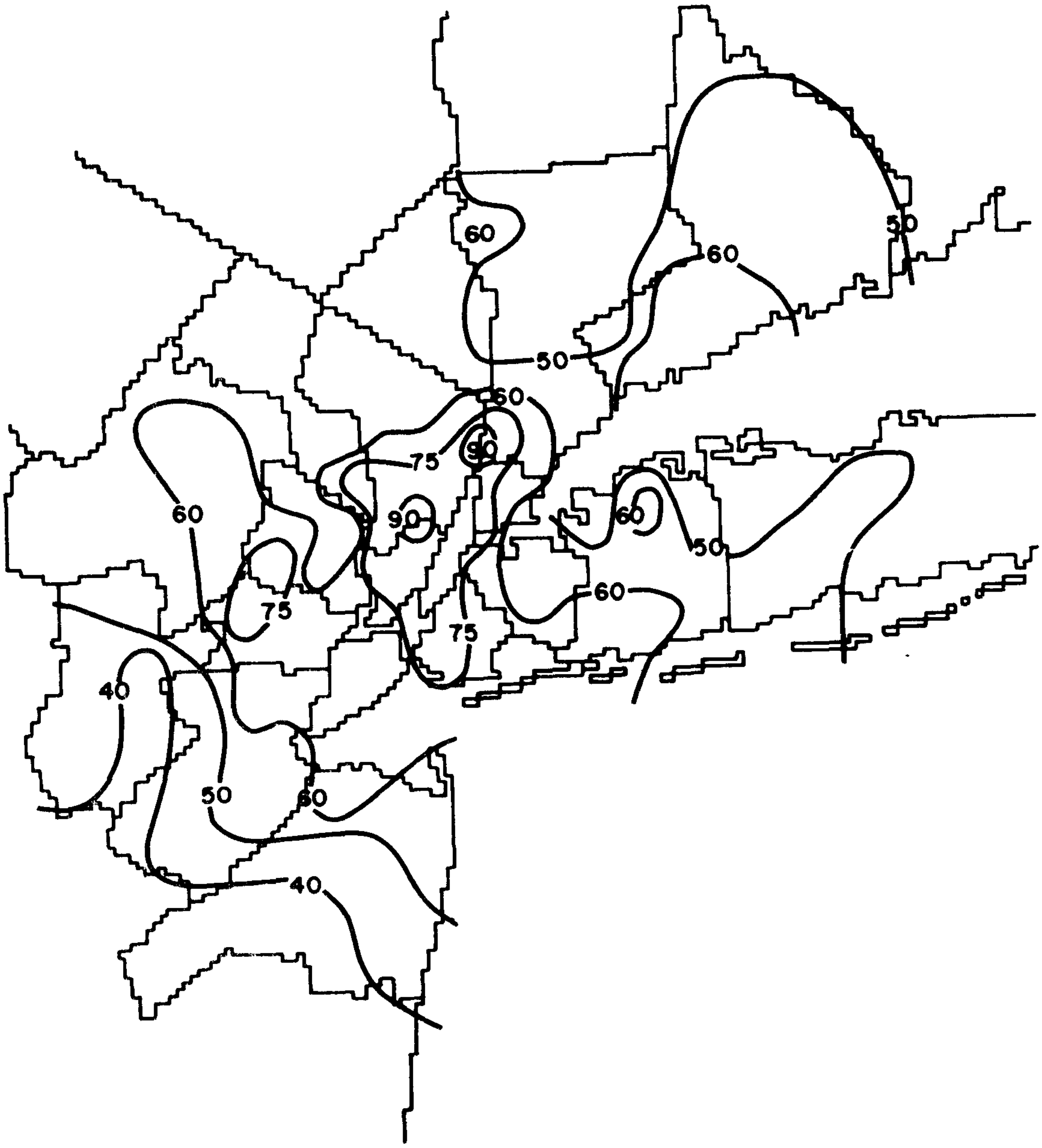

Figure 27: Concentration isopleths in 1973 ($\mu g/m^3$).

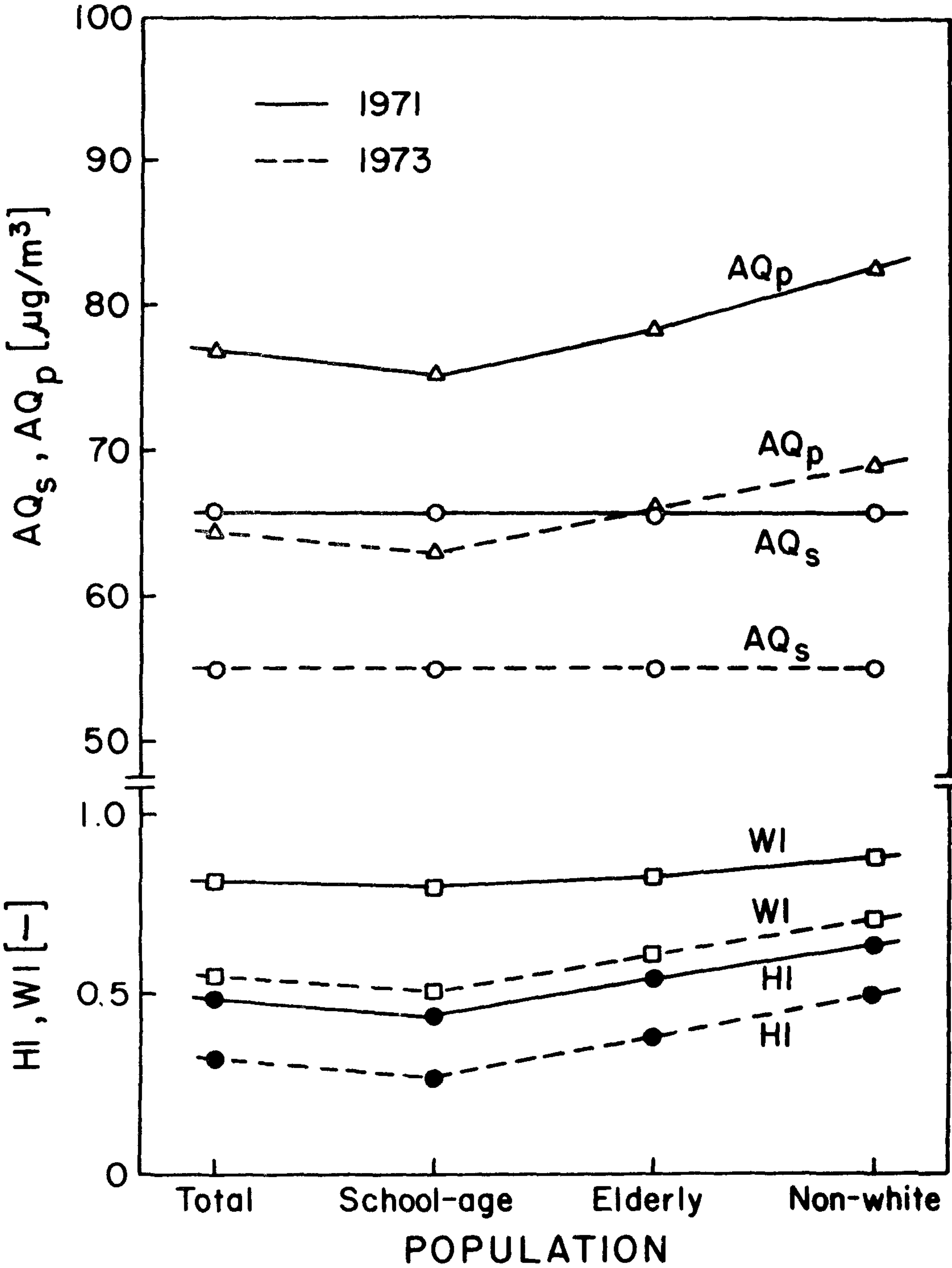

Figure 28: Values of air quality indices in 1971 and 1973.

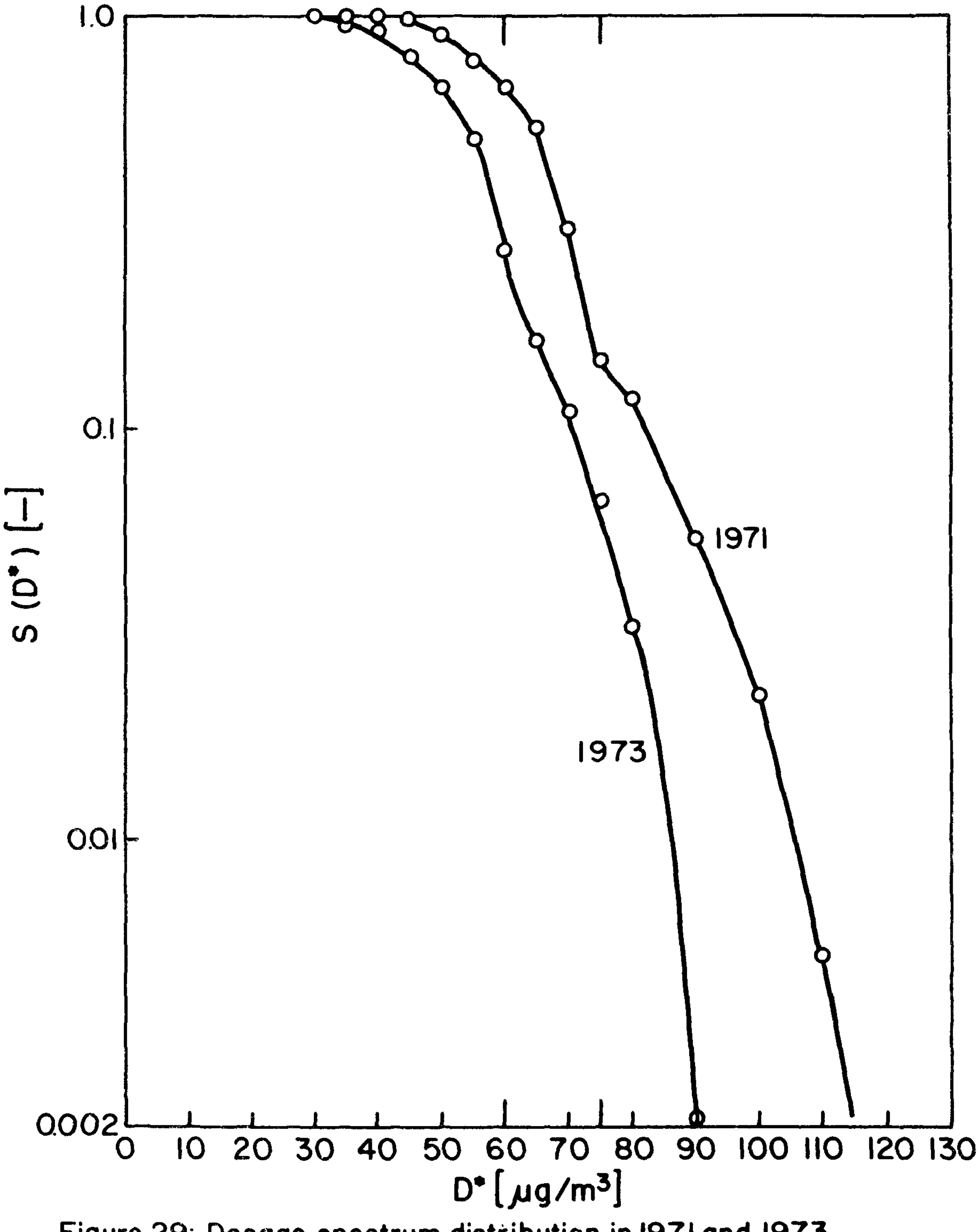

Figure 29: Dosage spectrum distribution in 1971 and 1973.

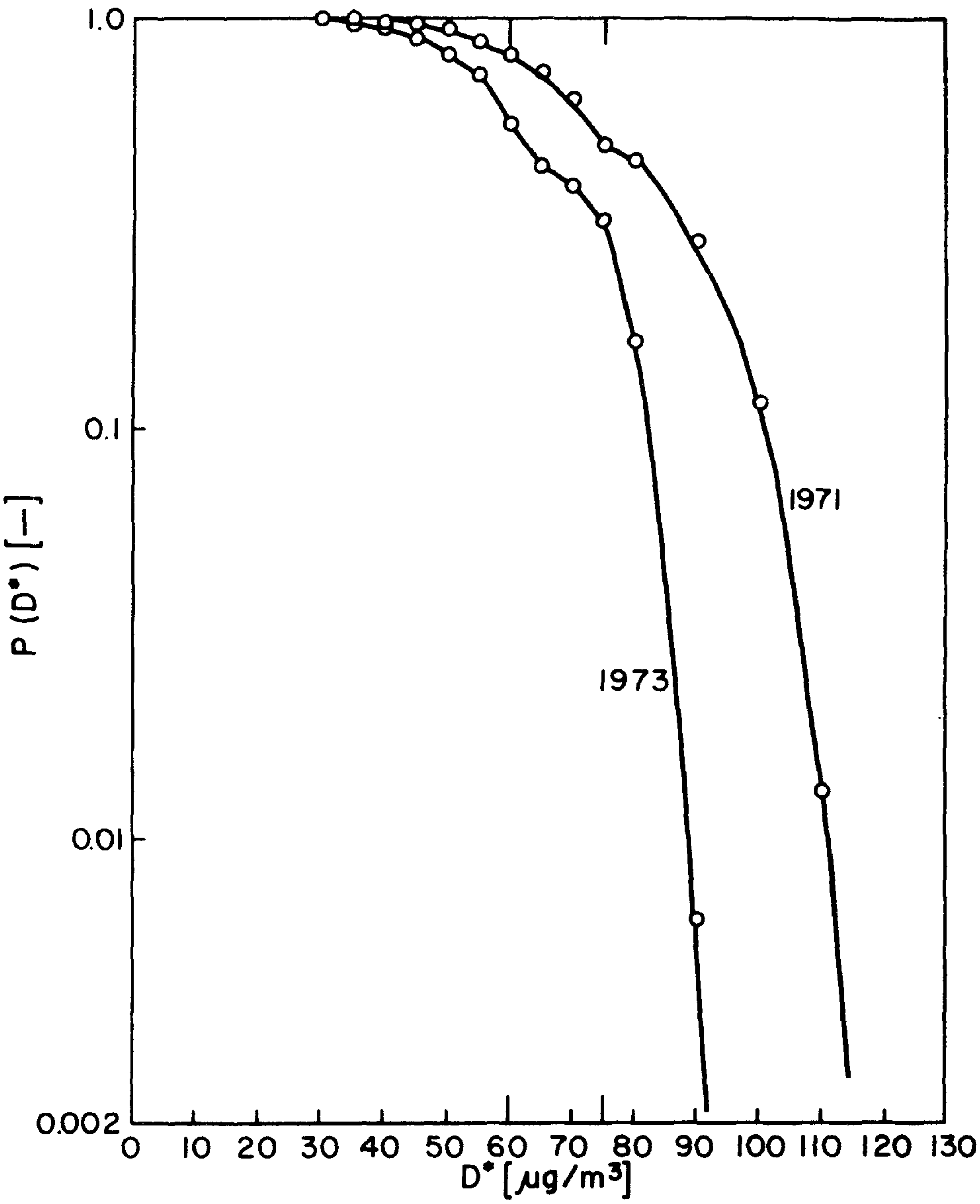

Figure 30: Population dosage spectrum distribution for total population.

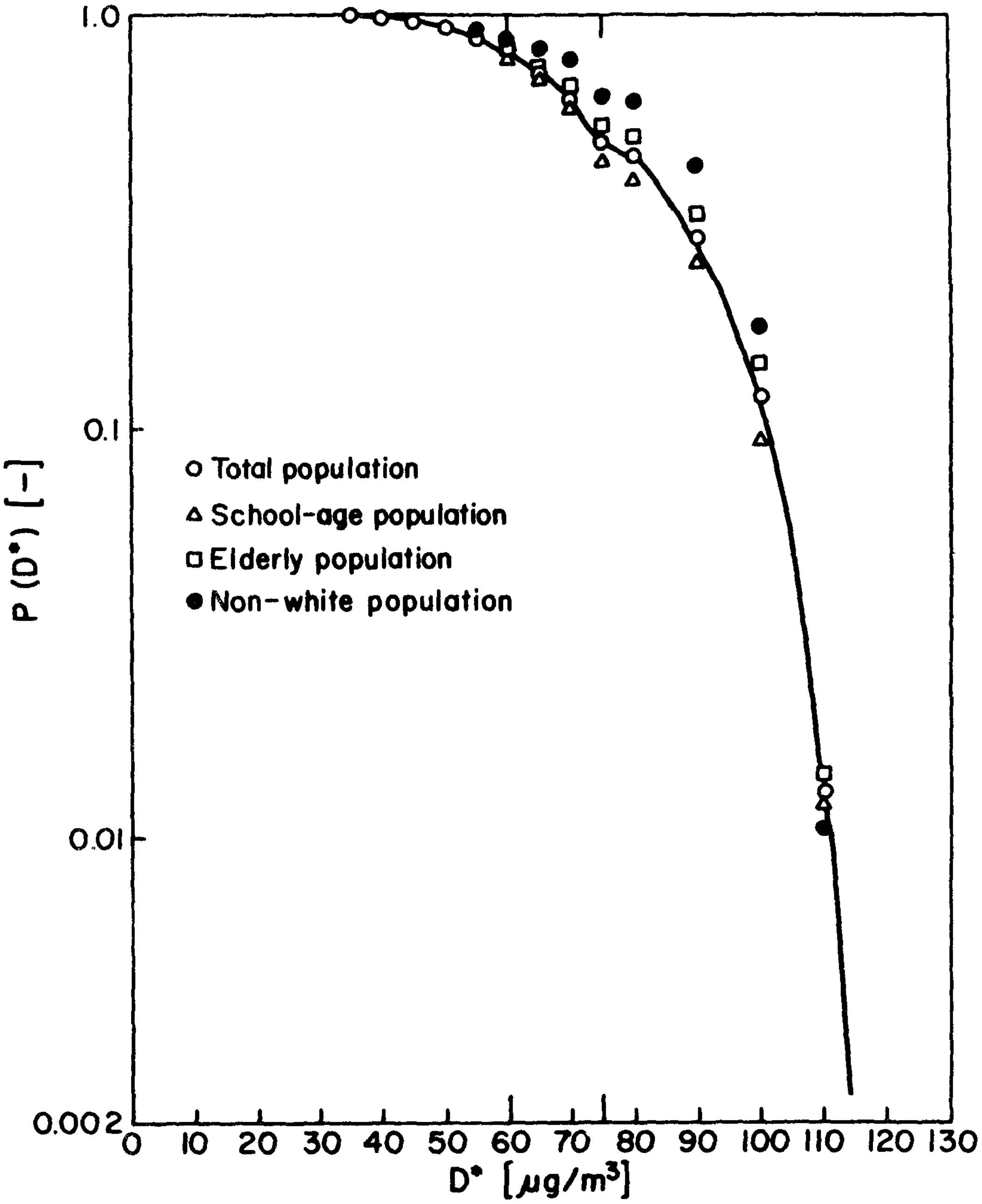

Figure 31: Population dosage spectra for four different populations in 1971.

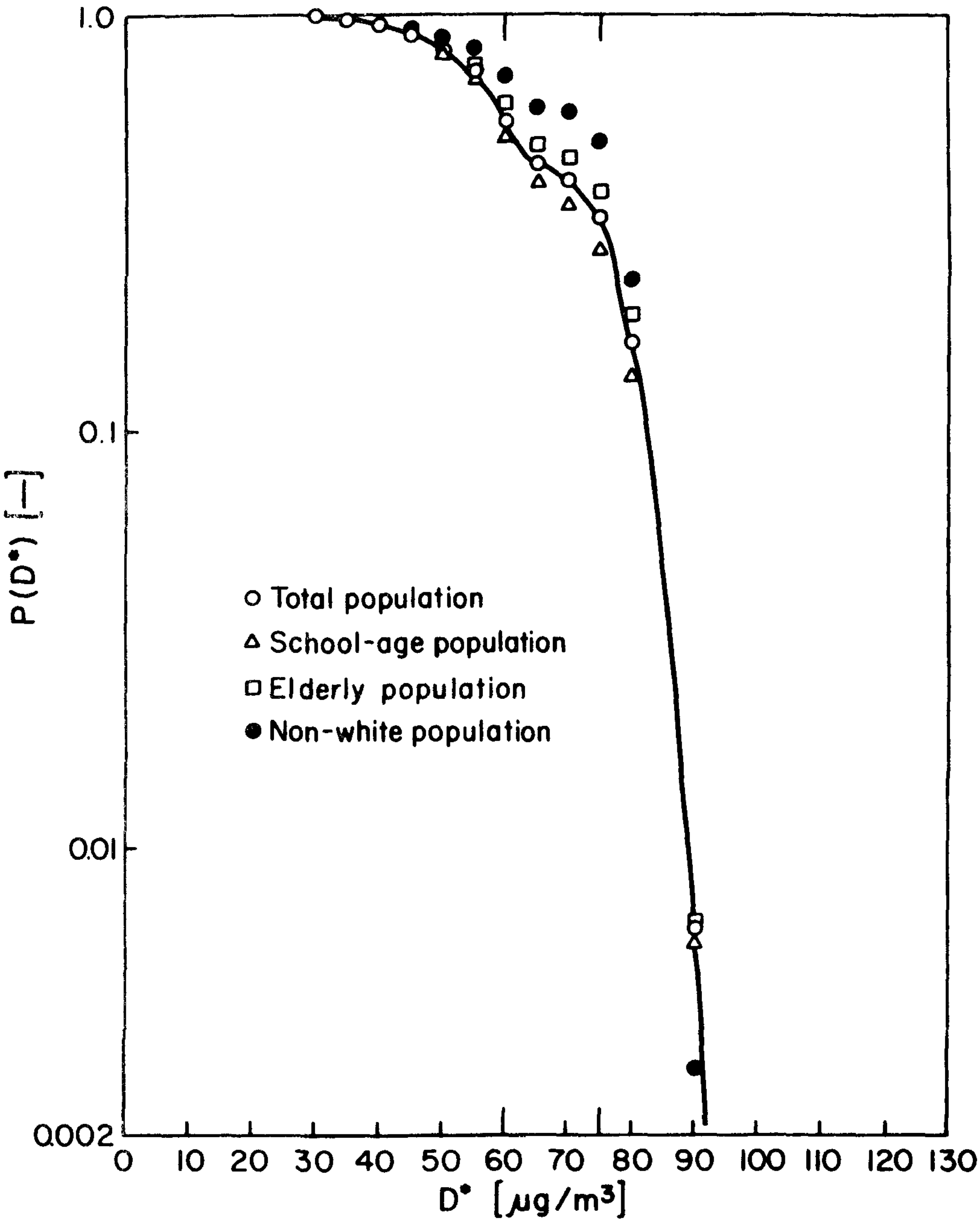

Figure 32: Population dosage spectra for four different populations in 1973.

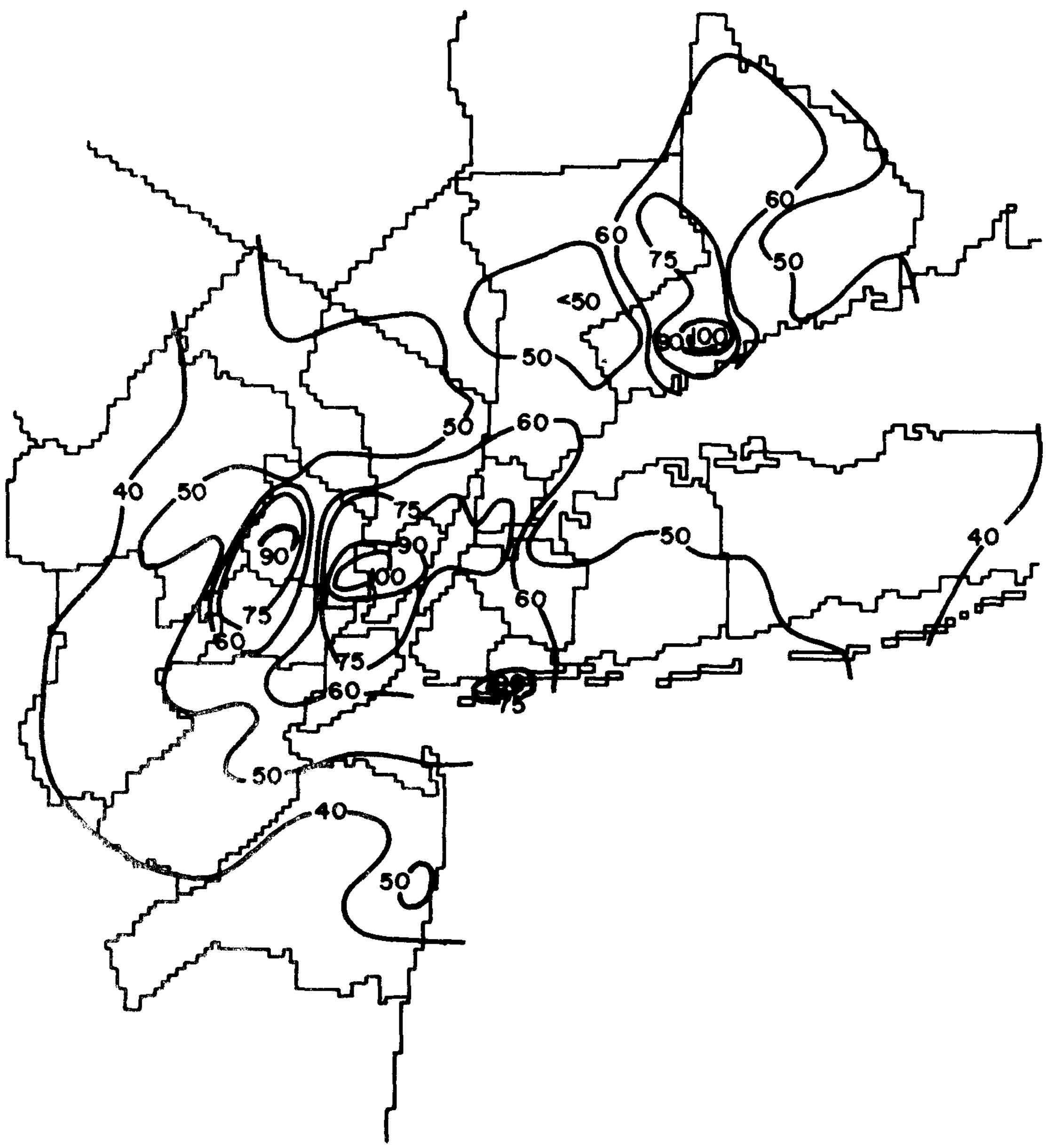

Figure 33: Isopleth map of geometric mean concentrations in 73/2 with 130 valid monitoring stations.

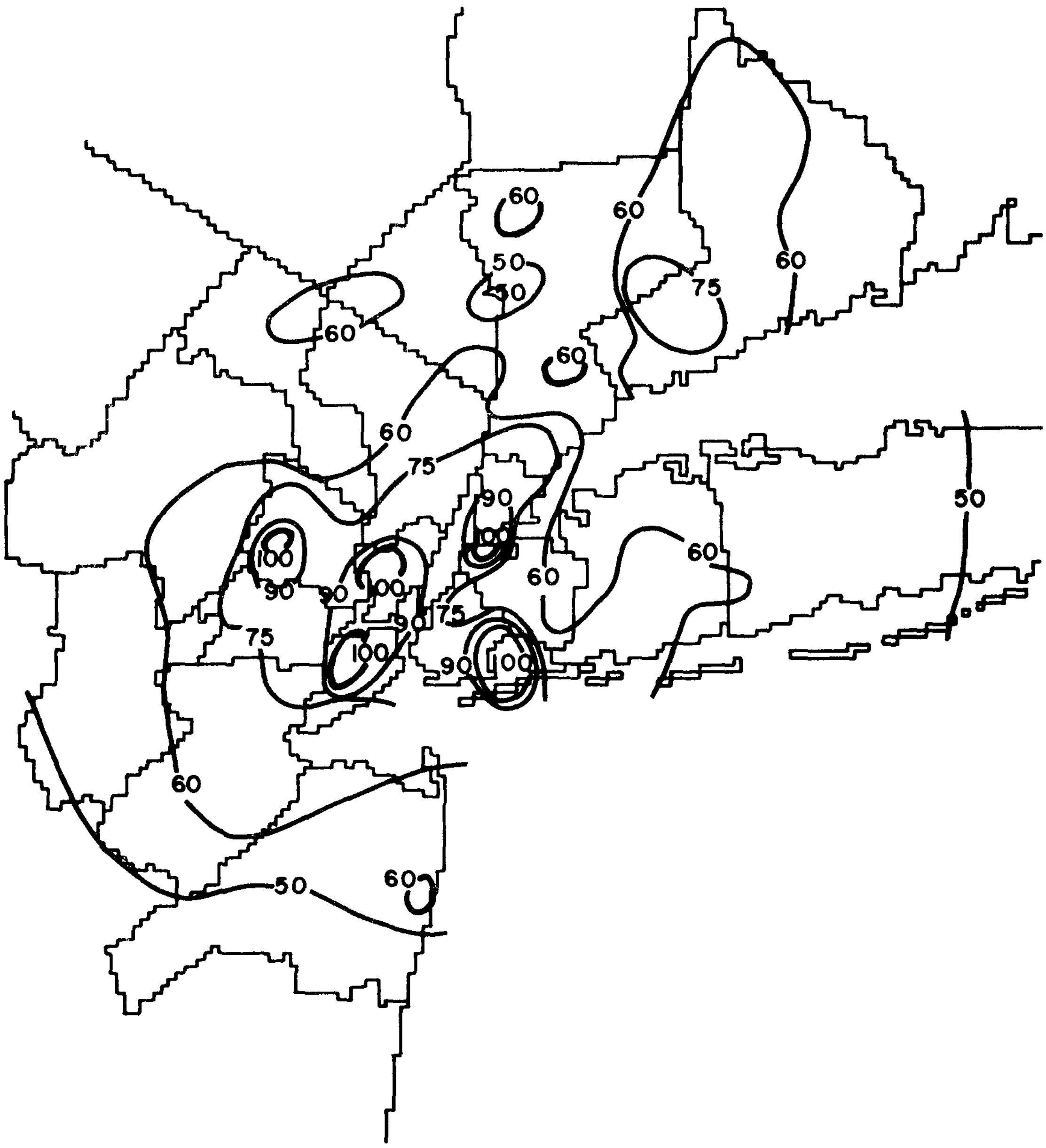

Figure 34: Isopleth map of geometric mean concentrations in 73/3 with 130 valid monitoring stations.

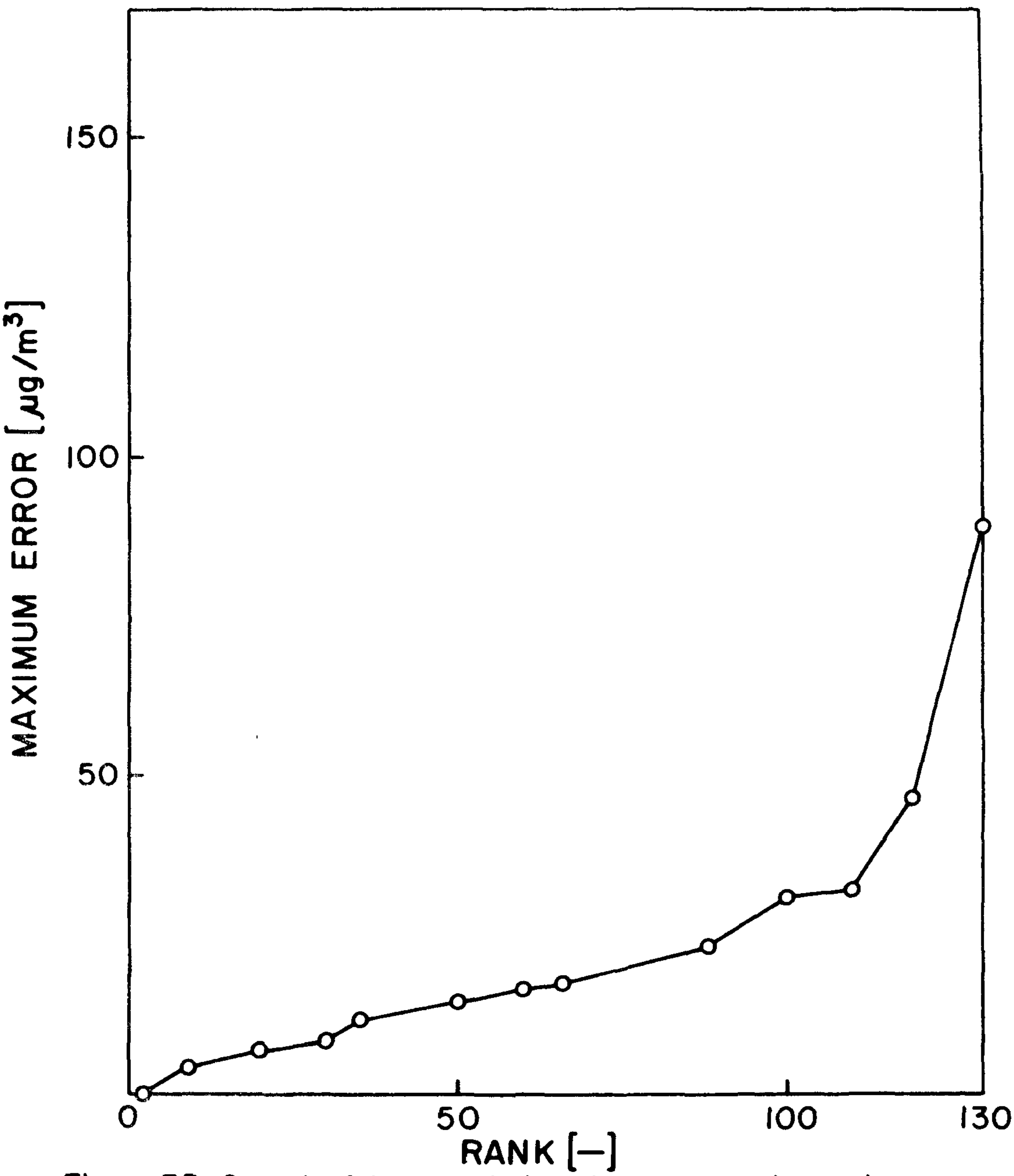

Figure 35: Growth of the error induced at each station under Scheme I.

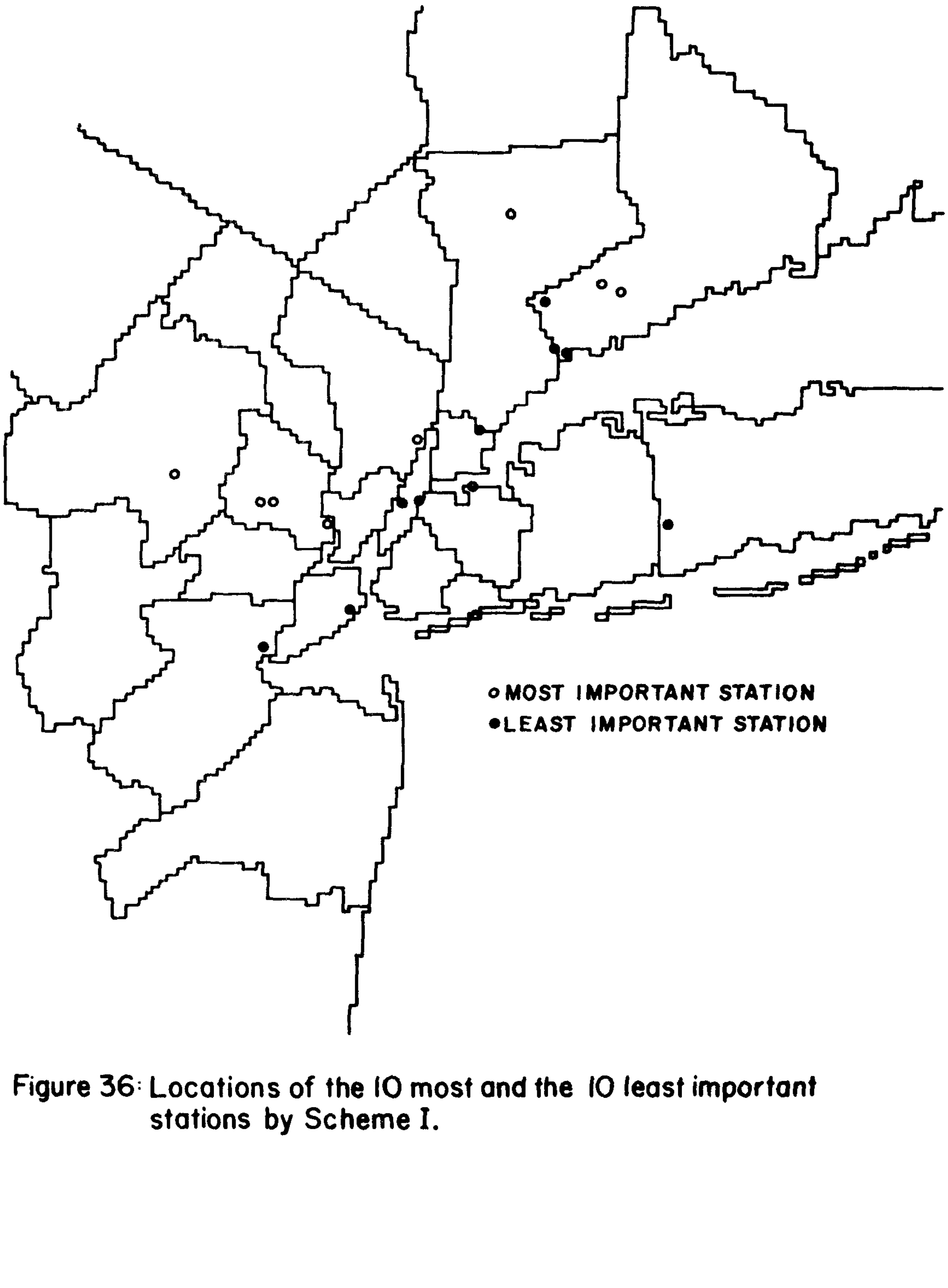

Figure 36: Locations of the 10 most and the 10 least important stations by Scheme I.

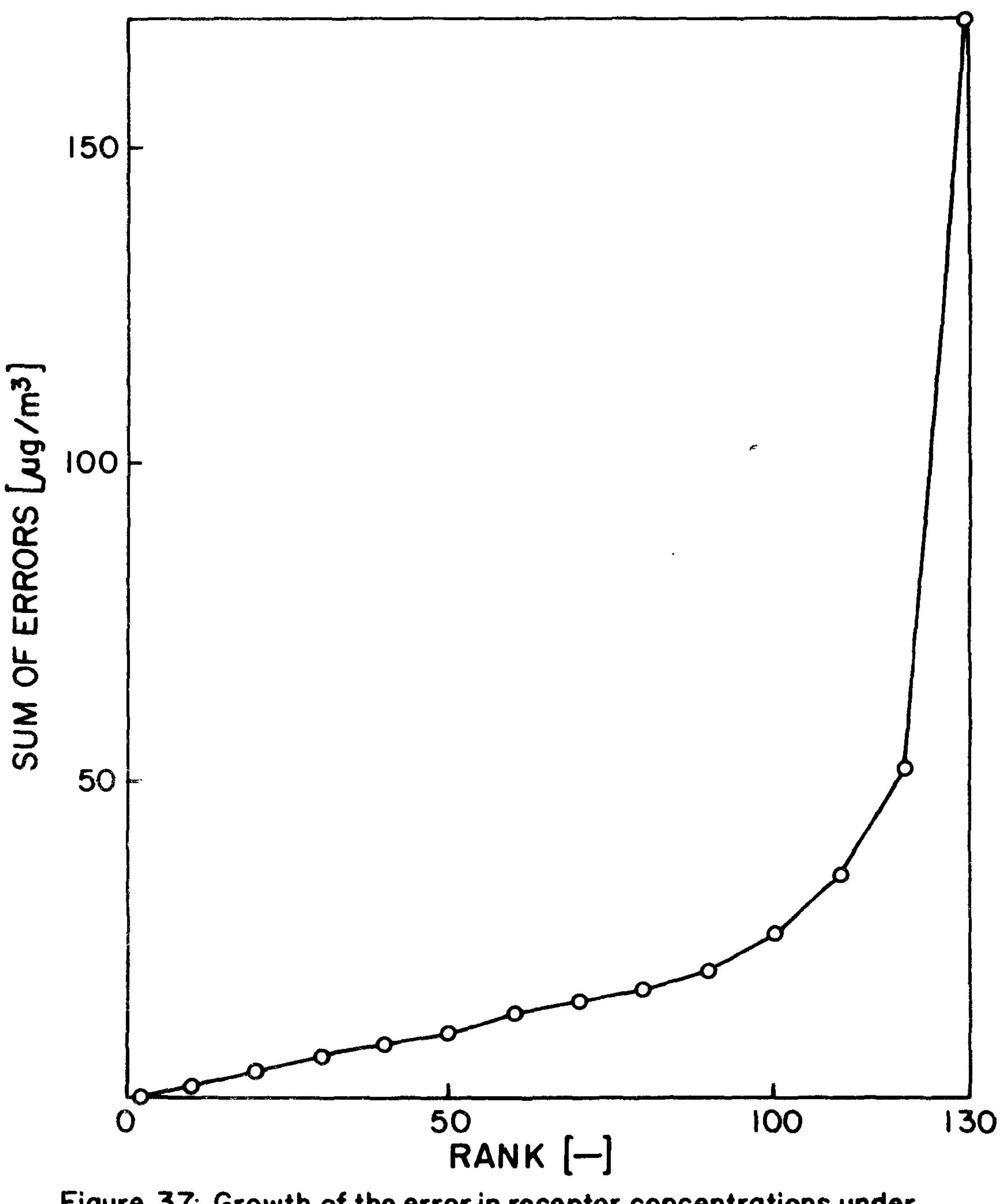

Figure 37: Growth of the error in receptor concentrations under Scheme II.

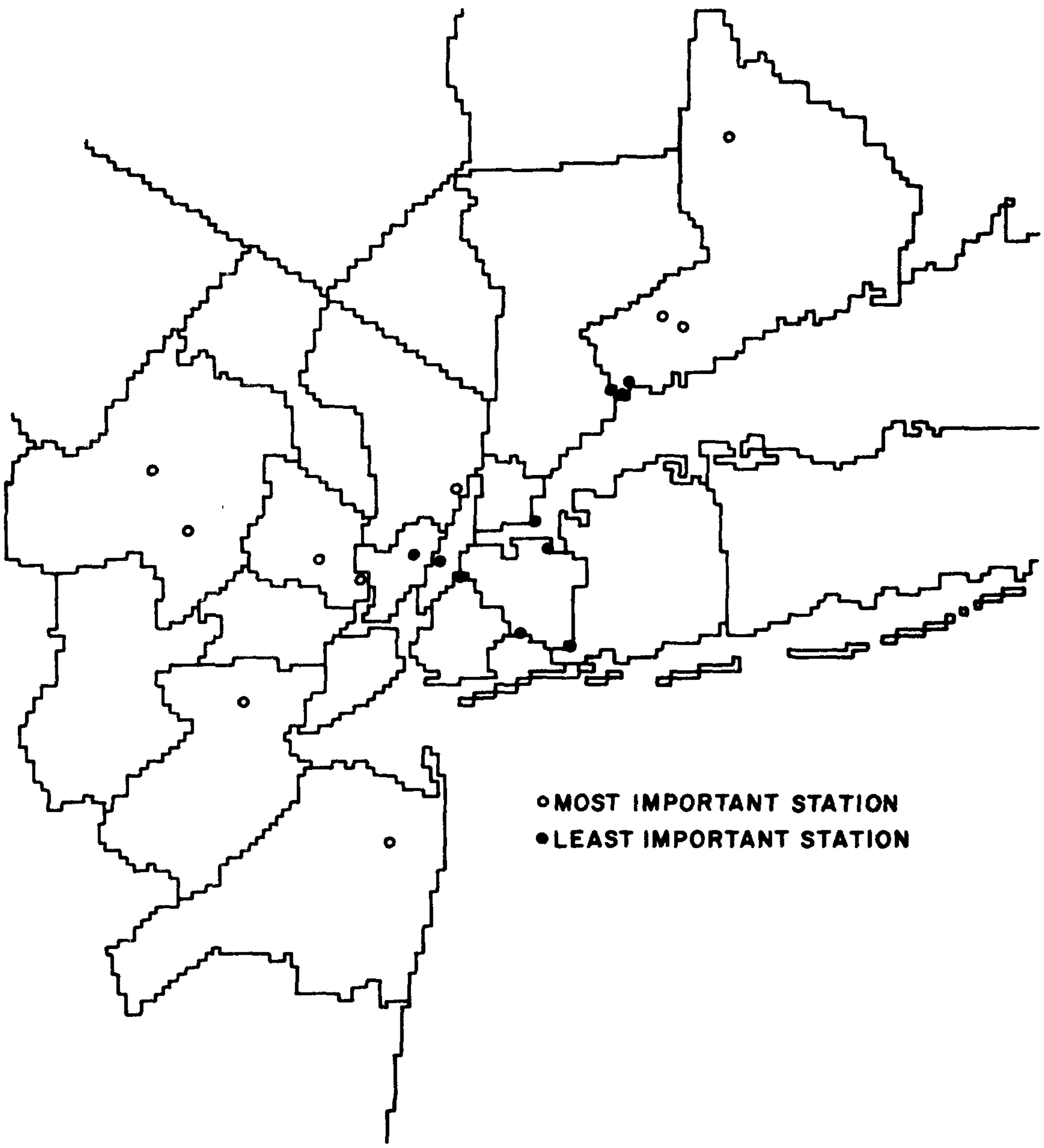

Figure 38: Locations of the 10 most and the 10 least important stations by Scheme II.

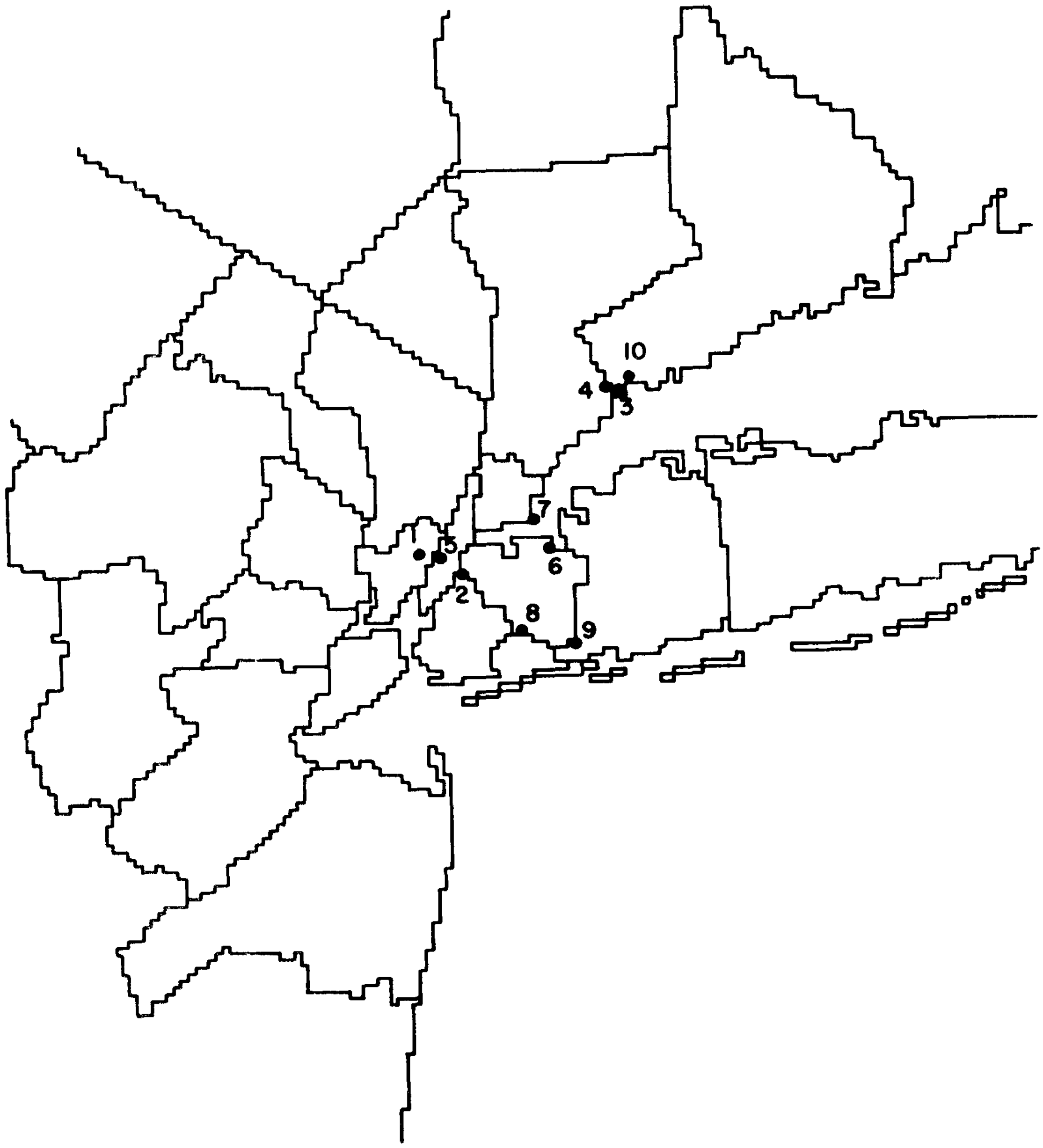

Figure 39: Locations of the 10 least important stations by Scheme III.

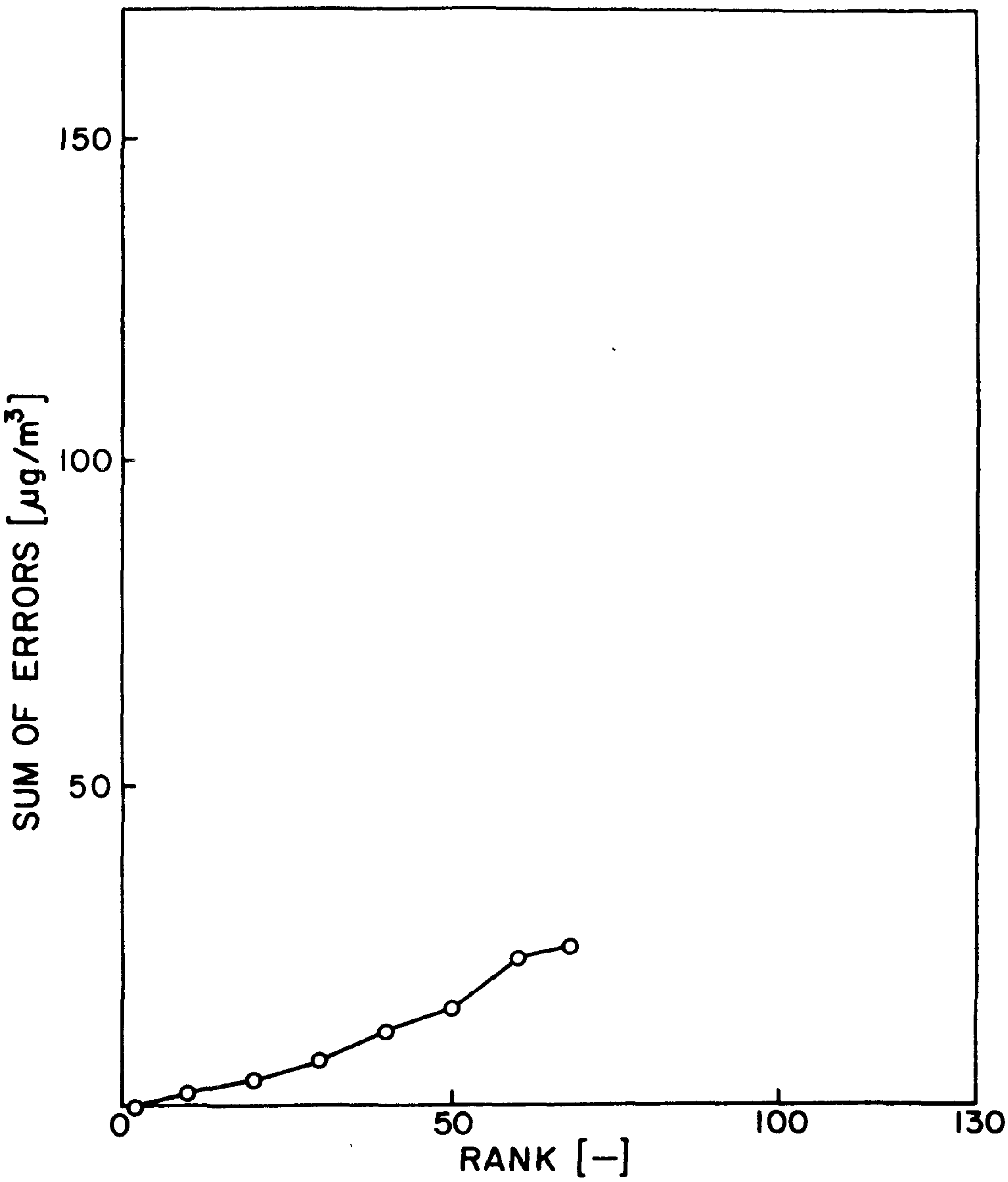

Figure 40: Growth of the error in receptor concentrations under Scheme III.

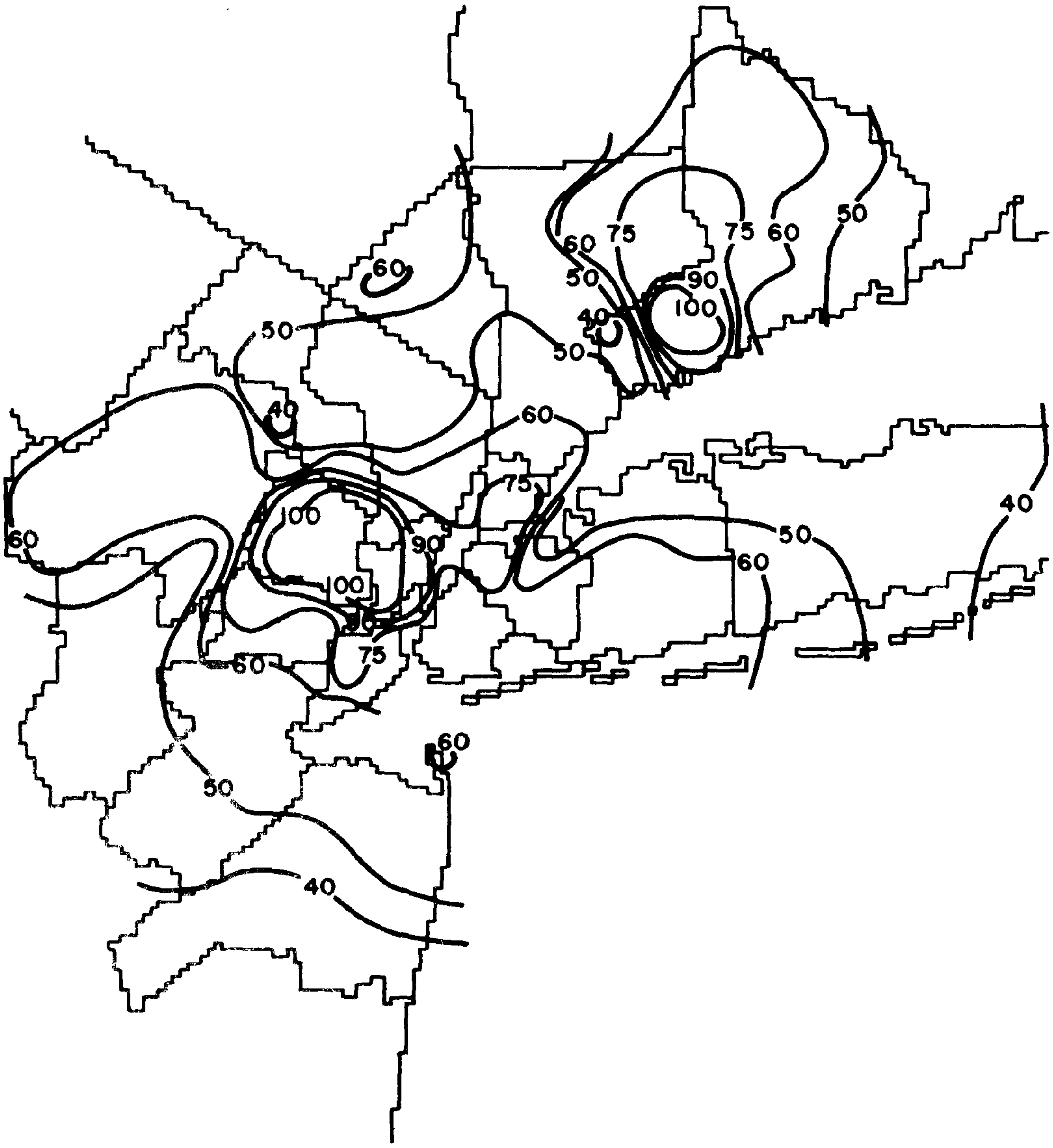

Figure 41: Isopleth map of geometric mean concentrations in 73/2 from 68 odd numbered stations.

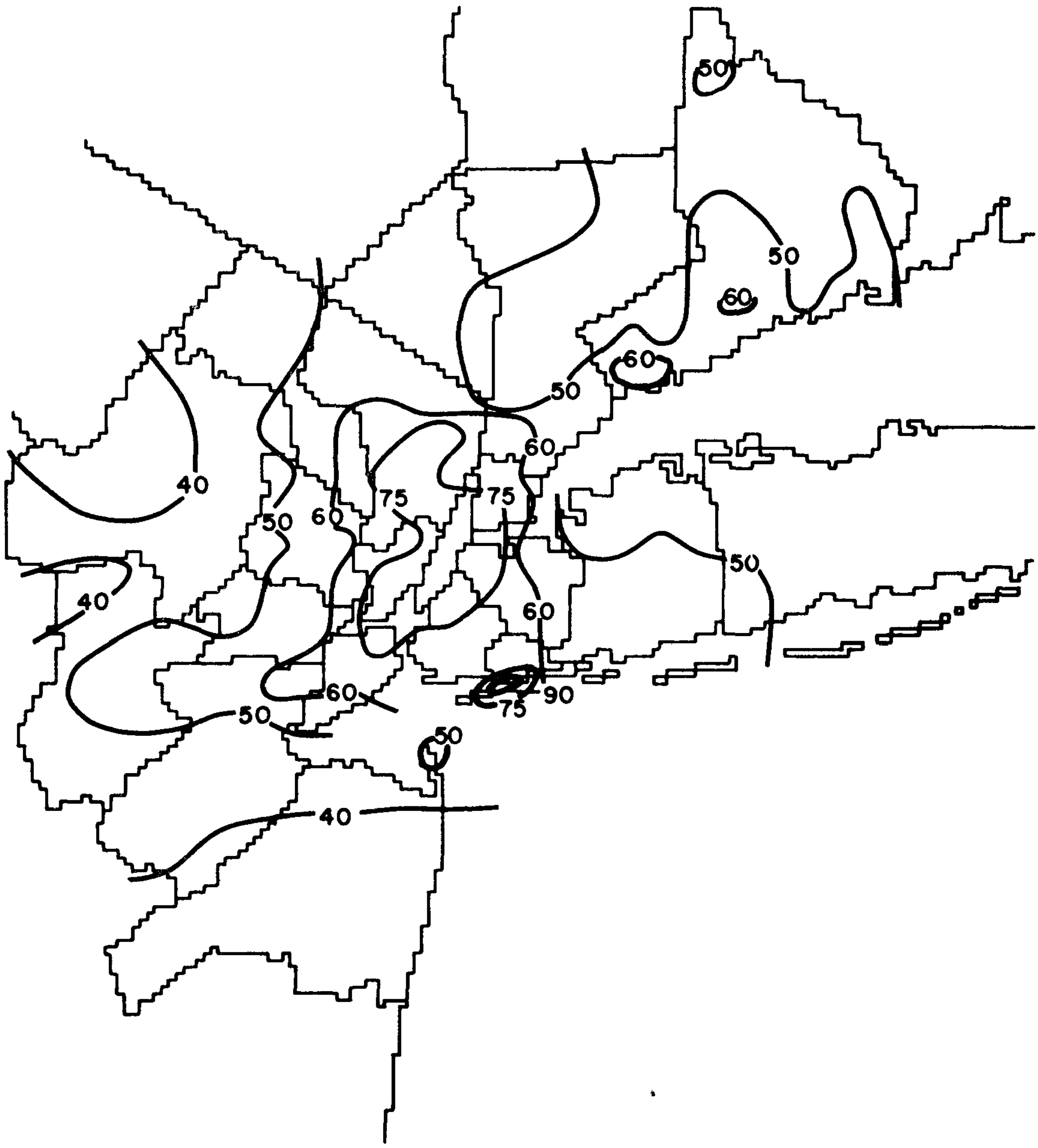

Figure 42: Isopleth map of geometric mean concentrations in 73/2 from 62 even numbered stations.

FIGURE 43 Key to the symbols used in Figures 44 through 47

Network subset	No. of stations	Symbol
Total network	130	——
Even # network	68	—
Odd # network	62	∿
Scheme I network	62	Δ
Scheme II network	62	□
Scheme III network	62	o

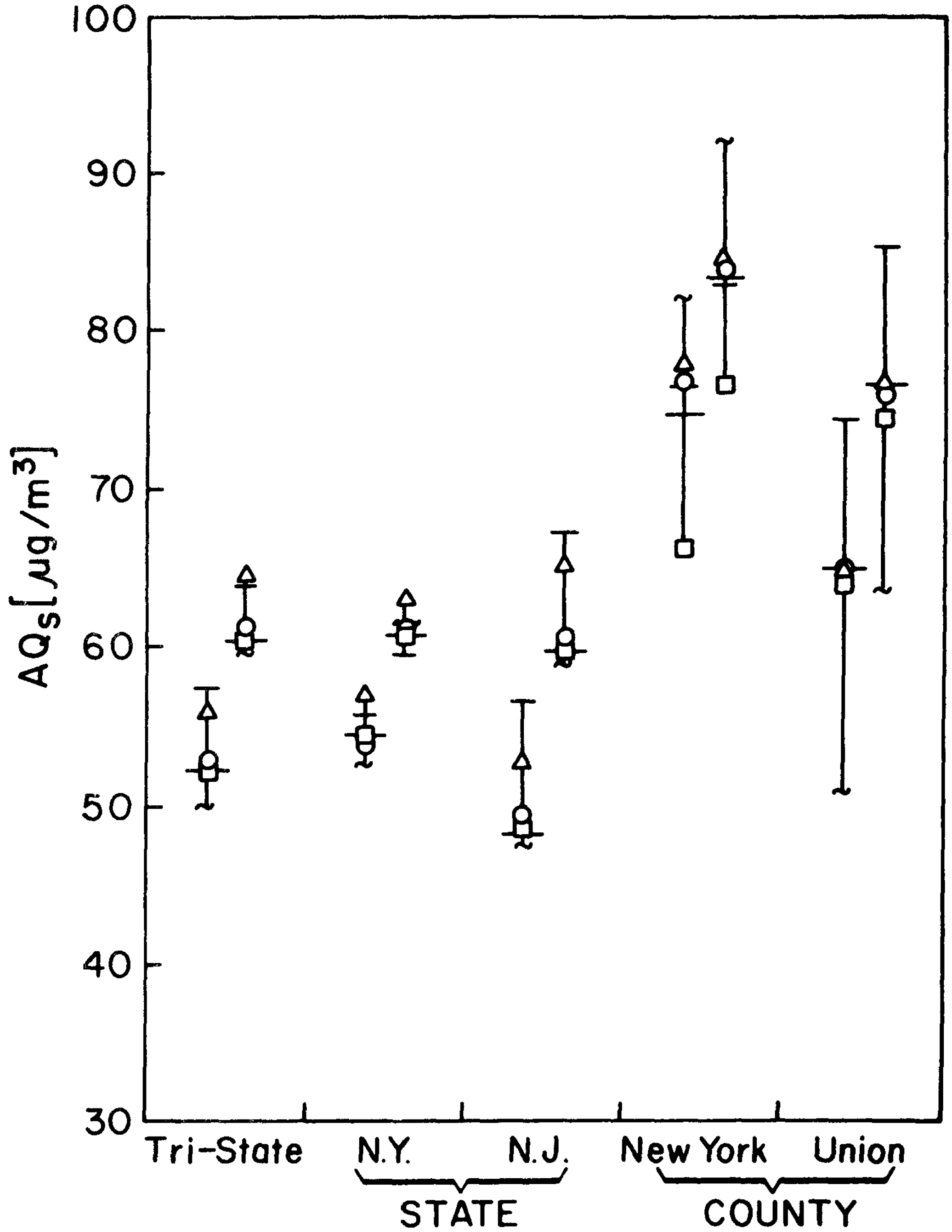

Figure 44: Space average air qualities estimated from the total network and from each of the five half size sub-networks.

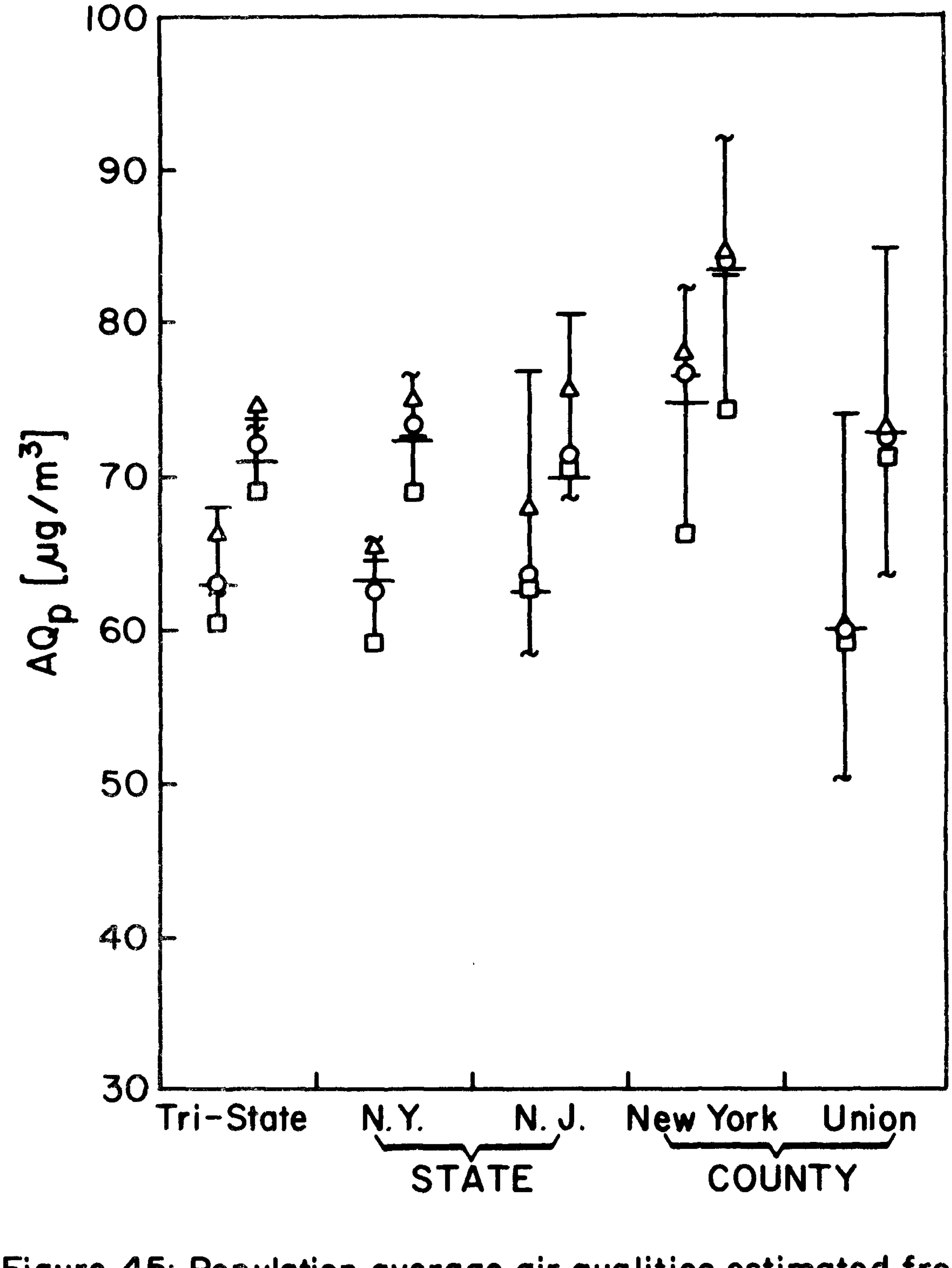

Figure 45: Population average air qualities estimated from the total network and from each of the five half size sub-networks.

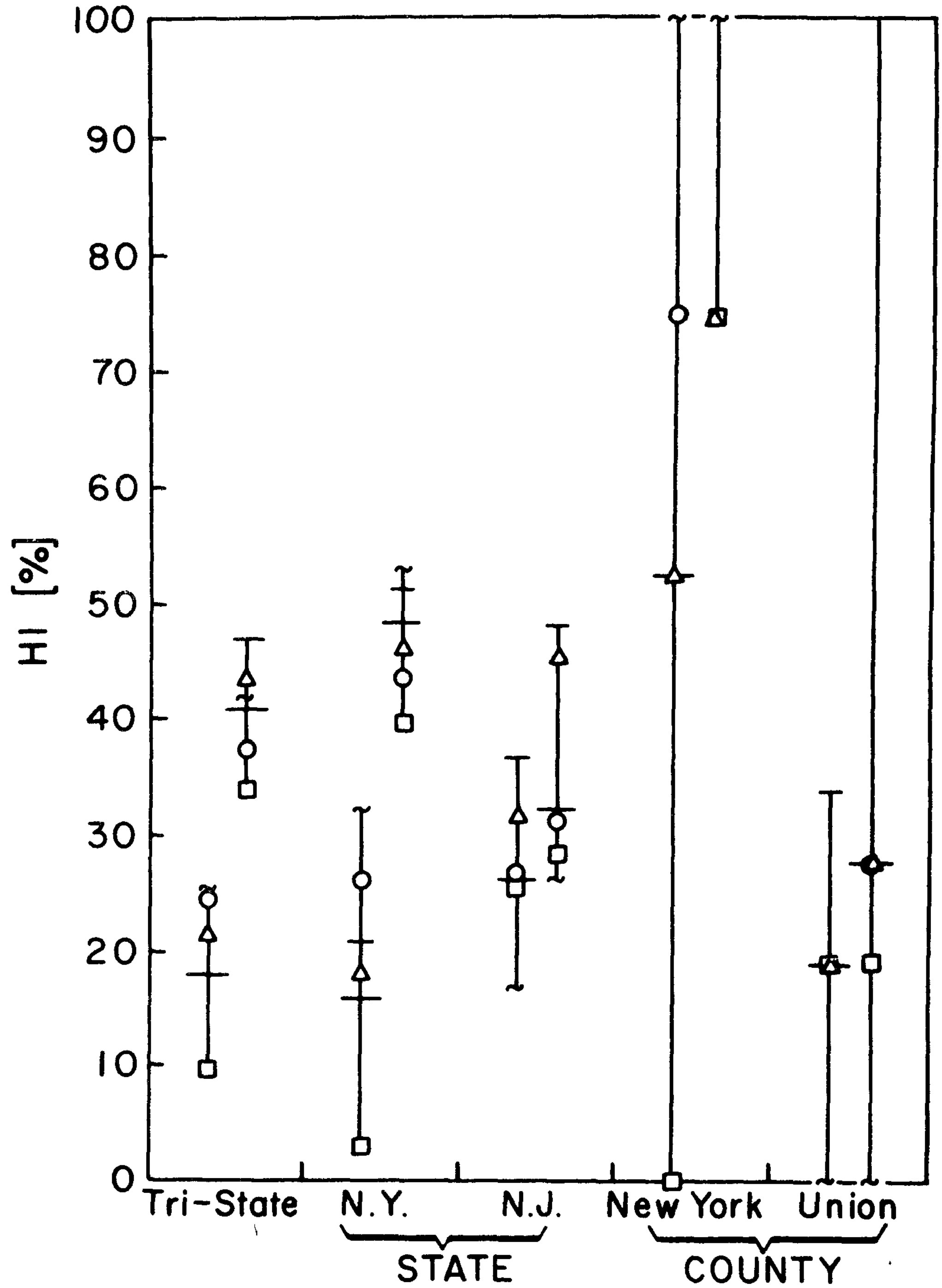

Figure 46: Health indices estimated from the total network and from each of the five half size sub-networks.

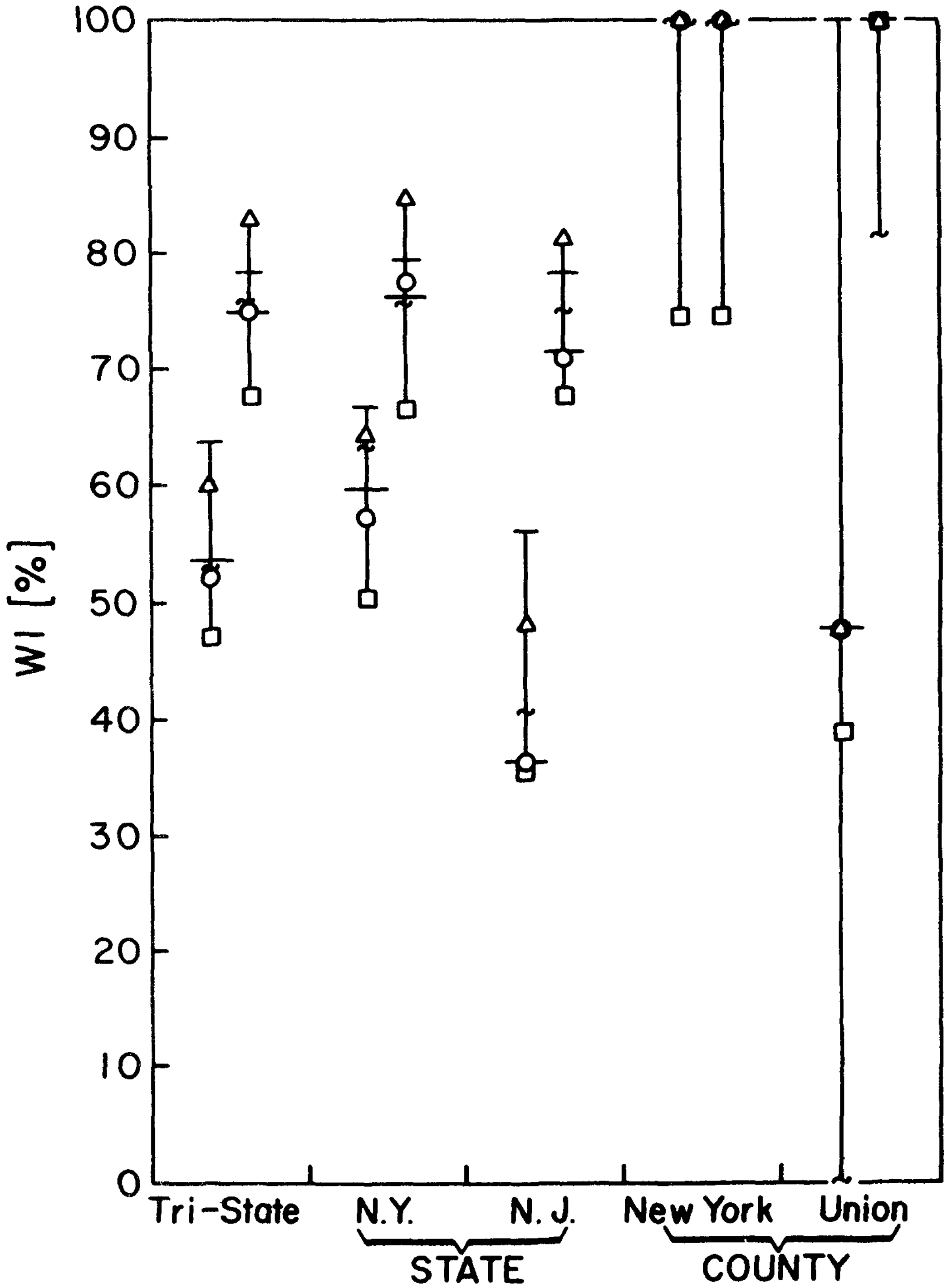

Figure 47: Welfare indices estimated from the total network and from each of the five half size sub-networks.

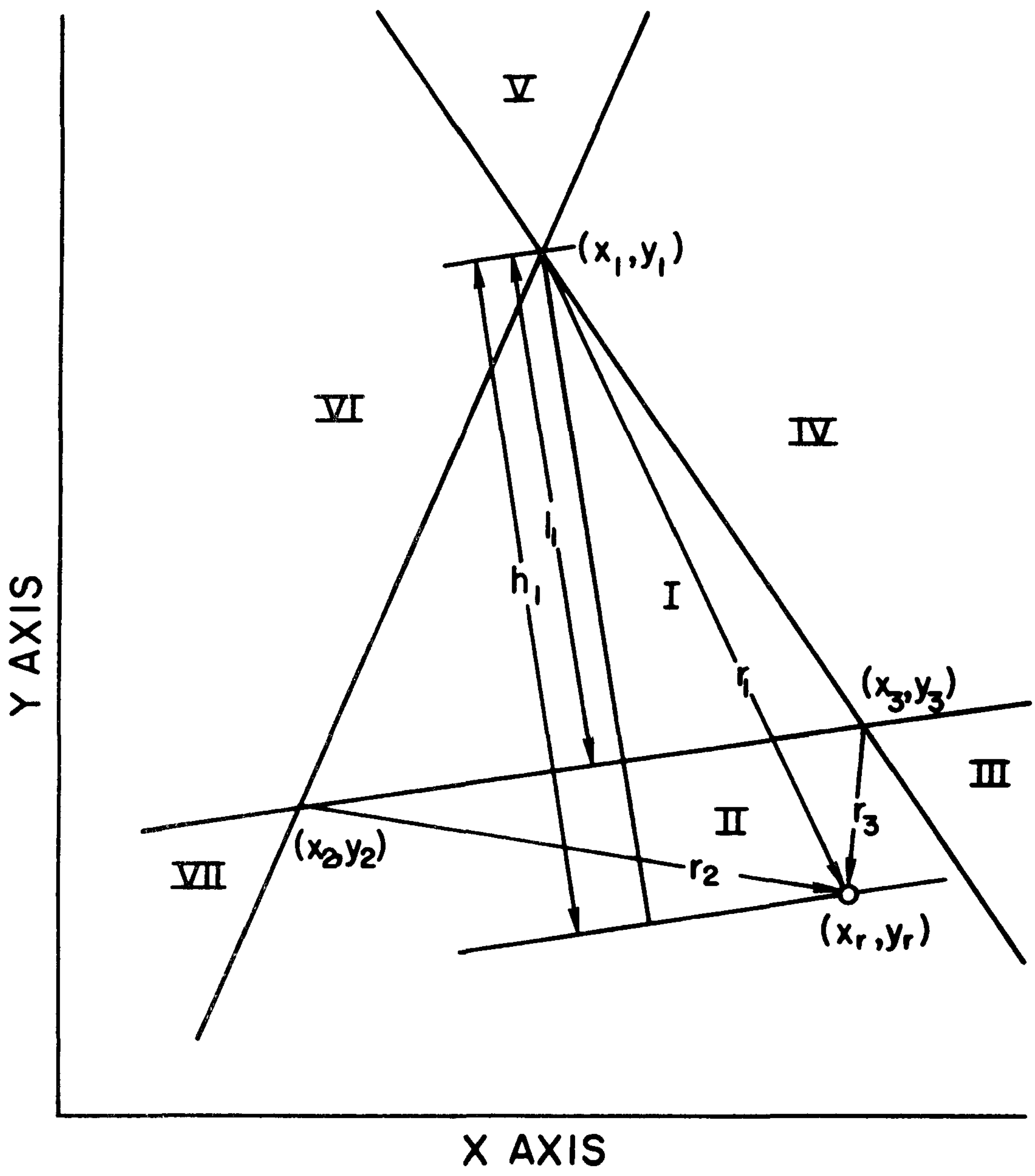

Figure A1: Pictorial representation of variables appearing in interpolation formula.

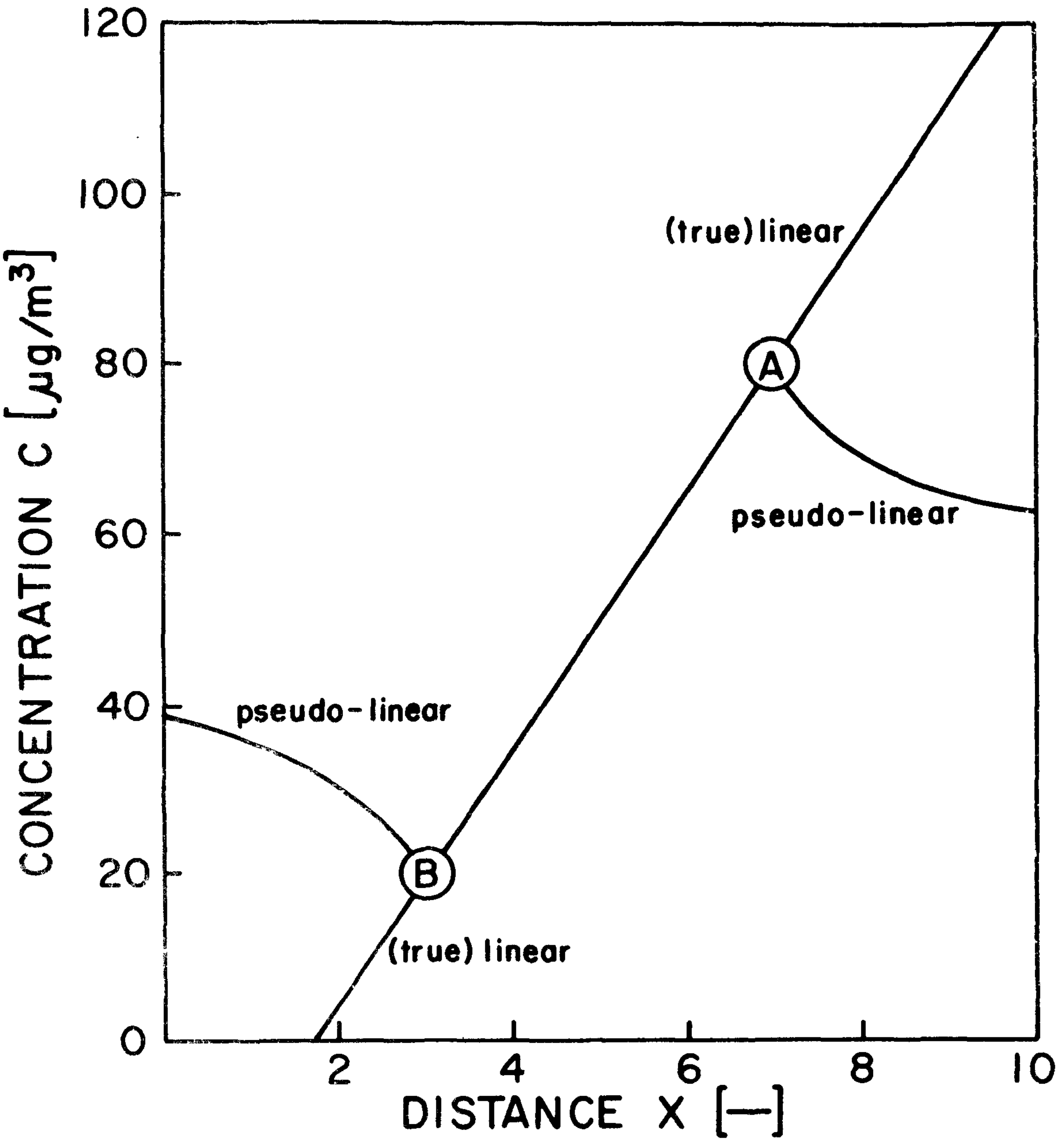

Figure A2: Performances of the linear and the pseudo-linear interpolation formula.

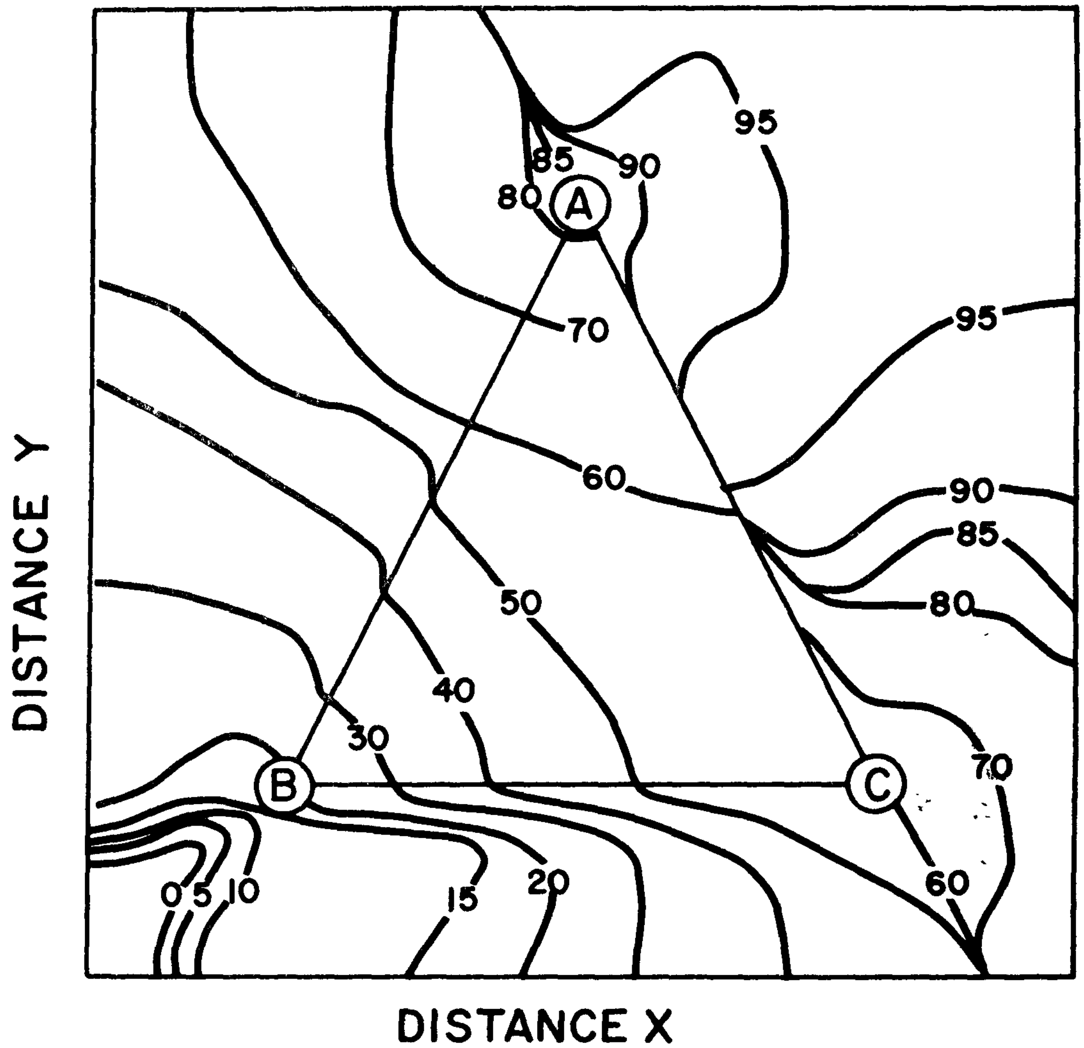

$$C = \left(\sum_{1}^{3} s_i C_i / r_i\right) / \left(\sum_{i=1}^{3} s_i / r_i\right)$$

Figure A3: Performance of the linear interpolation formula.

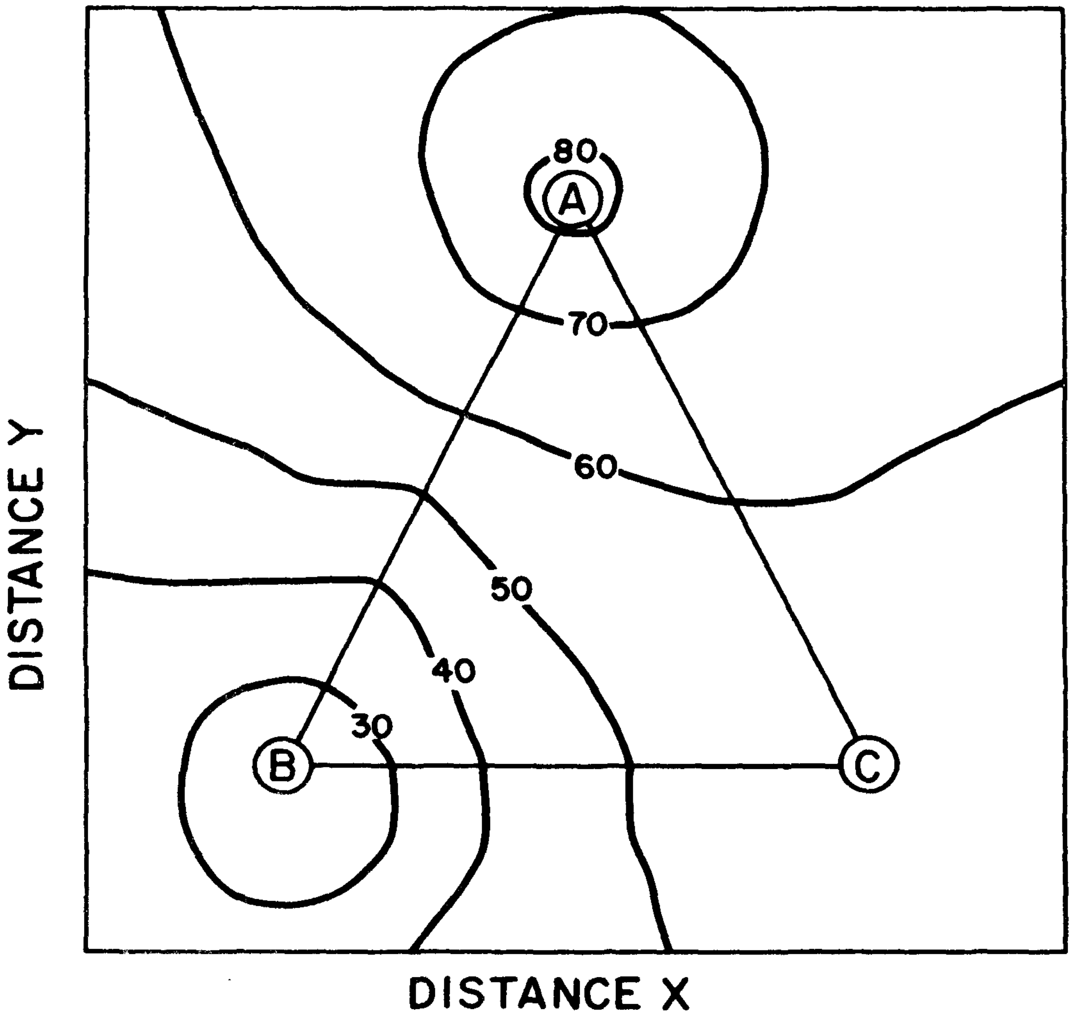

$$C = \left(\sum_{i=1}^{3} C_i / r_i\right) / \left(\sum_{i=1}^{3} 1/r_i\right)$$

Figure A4: Performance of the pseudo-linear interpolation formula.

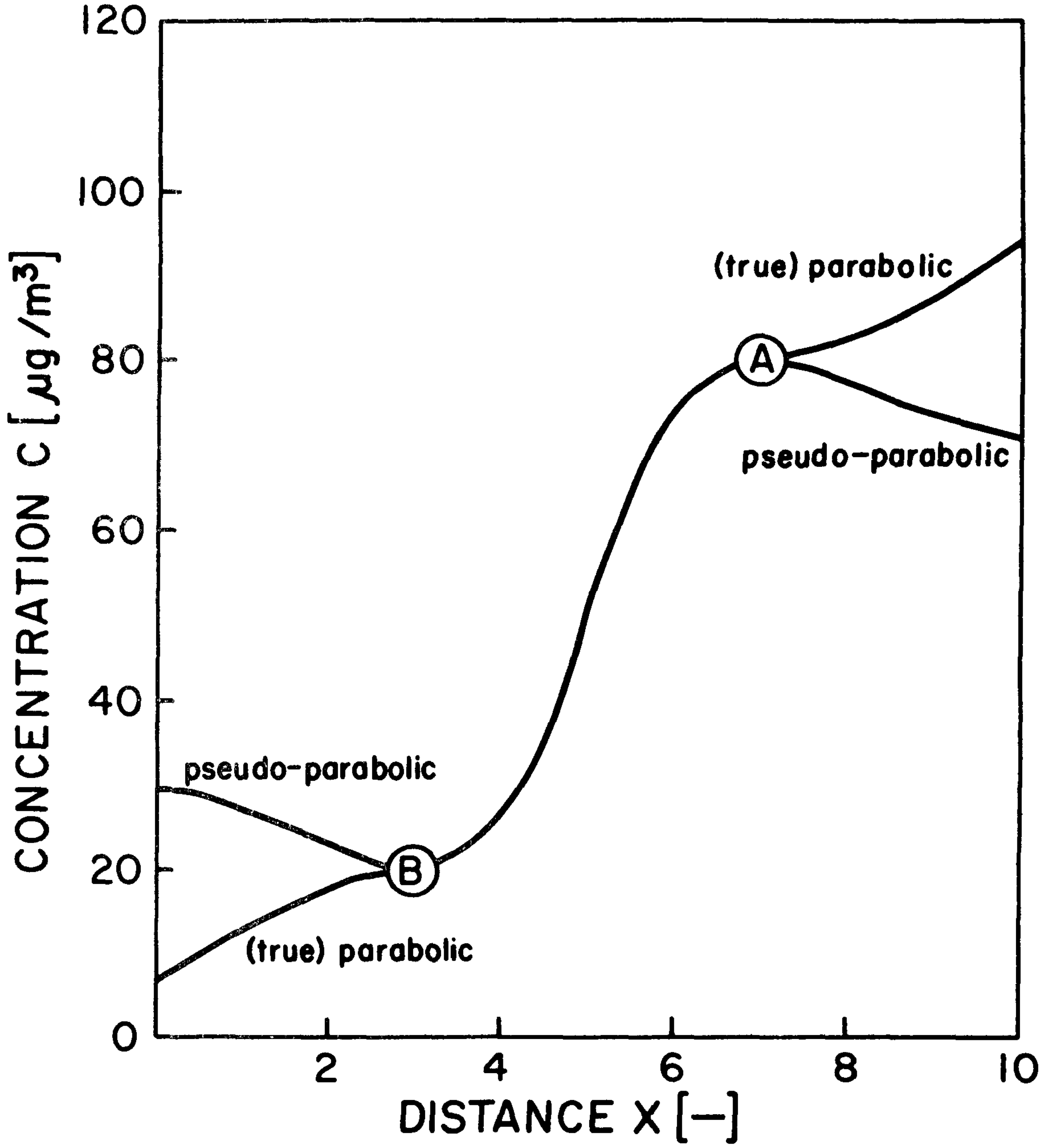

Figure A5: Performances of the (true) parabolic and the pseudo-parabolic interpolation formula.

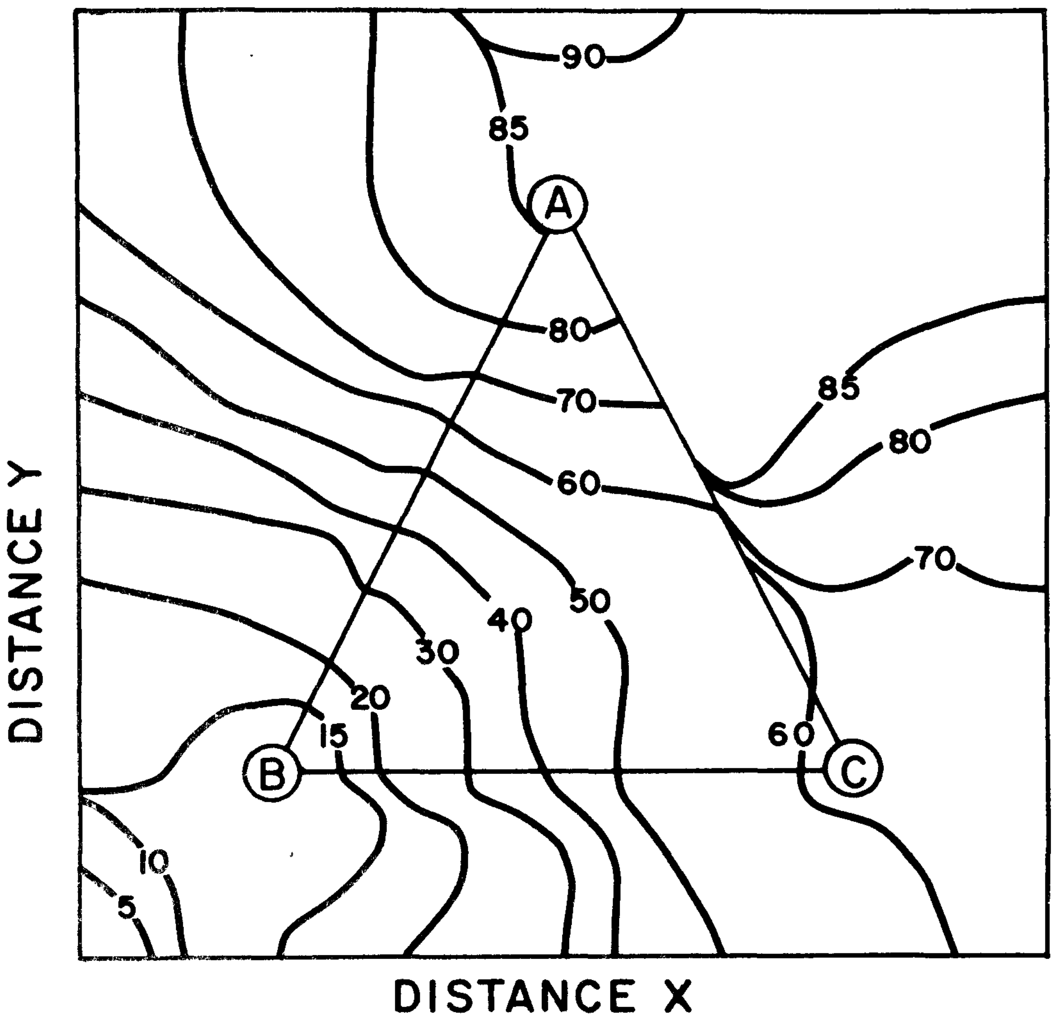

$$C = \left(\sum_{i=1}^{3} s_i C_i / r_i^2\right) / \left(\sum_{i=1}^{3} s_i / r_i^2\right)$$

Figure A6: Performance of the (true) parabolic interpolation formula.

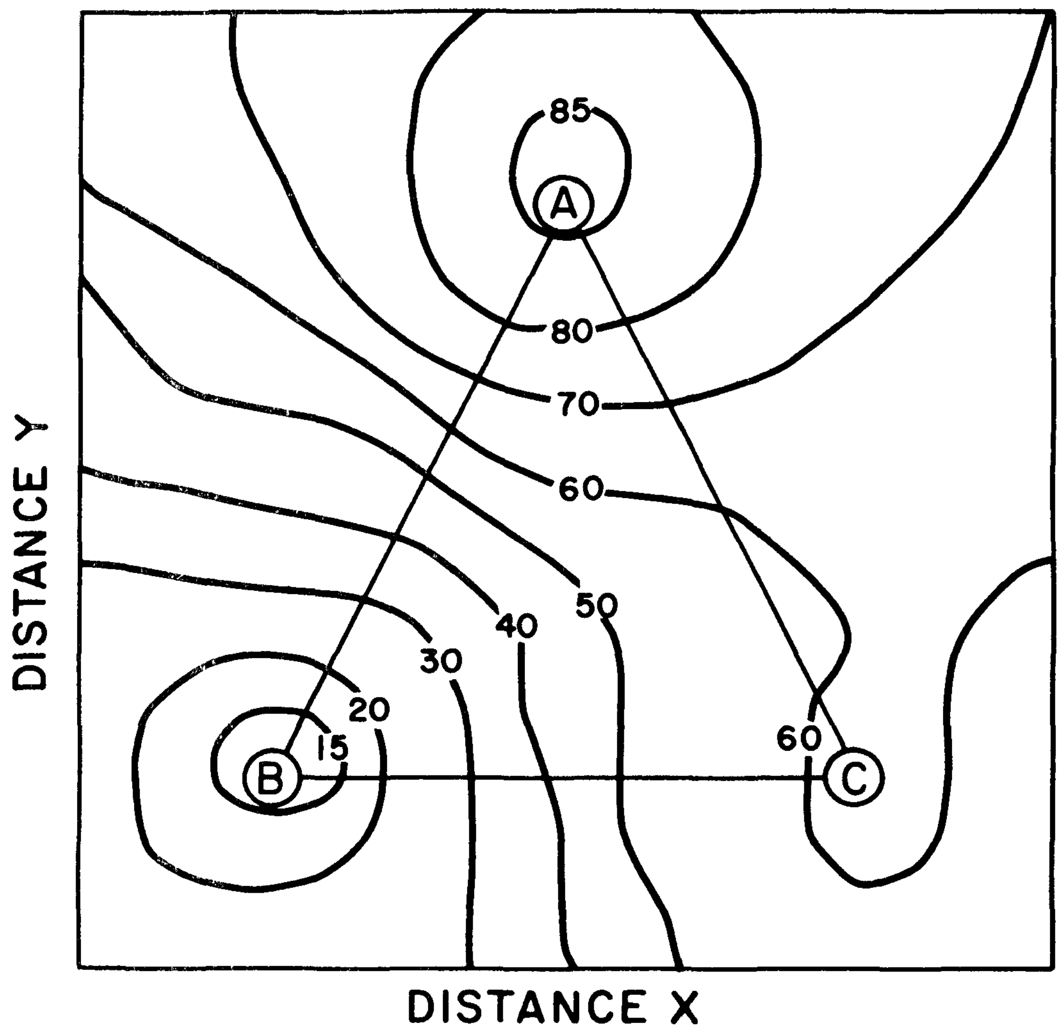

$$C=\left(\sum_{i=1}^{3} C_i/r_i^2\right)/\left(\sum_{i=1}^{3} 1/r_i^2\right)$$

Figure A7: Performance of the pseudo-parabolic interpolation formula.

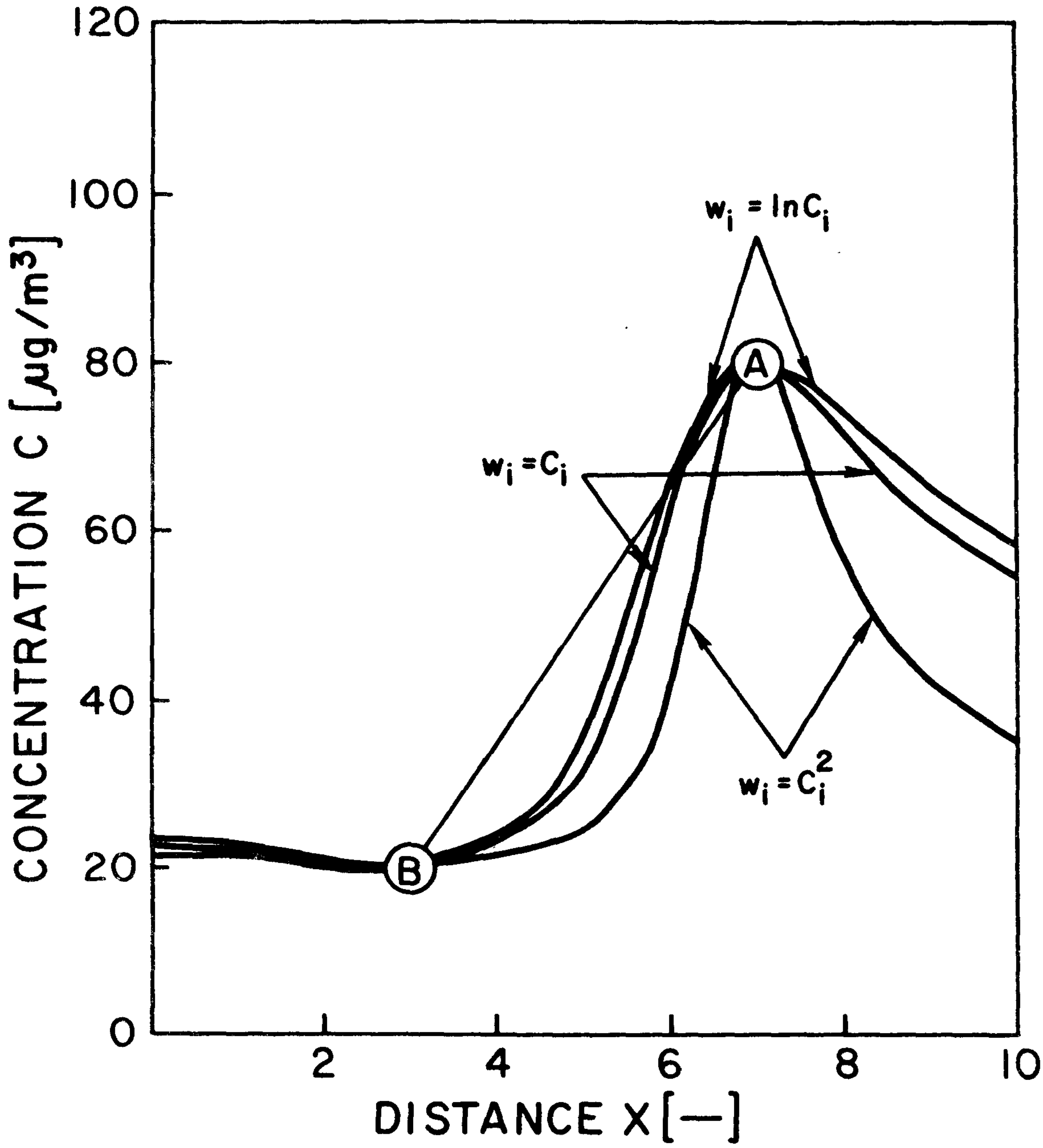

Figure A8: Performances of the three different weighted pseudo-parabolic interpolation formulae.

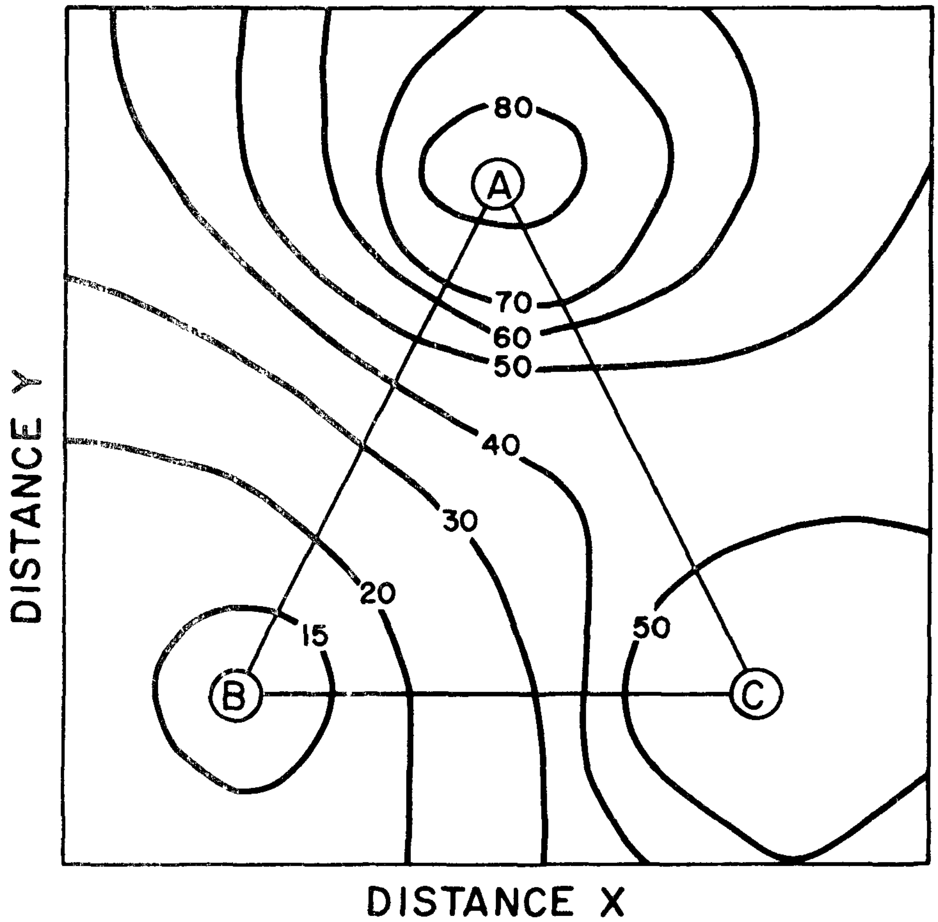

$$C = \left(\sum_{i=1}^{3} C_i / w_i r_i^2\right) / \left(\sum_{i=1}^{3} 1/w_i r_i^2\right)$$

Figure A9: Performance of the weighted pseudo-parabolic interpolation formula ($w_i = \ln C_i$).

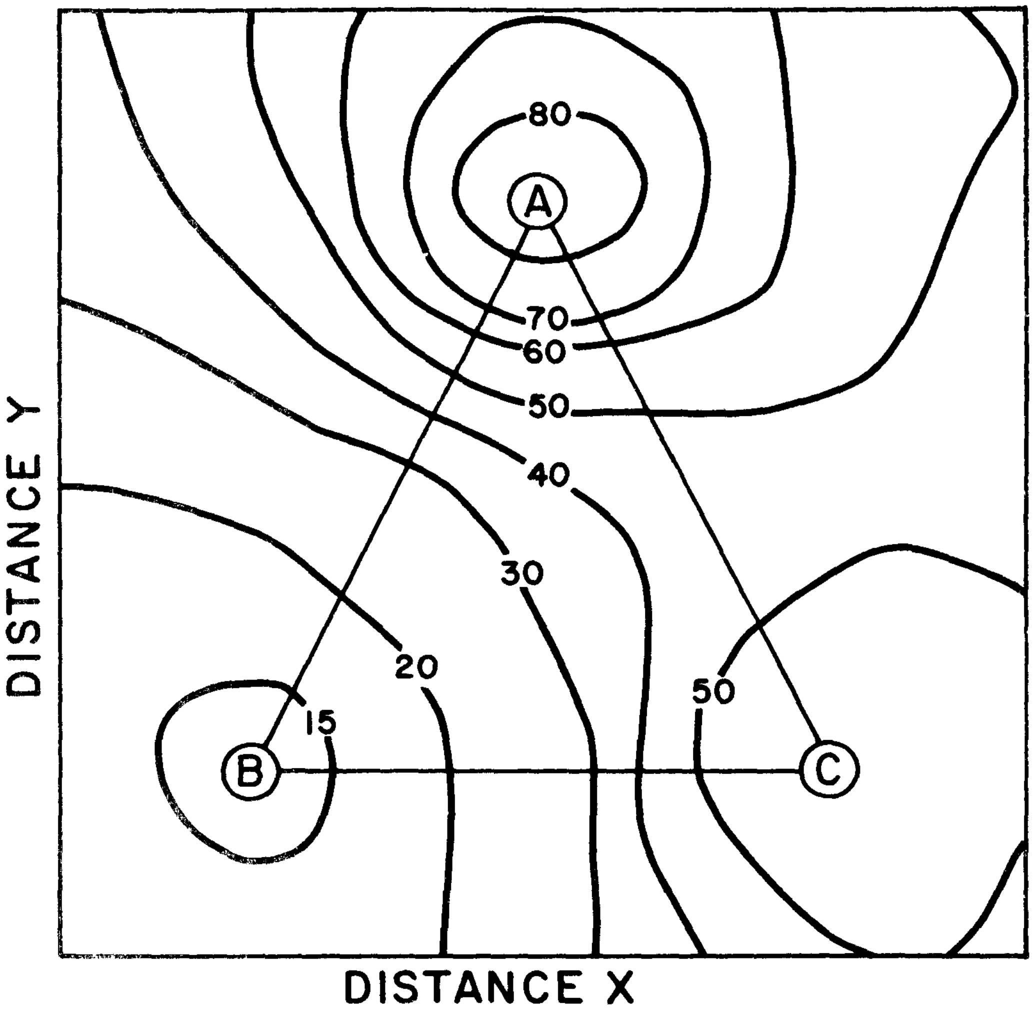

$$C=\left(\sum^{3} C_i / w_i r_i^2\right) / \left(\sum^{3} 1 / w_i r_i^2\right)$$

Figure A10: Performance of the weighted pseudo-parabolic interpolation formula ($w_i = C_i$).

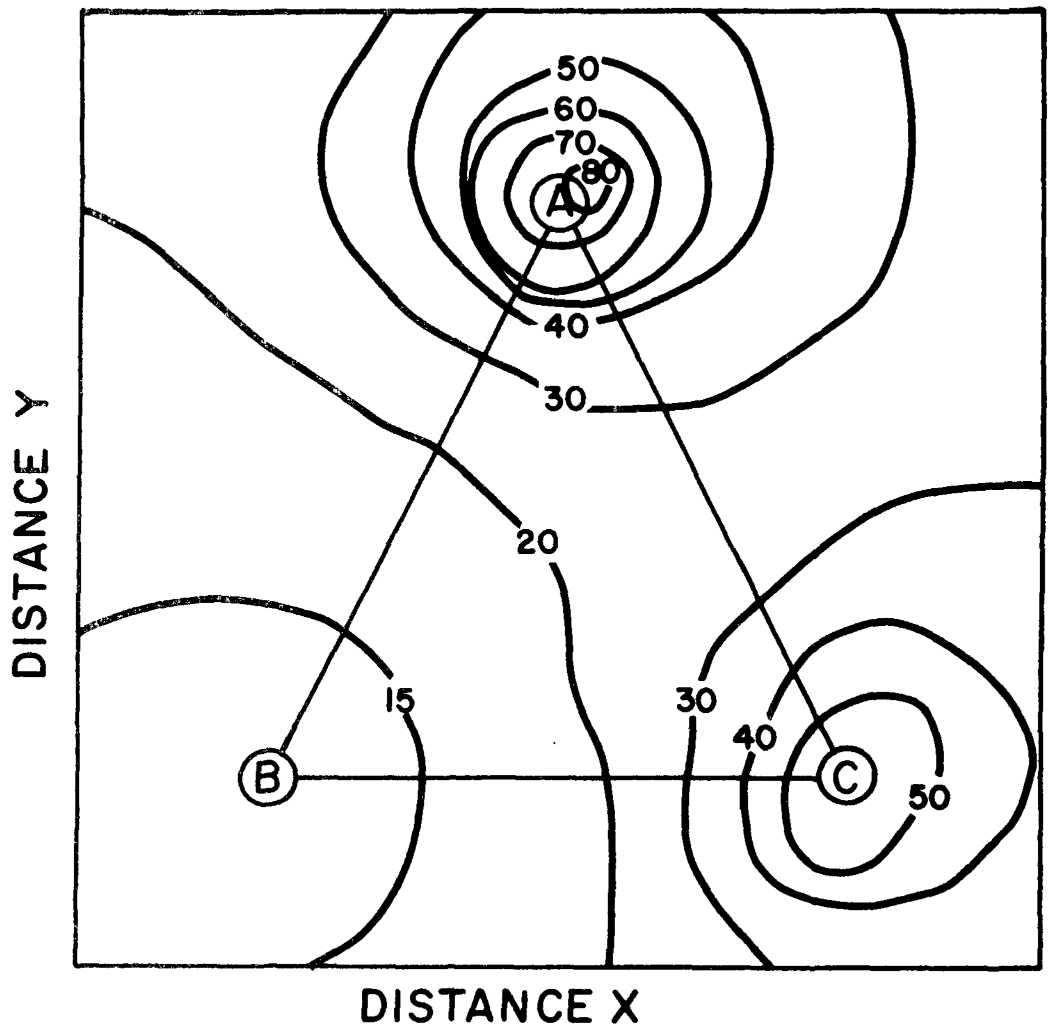

$$C = \left(\sum_{i=1}^{3} C_i / w_i r_i^2\right) / \left(\sum_{i=1}^{3} 1 / w_i r_i^2\right)$$

Figure AII: Performance of the weighted pseudo-parabolic interpolation formula ($w_i = C_i^2$)

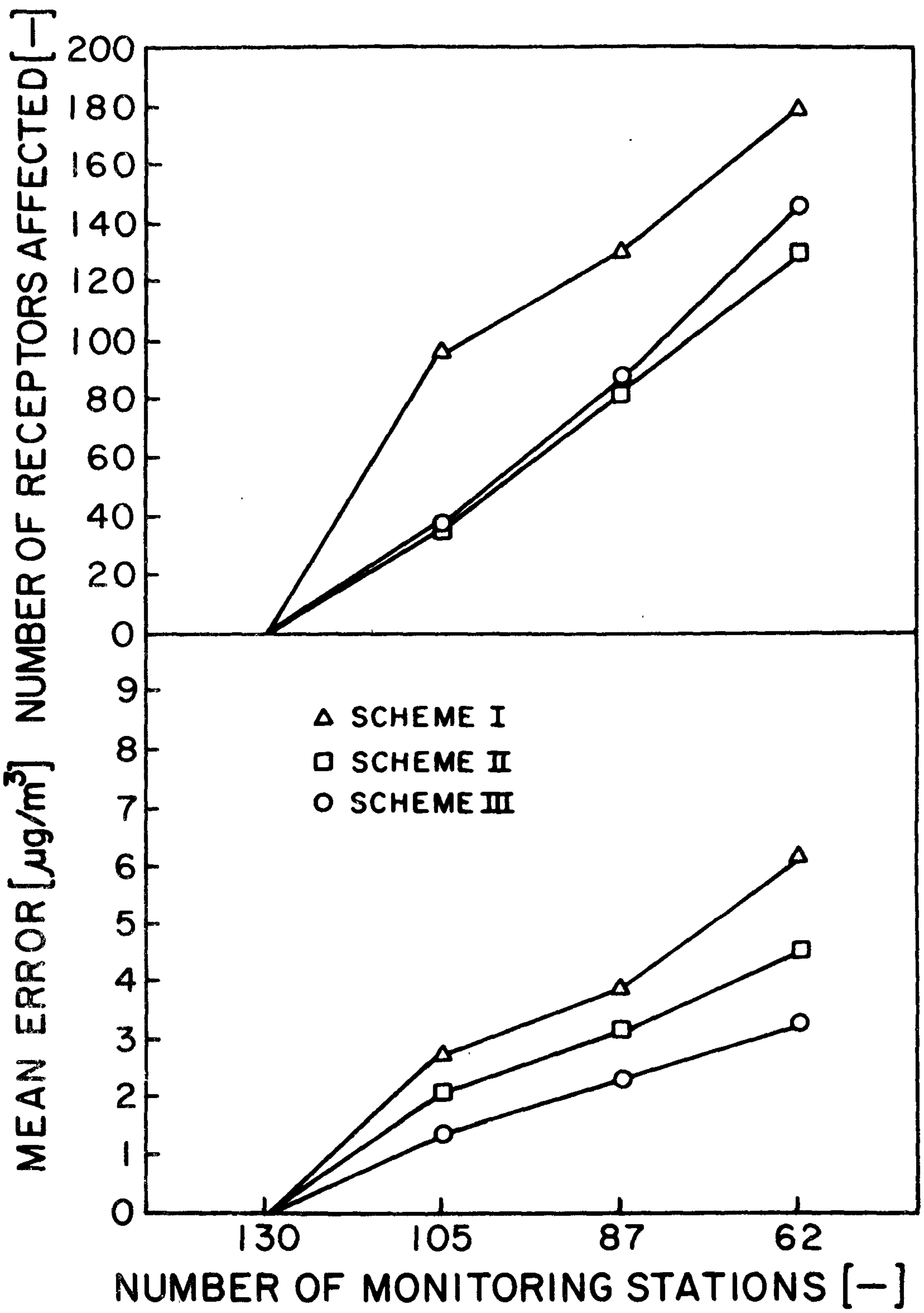

Figure C1: Performance of Schemes I, II, and III with less stations.